AD-A092 161 ROYAL AIRCRAFT ESTABLISHMENT FARNBOROUGH (ENGLAND) F/G 10/2
PROTON/ELECTRON DAMAGE RATIOS FOR SOME VIOLET, BLACK AND THIN S--ETC(U)
NOV 79 M W WALKDEN
UNCLASSIFIED RAE-TR-79133 DRIC-BR-71903 NL

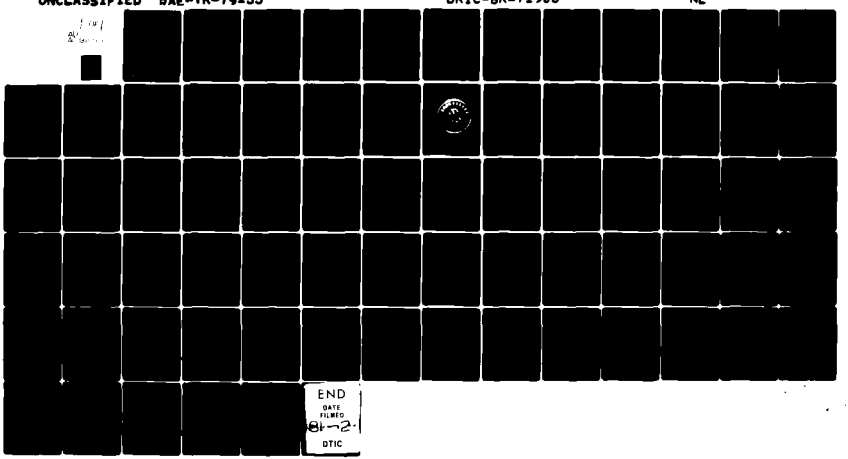

END
DATE FILMED
81-2
DTIC

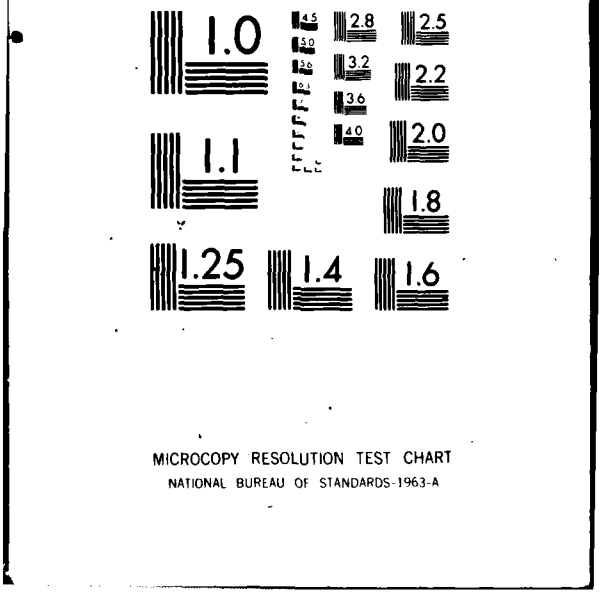

MICROCOPY RESOLUTION TEST CHART
NATIONAL BUREAU OF STANDARDS-1963-A

TR 79133

UNLIMITED

TR 79133

BR71903

LEVEL II

1

AD A092161

ROYAL AIRCRAFT ESTABLISHMENT

*

Technical Report 79133

November 1979

PROTON/ELECTRON DAMAGE RATIOS FOR SOME VIOLET, BLACK AND THIN SILICON SOLAR CELLS

by

M.W. Walkden

DTIC ELECTE NOV 26 1980 S D E

*

Procurement Executive, Ministry of Defence
Farnborough, Hants

DDC FILE COPY

80 10 31 032

UDC 629.19.066.5 : 621.383.5 : 620.192.63 : 629.199.31

ROYAL AIRCRAFT ESTABLISHMENT

Technical Report 79133

Received for printing 6 November 1979

PROTON/ELECTRON DAMAGE RATIOS FOR SOME VIOLET, BLACK AND THIN SILICON SOLAR CELLS

by

M. W. Walkden

SUMMARY

In order to predict the probable degradation of spacecraft solar cells and arrays in orbit it is necessary to know how the radiation environment and other factors may affect solar cell output power. It is convenient for this purpose to use proton damage ratios which relate the damage caused by protons of different energies to that caused by 1 MeV electrons.

To this end, four different types of modern silicon solar cell have been subjected to 1 MeV electrons and protons in the energy range from 2-50 MeV, followed at each irradiation stage by an exposure to photon irradiation. The cells included non-reflecting and violet cells of normal (200-250 μm) thickness and a thin (50 μm) cell. Cell performance measurements were made on new and irradiated cells at room and at elevated temperatures to obtain the proton damage ratios and to ascertain whether these were temperature dependent.

It was found that the proton damage ratio of one type of cell was approximately one half of that of the other three types. It was also found that the proton damage ratio for this type of cell was independent of temperature, which was not the case with the other types. One cause of these differences is attributed to photon induced changes in solar cell performance following electron and proton irradiation for the particular material from which this type of cell is made.

Report of tests carried out for the European Space Research and Technology Centre, Noordwijk, The Netherlands, under ESTEC Contract No.3301/NL/77HP. Responsibility for the contents resides in the author or organisation that prepared it.

Department Reference: Space 571

Copyright
©
Controller HMSO London
1979

LIST OF CONTENTS

Accession For
NTIS GRA&I
DDC TAB
Unannounced
Justification
By
Distribution/
Availability Codes
Dist | Avail and/or special
A

1 INTRODUCTION

In orbit, solar cell arrays are continuously bombarded by corpuscular radiation, composed mostly of multi-energetic protons and electrons. Particles with sufficient energy can pass through the cell coverglass and penetrate the cells. As a result, damage complexes are created in the cells which act as recombination centres for photogenerated carriers. The output from the solar cells and hence from the array will therefore decrease during the orbital life of the satellite. However, if the magnitude and rate of decrease in output can be predicted, it is possible to allow for this by making the array larger, and thus to satisfy the end of life power requirement of the spacecraft. The solar array designer has no control over such degradation factors as the duration of the mission, its timing with respect to the 11 year solar cycle and the altitude and inclination of the orbit. Optimisation of the design parameters of the array is therefore limited to the selection of solar cell type, and coverslide thickness, taking account of the mass and area limitations of the array.

In order to simplify the prediction of array degradation, the damage caused by an equivalent fluence of 1 MeV electrons is used. This is that fluence of 1 MeV electrons which would cause the same amount of damage to the cells, as that caused by the wide range of protons and electrons expected to be encountered by the array in a particular orbit for a given length of time. In order to calculate this equivalent fluence, it is necessary to know the proton damage ratios, by which the protons of different energies expected in a particular orbit can be 'converted' to equivalent 1 MeV electrons. The equivalent 1 MeV electron fluence may then be computed by summation of the products of the number of protons of a particular energy per unit time and the proton damage ratio for that energy.

As for most orbits the proton and electron energies and populations are now adequately predictable, it is necessary to obtain a knowledge of the proton damage ratios for modern high efficiency solar cells. When these are known, the equivalent 1 MeV electron fluence for any orbit can be computed as described above and that 1 MeV electron fluence applied to the solar cells to be used for the mission. By measuring the performance before and after that dose, the array degradation may therefore by predicted.

Damage ratios for protons in the energy range from 2 to 155 MeV were established for cells of initial efficiencies of 9-10% by RAE in 1972[1]. Since then, improvements in silicon solar cell technology have raised initial efficiencies to between 12 and 15%. In order to ascertain whether these damage ratios

133

were valid for more modern types of solar cell, a preliminary study[2] was made in 1976-77 in which seven types of modern silicon solar cell were subjected to 10 MeV proton, 1 MeV electron and photon irradiation. The results of this work indicated the need for further measurements, as differences in proton damage ratios between cell types were found at the single proton energy employed. These were found to be caused partly by photon induced damage of electron irradiated cells of a particular type, similar to one of the cells studied in the present work.

The cells were delivered to RAE in two stages. Types B and D (see Table 1), which were tested first, were of general interest and were measured at three temperatures. These were at the normal test temperature of 25°C and at 15°C and 65°C, temperatures applicable respectively to spinning and sun orientated arrays at geosynchronous altitude. On completion of this part of the programme, Types A and C were delivered and tested. Type A, with Type C, as a back-up, are intended for use on the ESA/NASA Space Telescope array, and as such had specific test requirements. The array temperature in orbit had been predicted by ESA and consequently cell performance measurements were required to be made at different temperatures ie 25°C, 55°C or 70°C and 90°C. Also, as the Space Telescope will be used in near earth orbit, the solar cell damage due to protons and electrons is expected to be relatively small. Irradiations were therefore commenced at lower thresholds than for Types B and D, but were continued beyond the fluence region expected for the Space Telescope mission, so that comparison with Types B and D could be made at the higher fluence levels.

2 SOLAR CELL SAMPLES

The four types of cell used in this programme were two violet cells (Types A and C), a 'black' or non-reflecting cell (Type B) and a thin cell (Type D). Full details of the cell parameters are given in Table 1.

All cells were calibrated on receipt, at 25°C, and divided into seven groups (5 in the case of Type D), such that the mean maximum power of each group of a particular cell type was the same. For example the mean maximum power of each of the Type A groups was 145 mW, while that of each of the Type B groups was 136 mW.

The first group of each cell Type received 1 MeV electron irradiation followed by photon irradiation, while the other six groups (4 in the case of D) received proton irradiation followed by photon irradiation. Table 2 gives the

proton energies used and the number of cells per group of each cell type, together with the initial mean maximum power of each type.

As described in section 1, the work was carried out in two stages, Types B and D being tested first. Only a few samples of Type D were available, and these were used to fill spare stations in the irradiation sample holder (Fig 1a). Hence there is a disparity in the number of cells per group for Types B and D. Also, in the second part of the programme, it was decided that as Type A was of major interest to ESA, this type of cell should be fully tested at the expense of Type C. There is therefore, a similar disparity in the number of cells per group between Types A and C.

As the cell holders for both irradiation and performance measurement were designed to accommodate cells of normal thickness, it was decided, because of their mechanical fragility to restrict the testing of Type D cells to a minimum. Hence spectral response measurements and performance measurements prior to photon irradiation (sections 4.2 and 5.4) were not made on this type of cell. For the same reason the measurement temperature was limited to 25°C (section 5.1).

3 IRRADIATION FACILITIES

3.1 Electron irradiation

For the 1 MeV electron irradiations, the van de Graaff accelerator at the Central Research Division of British Insulated Callenders Cables, London was used. This facility has been used for many years by RAE and ESA for electron irradiation testing, and is fully equipped for dosimetry measurement. The cells are mounted horizontally in a water cooled, 16 cm diameter aluminium block, enclosed in a vacuum chamber under a 125 μm aluminium diaphragm. During irradiation the vacuum was better than 10^{-3} torr and the beam was continuously monitored by means of a graphite Faraday cup of 1 cm^2 aperture located at the centre of the target block. The output from the Faraday cup was fed to a chart recorder via a vibrating reed electrometer. The electron beam from the accelerator tube in the generator was scanned electromagnetically, and this, combined with air scatter of the emergent beam gave a uniformity better than $\pm 5\%$ over the target area.

3.2 Proton irradiation

The 2, 4, 6 and 10 MeV proton irradiations were conducted on the Tandem van de Graaff accelerator at the Atomic Energy Research Establishment, Harwell. The proton exit window, 5 cm in diameter, limited the number of cells which could be irradiated at any one time to one 2 x 4 cm cell. Consequently a specially

designed holder (Fig 1a), integral with the flight tube, with 23 stations on its periphery to carry the cells was used. A 24th position carried a circular target divided into four insulated quadrants for beam intensity and uniformity measurement, by Faraday cup techniques. The wheel was indexed to the desired station by a remotely controlled electric actuator, and the cells were then accurately set in the 5 cm beam by lining up a mark on the wheel with a fixed pointer, using closed circuit TV. Beam uniformity was better than ±5% over the target area, and energy resolution was within ±0.2%.

The Variable Energy Cyclotron was used for 19 and 50 MeV proton irradiations. The same cell holder was used as with the Tandem van de Graaff accelerator, but in this case a cell which was to receive 50 MeV protons was superimposed on one to receive 19 MeV protons, with an absorber between them to give the required energy attenuation. Energy resolution was at worst 0.5%.

3.3 Photon irradiation

Photon stabilisation following either electron or proton irradiation was conducted using a Xenon arc solar simulator. The cells were mounted in the vertical beam on a constant temperature block which was maintained at 55°C. The lamp current and distance were adjusted to give an intensity of one solar constant (±5%) at the target area. Uniformity and intensity were determined in preliminary runs using a standard 2 x 2 cm cell to scan the target area. The intensity was continuously monitored during the period of cell irradiation.

4 SOLAR CELL MEASUREMENT FACILITIES

4.1 Voltage-current characteristics

All voltage-current characteristic (VI) measurements were made at RAE using the Large Area Pulsed Solar Simulator (LAPSS). This equipment, installed in a special building at RAE, comprises two Xenon flash tubes side by side which are simultaneously pulsed by a capacitive-inductive network to produce an intense flash of light lasting about 2 ms. During the period of the flat topped pulse, the load on the cell under test (13 m from the flash tubes) is swept from short circuit to open circuit condition and 40 near simultaneous voltage and current readings are taken at fixed time intervals. Associated with each pair of readings is a measurement of the short circuit current of a primary standard cell located in the target plane. The raw data are digitised and stored in a computer, automatically corrected to Air Mass Zero intensity by reference to the 'standard' cell of known short circuit current, and subsequently displayed on an X-Y plotter which produces a continuous trace of the 40 data points.

Fig 1b is a measurement of the spectral energy distribution of light at the target plane measured in August 1977, compared to AMO sunlight. With this spectral match it has been computed that if a cell irradiated to 3×10^{15} electron cm^{-2} at 1 MeV were measured against an unirradiated standard the error would be less than 1% low. In order to ensure uniformity of standard cells, it was decided to use one set only which had been irradiated to a 1 MeV electron fluence of 1×10^{14} electron cm^{-2}, for all measurements throughout the programme. Consequently the beginning of life performance figures are slightly high while those of the most heavily irradiated are slightly low. The standards used had been generated the previous summer at the RAE calibration test site in Malta, and the data corrected to AMO conditions.

4.2 Spectral response

The spectral response of one cell from each of Types A, B and C was found by means of a Hilger-Watts D285, fused silica prism monochrometer. The monochrometer is fed by a 1 kW tungsten-halogen lamp supplied from a stabilised dc power pack. The detector used was a Comsat non-reflecting cell with response ranging from 0.32 to 1.2 μm. The relative spectral response of this cell has been determined by the National Physical Laboratory, Teddington. By comparing the current generated in turn by the Comsat standard cell and the cell under test and dividing, the relative spectral response of the irradiated cells was found.

5 TEST PROGRAMME

5.1 Initial measurements

The voltage-current characteristics of all 84 cells were measured initially at 25°C and the cells divided into groups as indicated in Table 2. Types A and C were remeasured at temperatures of 25°C, 55°C or 70°C and 90°C, while Type B was measured at 15°C, 25°C and 65°C. In order to minimise handling of the 50 μm cells it was decided to measure Type D at 25°C only. The relative spectral response of one cell from each group of Types A, B and C was also measured at 25°C.

5.2 Electron irradiations

Sequential electron irradiations at 1 MeV of 'electron groups' of each cell type were performed at BICC using facilities described in section 3.1. Cumulative fluences received by the cells from zero to 3×10^{15} electron cm^{-2} are given in Table 3.

5.3 Proton irradiations

Sequential proton irradiations at 2, 4, 6 and 10 MeV were performed, at AERE using facilities described in section 3.2. Cumulative fluences received by the cells from zero to 1.1×10^{12} protons are given in Table 4.

The 19 and 50 MeV proton groups received three fluences only, which are given in Table 5.

5.4 Measurements following corpuscular radiation

After either proton or electron irradiation, the cells were returned to the RAE, where two cells from each group (except Type D) were measured at 25°C using the LAPSS. All cells were then placed under illumination from the Xenon lamp and subjected to photon irradiation at one solar constant (AMO) for 6 hours. The irradiation was then stopped and the same two cells from each group were removed and remeasured. The cells were replaced, and the photon irradiation continued for a further 18 hours, after which the same cells were measured again.

By comparison of the cell performance after proton or electron irradiation only, with that after the additional 6 and 24 hours of photon irradiation, it was possible to decide whether changes induced by photon exposure was complete. Only after the largest fluence of both proton and electrons was it found necessary to give the cells further photon exposure (20 hours) to ensure stability. Once this was achieved all cells were measured at 25°C. Also at this stage the relative spectral response of one cell from each of groups A, B and C was measured as described in section 4.2.

After this time and just prior to the next fluence dose, all cells were remeasured at 25°C and at the temperatures given in section 5.1.

6 RESULTS

6.1 V-I characteristics and maximum power

Fig 2 shows the mean voltage-current characteristics of Type A cells, initially, and after various fluences of 1 MeV electrons. In this case the cell temperature when measured was 25°C. From this and similar characteristics obtained for the other cell measurement temperatures, and for proton irradiation in the energy range 2-50 MeV, Figs 3 to 16 were constructed. Figs 3 and 4 show cell maximum power versus 1 MeV electron fluence at the temperatures used for groups A and B respectively. Fig 5 gives the same parameters for Type C, and Type D at 25°C only. In Figs 6 to 9 cell maximum power versus proton fluence is

illustrated for the six energy levels at the four temperatures used for Type A cells, and Figs 10 to 12 show similar curves for Type B cells for the three temperatures used. In Fig 13 maximum power degradation at 25°C versus proton fluence for Types C and D is given and Figs 14 to 16 show that of Type C at the higher temperatures.

6.2 Spectral response

The effect of 1 MeV electron and 2 and 50 MeV proton irradiation on the cell absolute spectral response is illustrated in Figs 17 to 19. All of these measurements were made after photon stabilisation as described in section 4.2. Cell Types A and B are shown, Type C behaved in a similar way to Type B.

6.3 Proton damage ratios

Proton damage ratios (pdrs) are defined as:

The number of 1 MeV electrons required to reduce the cell maximum power measured at temperature T , by x per cent; divided by the number of protons of energy E required to reduce the cell maximum power measured at the same temperature by the same percentage.

Proton damage ratios were obtained from large scale plots of Figs 3 to 16 for maximum power degradations of 5, 10, 15 and 20% and are given in Figs 20 to 49. At the top of each figure is shown

(a) the cell type - violet or black

(b) the base resistivity of the cell - 1 or 10Ω cm

(c) the temperature at which the irradiated cells were measured, T°C and

(d) the percentage degradation of maximum power for which the proton damage ratios were calculated - 5, 10, 15 or 20%.

In addition to the pdr for uncovered cells, derived as described above, pdrs for cells covered with three typical thicknesses of coverslide are shown. These were calculated from the uncovered cell pdr and the known stopping power of ceria doped microsheet (CMS) material.

For Type D cells, where only the whole of the 2 and 10 MeV groups survived intact, pdrs are shown in tabular form in Table 6.

7 DISCUSSION OF RESULTS

7.1 The effect of photon irradiation

For Type A cells, it was found that photon exposure following 1 MeV electron irradiation produced a significant further degradation, amounting to some 4-6% for electron fluences in excess of 5×10^{13} electron cm^{-2} (Table 7). In contrast to this, cell Types B and C showed annealing of the electron radiation damage of between 1 and 4% over the same 1 MeV fluence range. Hence the difference between Type A cells and those of Types B and C due to photon irradiation amounted to between 5 and 10% depending on the total electron fluence. Moreover as Types B and C were made from 10Ω cm CZ silicon, the rate of degradation due to electron irradiation only, was, as expected less than that of the 1Ω cm FZ, Type A, although these results are somewhat obscured as the cells were subjected to photon exposure at each electron fluence stage. Hence after the final fluence, including photon exposure, Type A cells had fallen from an initial maximum power of 145 mW to 79 mW (45% fall). Type B on the other hand fell from 136 mW initially to 102 mW (25% fall), and Type C from 133 mW to 93 mW (30% fall). Type D, being a thin cell fell less, from 60.2 mW initially to 48.5 mW (19% fall).

The effect of photon exposure on proton irradiated cells is illustrated in Table 8. It will be seen that in general there was little change in cell performance for Type A cells, whereas Types B and C exhibited some 2-3% annealing. The small changes in cell performance, in general showed some correlation with proton energy (Table 8). Those cells exposed to lower energy protons - hence damaged more - showed a tendency to degrade (Type A) or anneal (Types B and C) slightly more than those groups exposed to the higher energy protons. Although Table 8 illustrates the behaviour only after a cumulative fluence of 10^{11} p cm^{-2}, it is typical of the results obtained for all other fluences.

7.2 Proton damage ratio and cell types

The behaviour of Type A cell, as illustrated in Table 7, clearly has a significant effect on the proton damage ratios in comparison with those of Types B and C. This is illustrated in Fig 50, which shows the pdr of Types A, B and C for uncovered cells at 25°C, based on cell maximum power degradation of 20%.

In the previous study[2], which was limited to 10 MeV proton and 1 MeV electron irradiation plus photon exposure, the pdrs of similar cells to the present Types A and B were 1.3×10^3 and 2.0×10^3 respectively which are in good agreement with the results reported here.

The cell similar to Type A (1Ω cm, low dislocation FZ silicon) in fact had a textured front surface and was thinner (200 μm). Evidently neither of these parameters has a significant effect on the pdr. The pdrs established in 1971 for Intelsat IV cells[1] appear to be more energy dependent than those obtained in this study, although at 10 MeV the pdr is almost identical (2.2×10^3) to that of Types B and C. Intelsat IV, and Types B and C were all made from 10Ω cm CZ silicon. Different manufacturing techniques, improved collection efficiency, a shallower junction and hence superior blue spectral response of the more modern cells could be responsible for this energy dependence difference.

7.3 The effect of temperature on the proton damage ratio

Fig 51 shows the effect of cell temperature on the pdrs. It can be seen that Type A again behaves differently compared with Types B and C. The latter show significant increases in pdr as the cell temperature is raised which is in agreement with previous work[3]. Type A on the other hand shows no significant increase in pdr as the temperature is raised from 25 to 70°C, or indeed 90°C (Fig 51).

7.4 The percentage degradation on which the proton damage ratios are based

Another item of interest is to determine whether pdrs showed a significant difference if they were based on different percentage degradations of maximum power. It can be seen (Fig 52) that there are insignificant differences in pdr for maximum power degradations of 15 and 20%. The pdr based on 10% degradation is in general between the 15-20% cures and that based on 5% degradation as would be expected. The reason for the differences is due to the shape and position of the 'knee' of the maximum power versus fluence curves (Figs 3 to 16), that is, the start of a true logarithmic decrement.

8 CONCLUSIONS AND RECOMMENDATIONS

Proton damage ratios in the energy range 2-50 MeV have been established for a number of types of solar cell. The effect of cell temperature and coverglass thickness on the proton damage ratios have been investigated. From the present work it is concluded that:

(1) The 'traditional' value of 3000, 1 MeV electrons per 10 MeV proton is somewhat high for present day solar cells (cf 2300).

(2) Proton damage ratio of 10Ω cm CZ (B and C) solar cells are greater than 1Ω cm FZ (A) cells by a factor of 1.8 to 2.0 at 25°C depending on the proton energy.

(3) Proton damage ratios of 10Ω cm CZ cells increase by a factor of approximately 1.3 for a temperature rise of 40°C, whereas there is no corresponding increase for 1Ω cm FZ cells. Hence at 65°C proton damage ratios for 10Ω cm CZ cells are higher than those of 1Ω cm FZ cells by a factor of approximately 2.5.

(4) Proton damage ratios for slightly damaged cells (~5% degradation of maximum power) are slightly higher than for moderately damaged cells (>10% degradation of maximum power).

(5) Photon exposure following electron irradiation causes further permanent degradation of 1Ω cm FZ cells whereas 10Ω cm CZ cells are annealed.

(6) Photon exposure following proton irradiation has little effect on 1Ω cm FZ cells whereas 10Ω cm CZ cells are again annealed.

(7) Proton damage ratios of thin (50 μm) cells (Table 6) are approximately the same as those of greater thickness.

Electron damage ratios have not been measured in this or the previous work. In view of the anomalous behaviour of 1Ω cm FZ cells after electron irradiation and photon exposure, it would be desirable to conduct electron irradiations at other energies. In addition to providing electron damage ratios for present day cells it could be of benefit to those workers studying the photon induced phenomena from the theoretical viewpoint.

In the future, most arrays for all but small spacecraft will probably be constructed from cells mounted on thin plastic sheets which are deployed from the spacecraft by unrolling or unfolding. This type of array does not have the benefit of the shielding afforded by the spacecraft body of a 'drum' spacecraft, or the relatively dense aluminium honeycomb panels of rigid deployed arrays. Protons and electrons can therefore enter the cells from the rear as well as through the front coverglass.

In order to improve the accuracy of computed equivalent 1 MeV electron fluences and hence a better estimate of array lifetime, it is recommended that further work should be carried out in both of these areas.

Acknowledgments

The author wishes to thank ESA for their permission to publish this paper and his colleagues M.A.H. Davies and G. Lovell for carrying out the very large number of solar cell performance measurements.

Table 1

CELL CHARACTERISTICS

Type	A (violet)	B (black)	C (violet)	D
Manufacturer	AEG	AEG	AEG	SOLAREX
Size (cm)	4.035 x 2.095	4 x 2	4.035 x 2.095	2 x 2
Thickness (μm)	250	200	250	50
Surface finish*	Spec	Text	Spec	Spec
Base resistivity (ohm-cm)	1	10	10	2
Back surface field	No	No	No	Yes
Crystal**	FZ	CZ	CZ	CZ
Initial efficiency (%)	12.6	12.5	11.5	11.0

NOTE : *Spec = Specular
Text = Textured or non-reflecting

**FZ = Float zone refined
CZ = Czochralski grown

Table 2

NUMBER OF CELLS PER GROUP

Type	Initial maximum power of each group (mW)	Number of cells per group						
		Electron group	Proton groups					
		1 MeV	2 MeV	4 MeV	6 MeV	10 MeV	19 MeV	50 MeV
A	145	5	4	4	4	4	4	4
B	136	6	4	4	4	4	4	4
C	133	5	1	1	2	2	2	2
D	60	2	2	2(0)*	2(0)*	2	0	0

*Mechanical damage during irradiation/measurement handling

Table 3

ELECTRON FLUENCE

Type	Electron fluence cm^{-2}
A	0, 1E13, 5E13, 2E14, 1E15, 3E15
B	0, 3E13, 1E14, 3E14, 1E15, 3E15
C	0, 1E13, 5E13, 2E14, 1E15, 3E15
D	0, 3E13, 1E14, 3E14, 1E15, 3E15

Note : 3E15 means 3×10^{15} etc

Table 4

PROTON FLUENCES (2 to 10 MeV)

Type	Proton fluence cm^{-2}
A	0, 1E9, 1E10, 3E10, 1E11, 1E12
B	0, 1E10, 3E10, 1.1E11, 3.1E11, 1.11E12
C	0, 1E9, 1E10, 3E10, 1E11, 1E12
D	0, 1E10, 3E10, 1.1E11, 3.1E11, 1.11E12

Table 5

PROTON FLUENCES (19 and 50 MeV)

Type	Proton fluence cm^{-2}
A	0, 2E10, 1E11, 1.1E12
B	0, 1E11, 5E11, 1.5E12
C	0, 2E10, 1E11, 1.1E12

Table 6

PDR OF TYPE D CELLS

Proton energy (MeV)	PDR at 25°C (mean of 10, 15 and 20% p max degradation)
2	6.5 E3
10	2.0 E3

Table 7

EFFECT OF PHOTON IRRADIATION ON MAXIMUM POWER OF TYPES A, B AND C AFTER 1 MeV ELECTRON IRRADIATION

1 MeV electron fluence (cm^{-2})	Maximum power (mW), 25°C								
	Type A (145 mW initial)			Type B (136 mW initial)			Type C (133 mW initial)		
	After electrons	After electrons plus photon stabilisation	Δ (%)	After electrons	After electrons plus photon stabilisation	Δ (%)	After electrons	After electrons plus photon stabilisation	Δ (%)
1E13	143.0	141.3	-1.2	-	-	-	131.6	131.1	-0.4
3E13	-	-	-	134.2	133.8	-0.3	-	-	-
5E13	133.8	128.6	-3.9	-	-	-	126.0	128.0	+1.6
1E14	-	-	-	129.5	131.3	+1.4	-	-	-
2E14	120.0	114.2	-4.8	-	-	-	118.5	121.1	+2.2
3E14	-	-	-	121.3	124.3	+2.5	-	-	-
1E15	100.0	94.3	-5.7	110.7	113.3	+2.3	101.3	105.0	+3.7
3E15	82.5	78.8	-4.5	98.8	102.3	+3.5	89.5	93.4	+4.4

Table 8

EFFECT OF PHOTON IRRADIATION ON MAXIMUM POWER OF TYPES A, B AND C AFTER A CUMULATIVE PROTON FLUENCE OF ~1E11 p cm^{-2}

Proton energy (MeV)	Maximum power (mW), 25°C								
	Type A			Type B			Type C		
	After protons	After protons plus photon stabilisation	Δ (%)	After protons	After protons plus photon stabilisation	Δ (%)	After protons	After protons plus photon stabilisation	Δ (%)
2	107.6	105.8	-1.7	112.3	115.6	+2.9	106.8	110.9	+3.8
4	114.6	113.1	-1.3	115.6	119.1	+3.0	112.0	114.8	+2.5
6	117.6	116.6	-0.9	119.8	122.4	+2.2	116.1	119.7	+3.1
10	120.5	120.8	+0.2	122.5	125.1	+2.1	119.0	122.0	+2.5
19	123.2	122.4	-0.6	125.6	128.7	+2.5	121.3	123.8	+2.1
50	125.5	125.0	-0.4	128.5	130.9	+1.9	120.5	122.1	+1.3

Note : For types A and C the 2 to 10 MeV samples received a discrete proton fluence of 7E10, and the 19 and 50 MeV samples a discrete proton fluence of 8E10 p cm^{-2}.
For type B, the 2 -10 MeV samples received a discrete fluence of 8E10 p cm^{-2} (1.1E11 cumulative) and the 19 and 50 MeV samples a fluence of 1E11

REFERENCES

No.	Author	Title, etc
1	A. Meulenberg Jr F.C. Treble	Damage in silicon solar cells from 2-155 MeV protons. Xth IEEE Photovoltaic Specialists Conference, November 1973, Palo Alto, California, USA
2	A.A. Dollery M.W. Walkden R.L. Crabb	The effect of protons, electrons and photons on some new types of high efficiency solar cells. XIIIth IEEE Photovoltaic Specialists Conference, 1978 Washington DC, USA
3	M.W. Walkden	Optimisation of solar cell shielding for geostationary missions. International colloquim 'Evaluation of space environment on materials'. Toulouse 1974

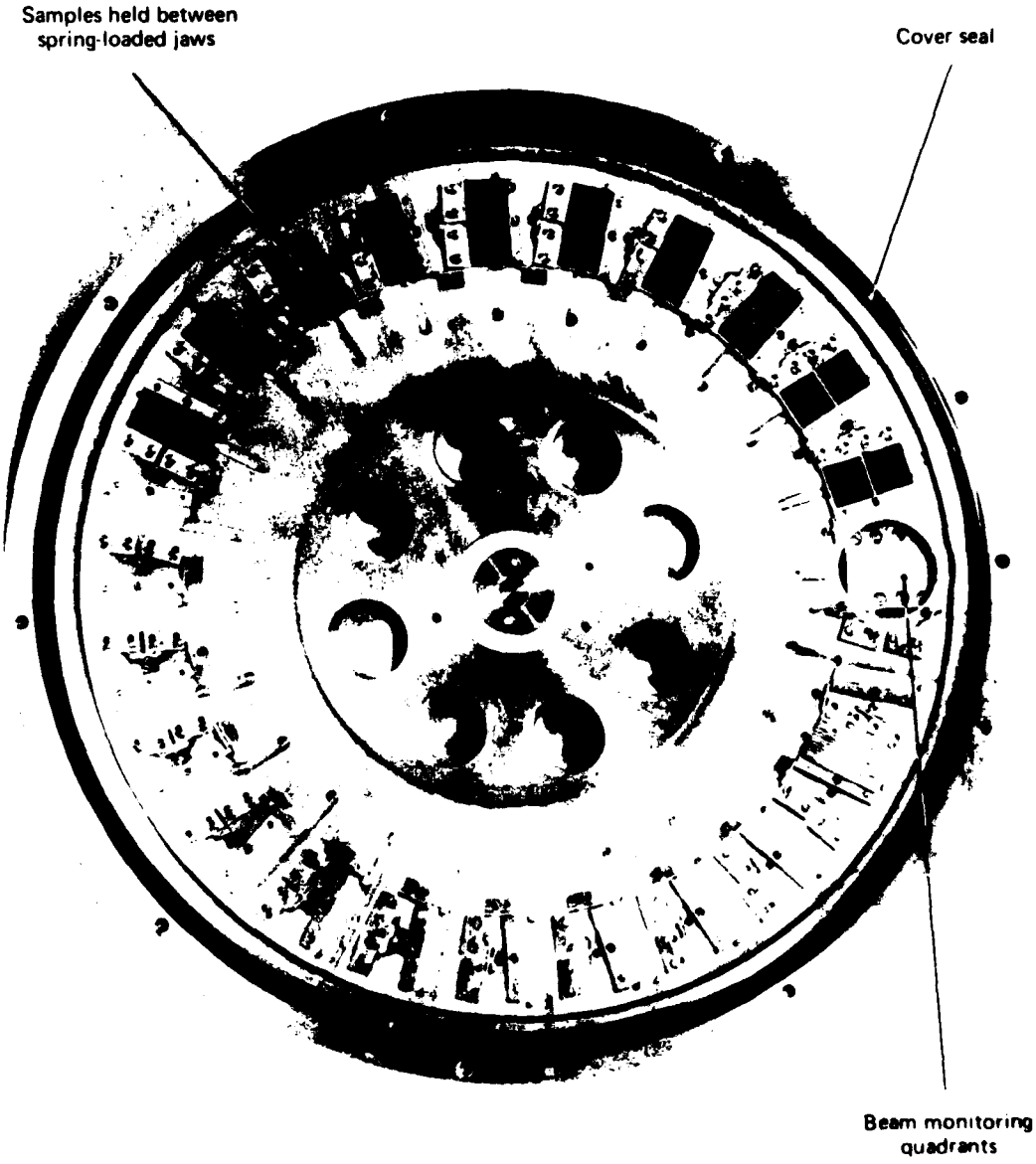

TR 79133 C15813

Fig 1a Sample holder for tandem van de Graaff and variable energy cyclotron

Fig 1b

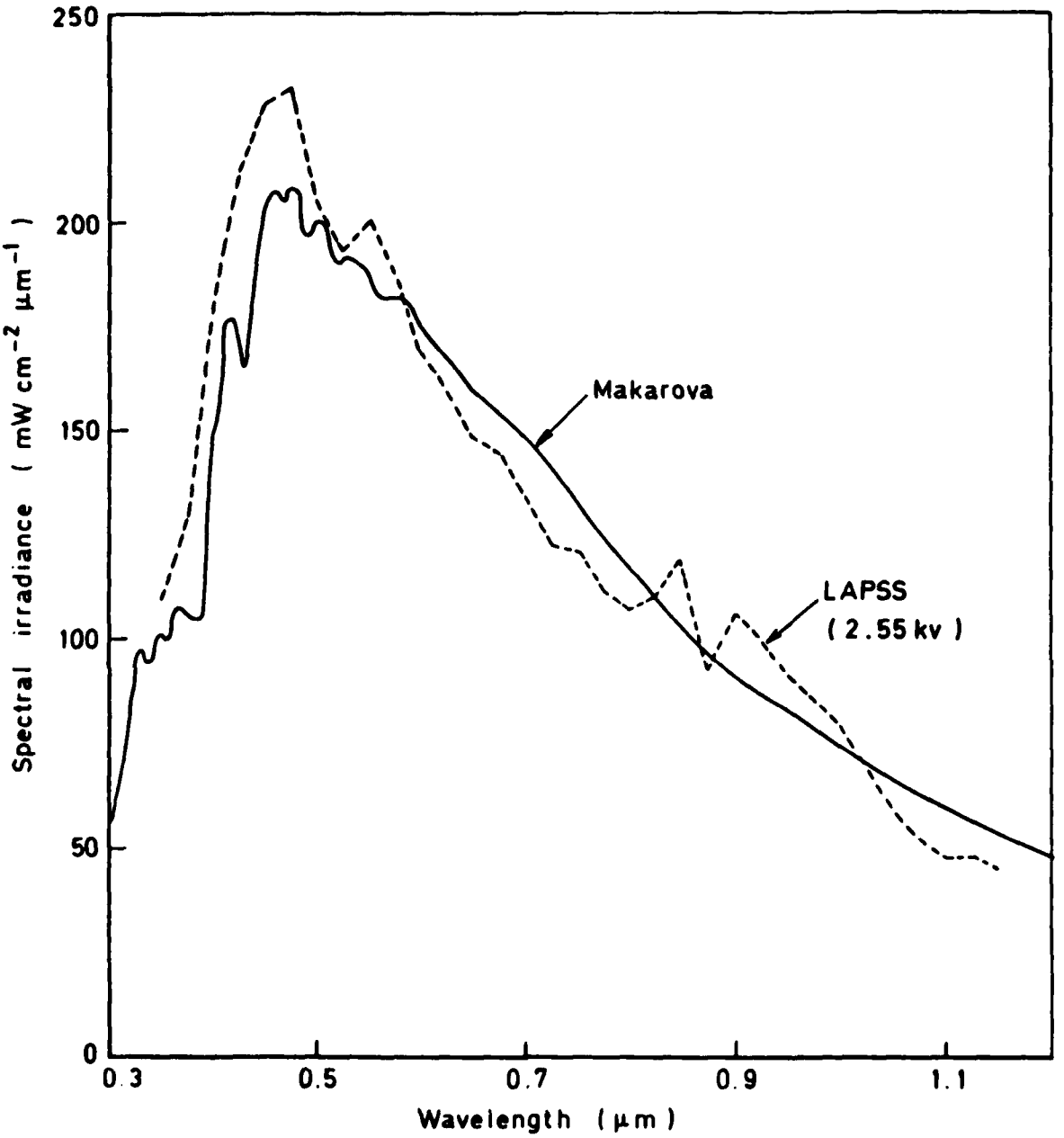

TR 79133

Fig 1b LAPSS spectral energy distribution

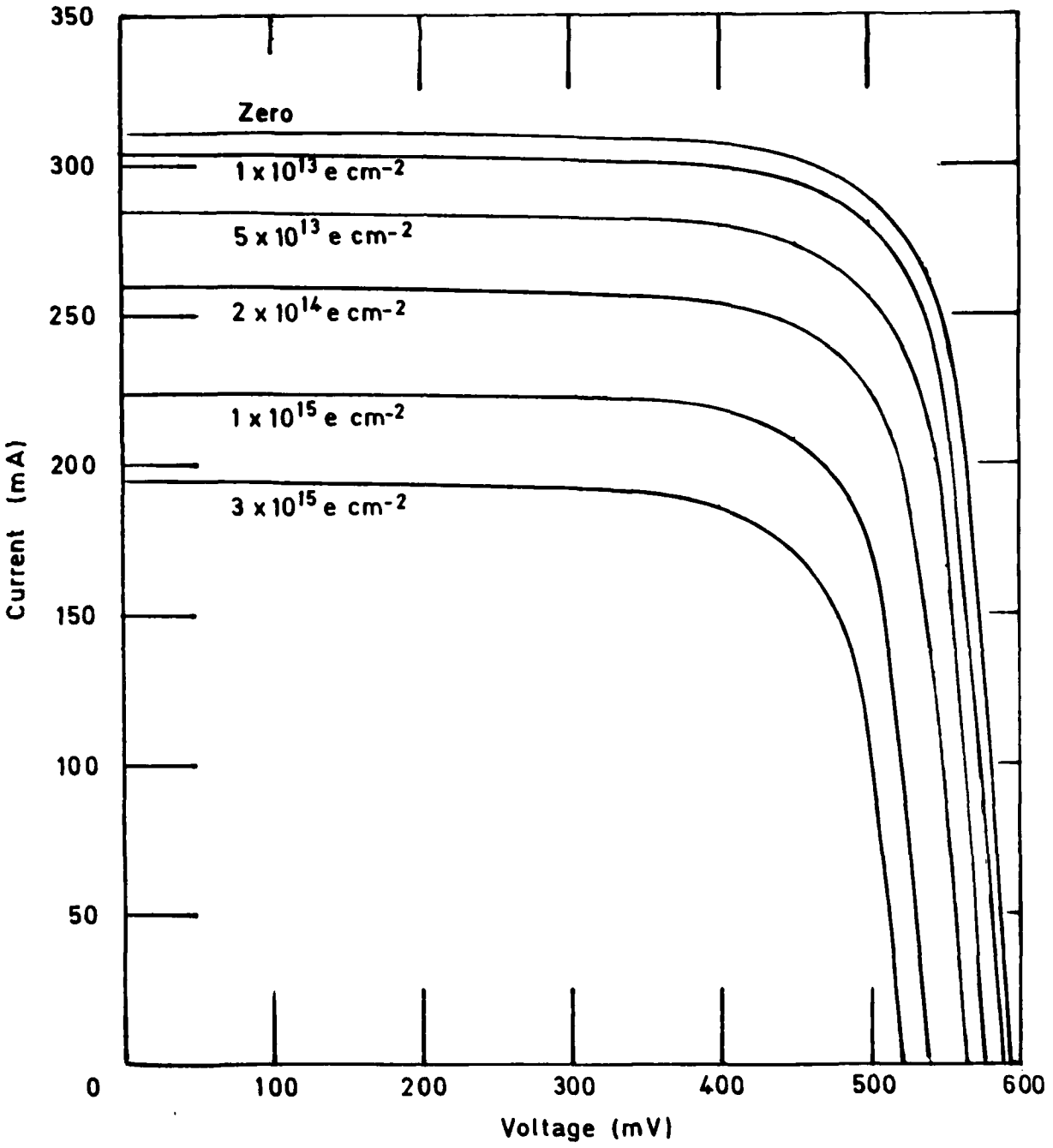

TR 79133

Fig 2 Effect of 1 MeV electron irradiation on type A cells (25°C)

Fig 3

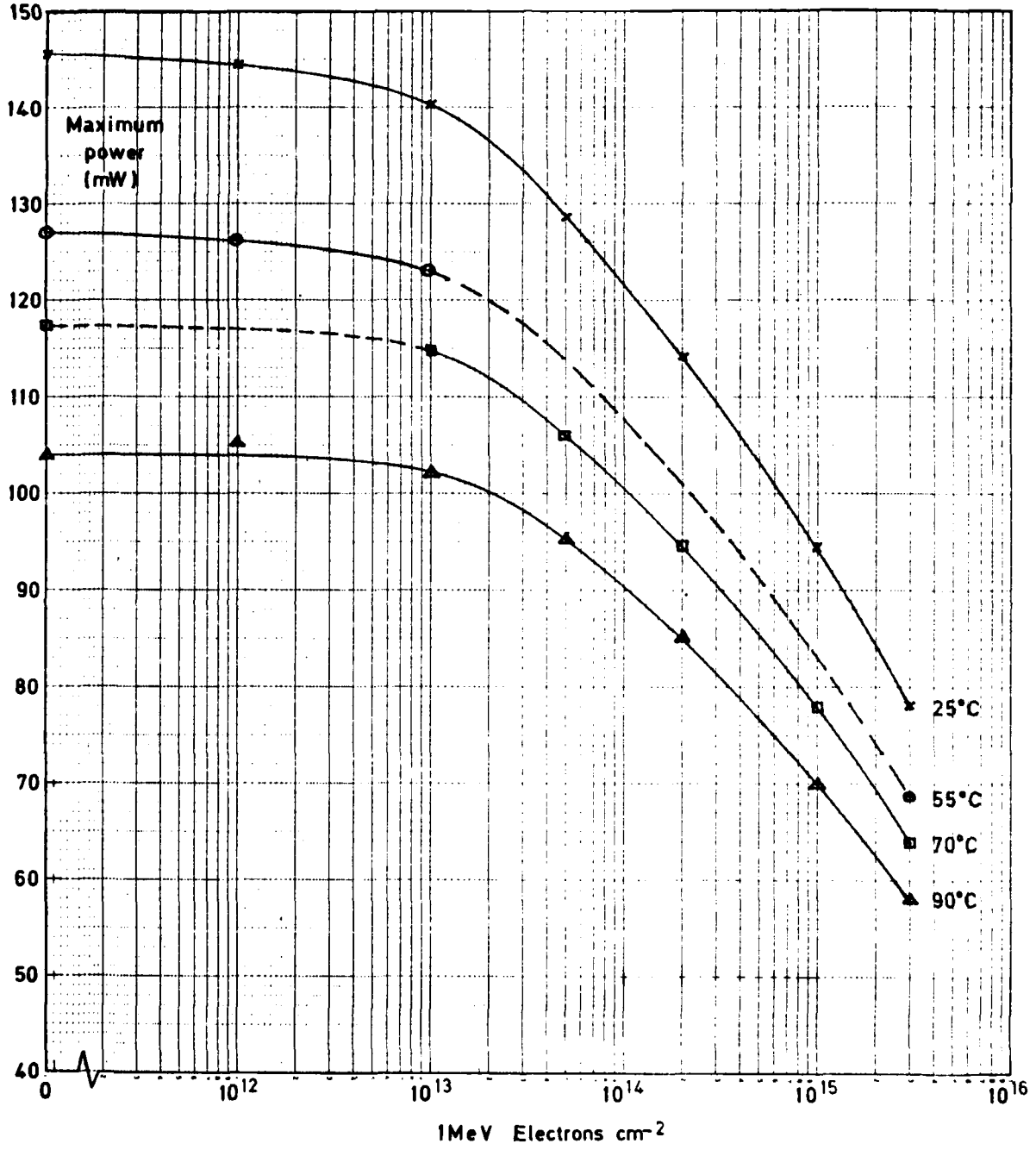

TR 79133

Fig 3 Type A, 25-90°C, 1 MeV electron irradiation

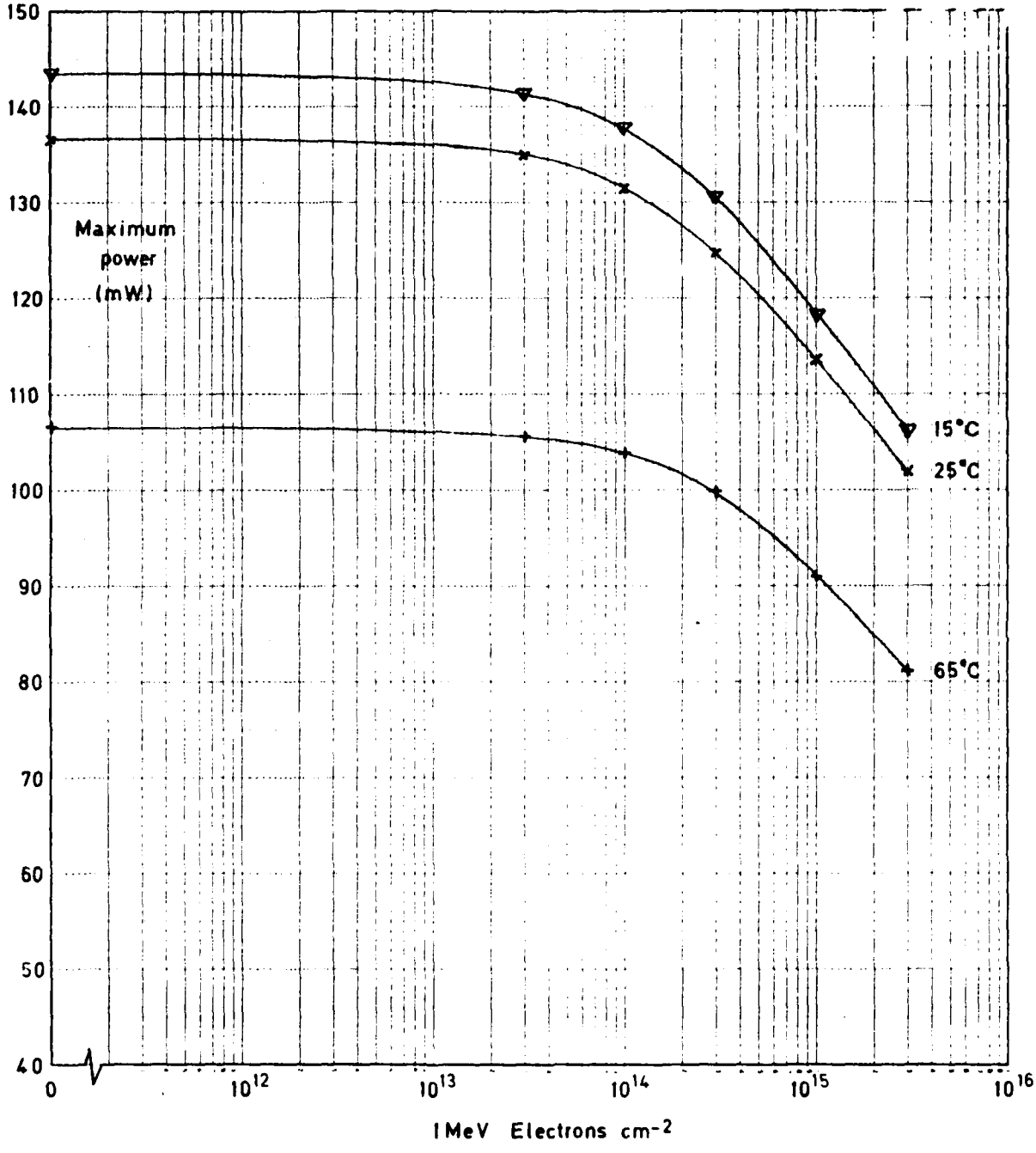

TR 79133

Fig 4 Tybe B, 15-65°C, 1 MeV electron irradiation

Fig 5

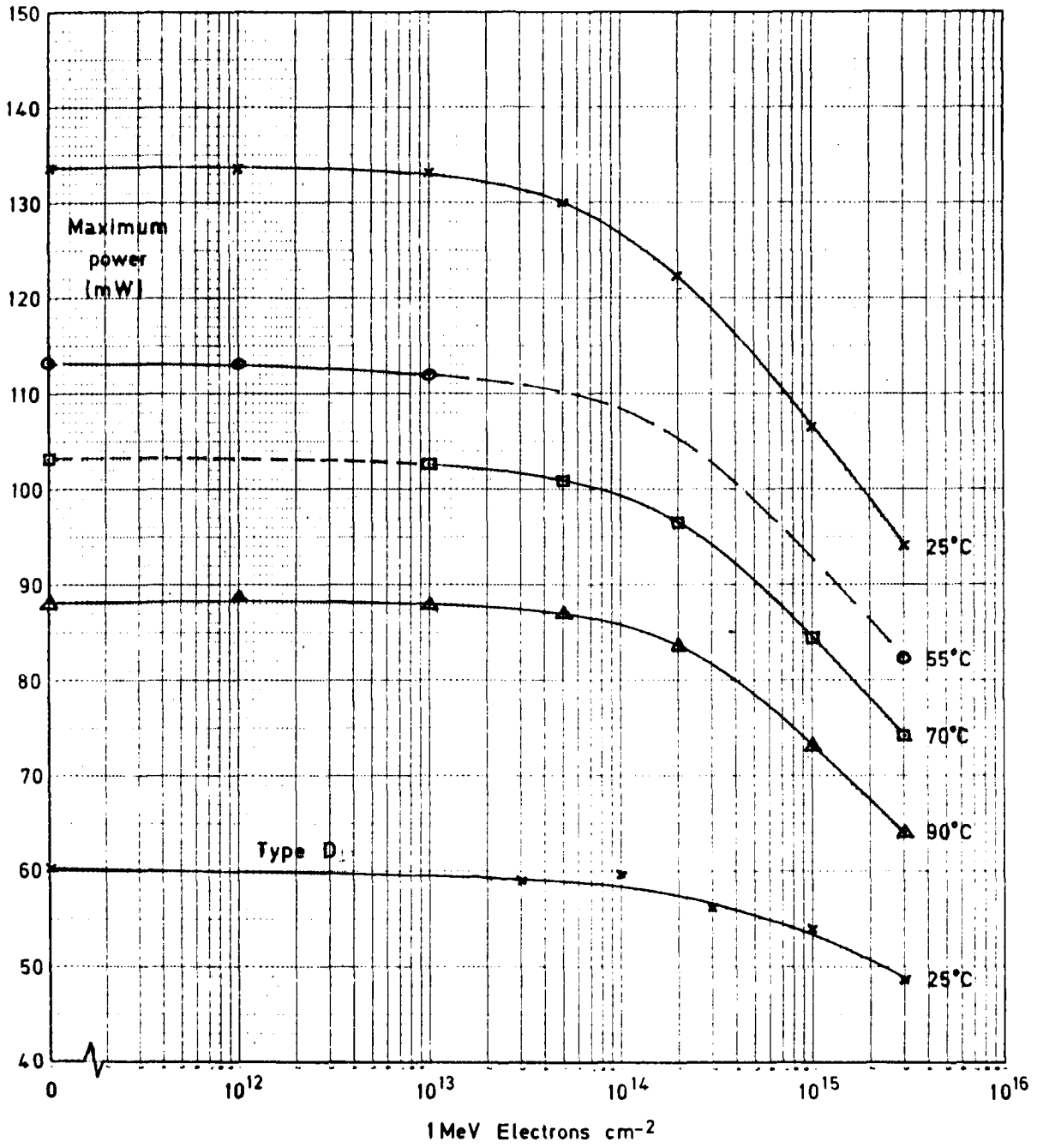

TR 79133

Fig 5 Type C, 25-90°C, 1 MeV electron irradiation; type D, 25°C, 1 MeV electron irradiation

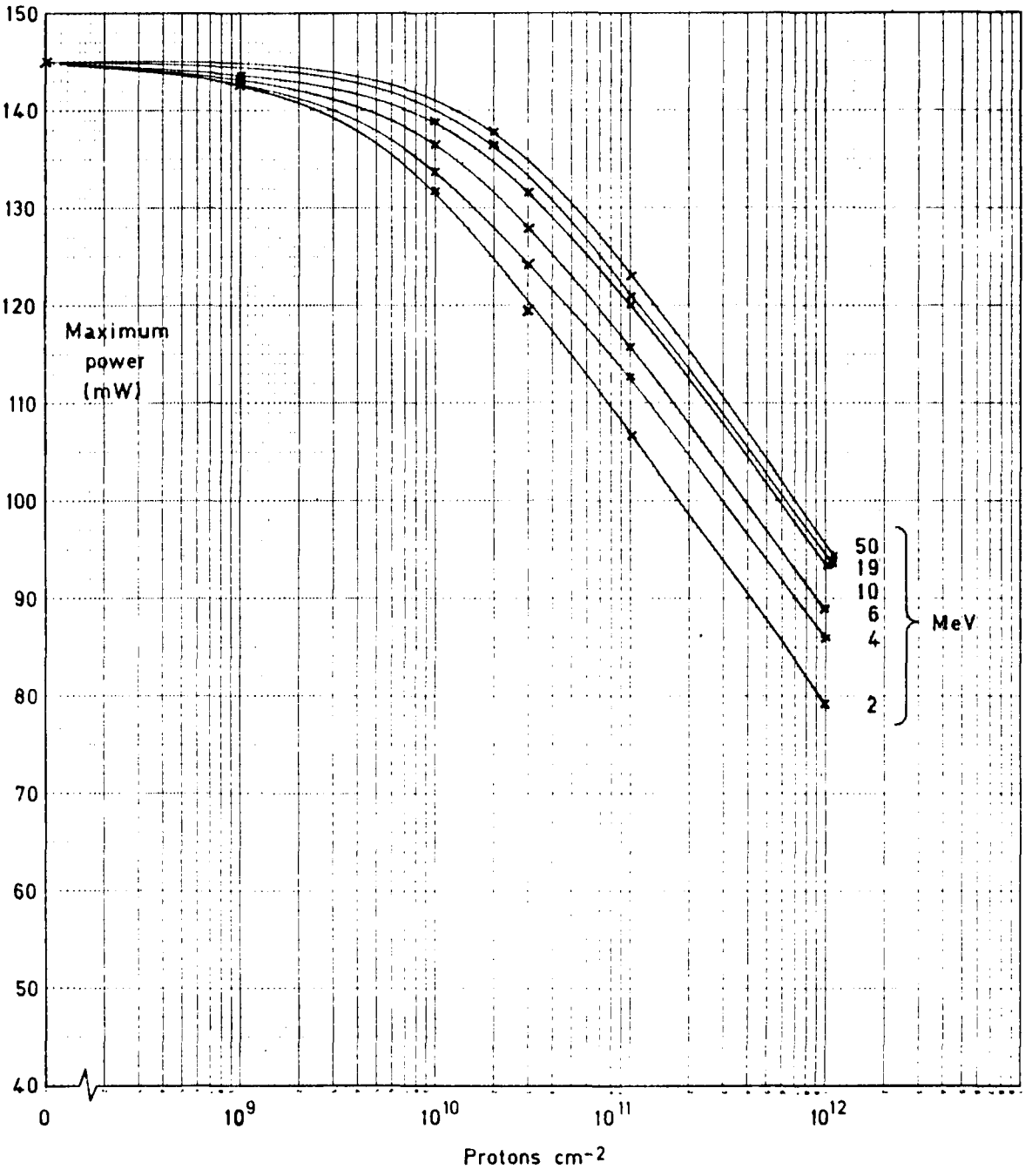

TR 79133

Fig 6 Type A, 25°C, 2-50 MeV proton irradiation

Fig 7

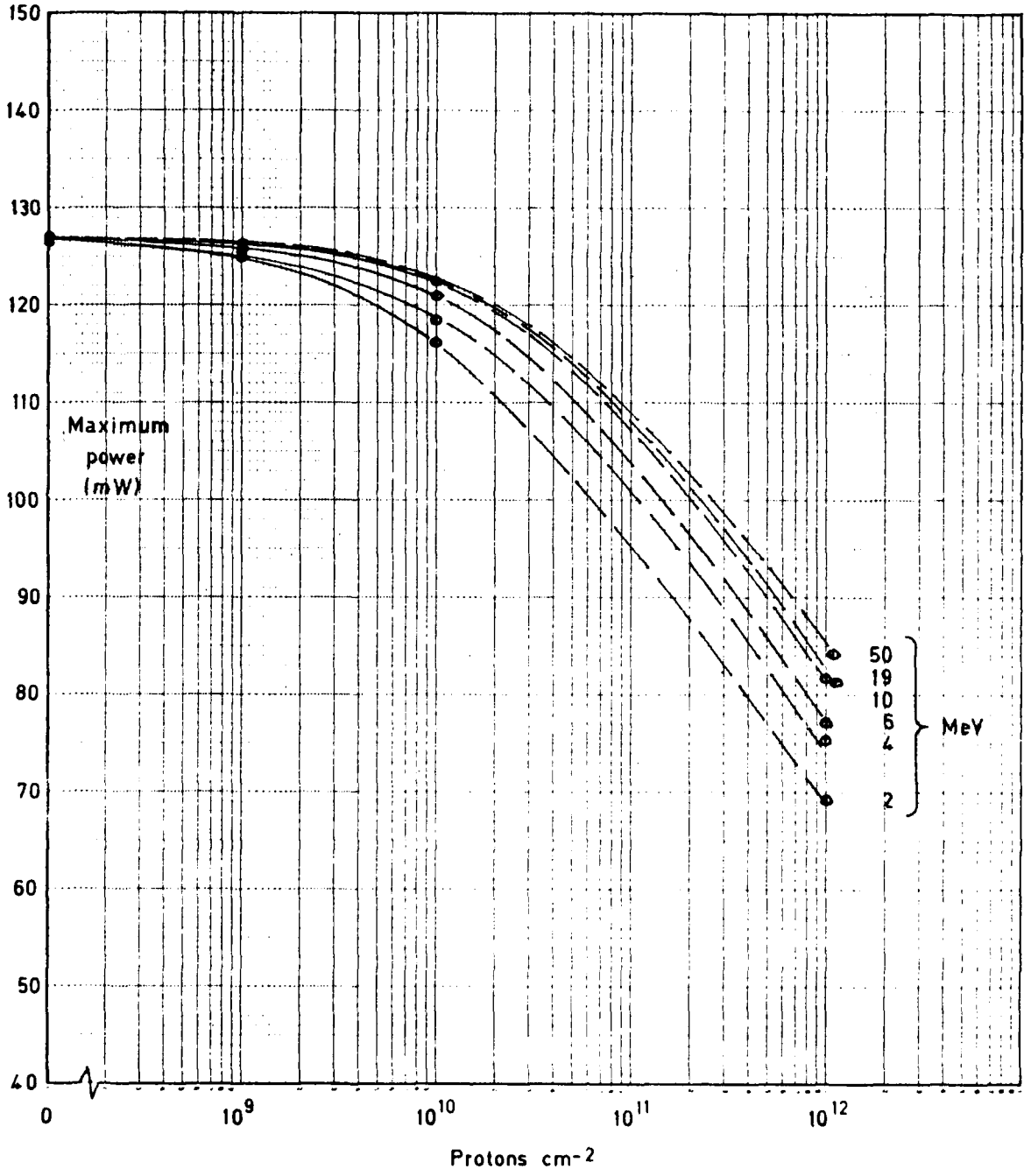

TR 79133

Fig 7 Type A, 55°C, 2-50 MeV proton irradiation

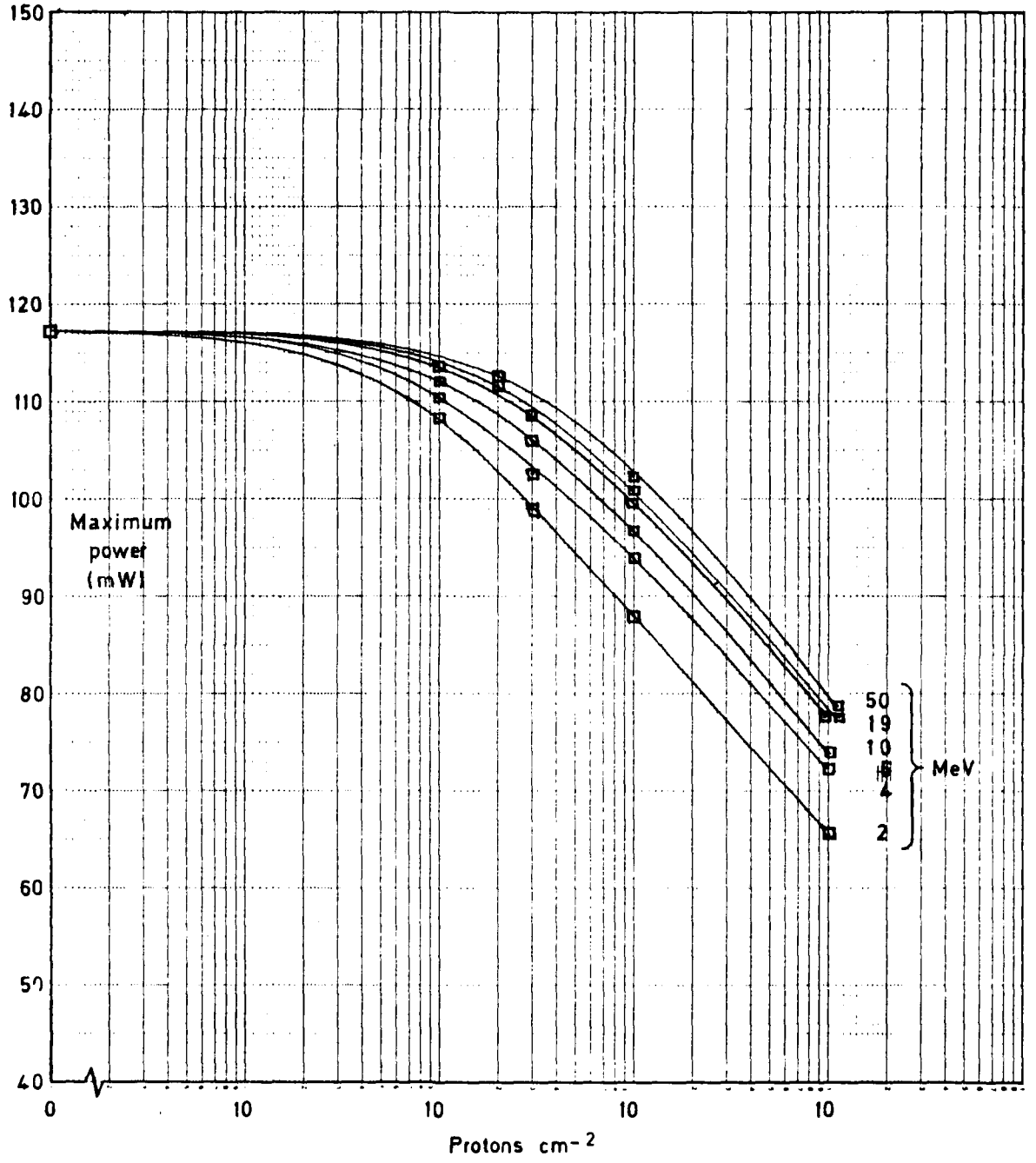

TR 79133

Fig 8 Type A, 70°C, 2-50 MeV proton irradiation

Fig 9

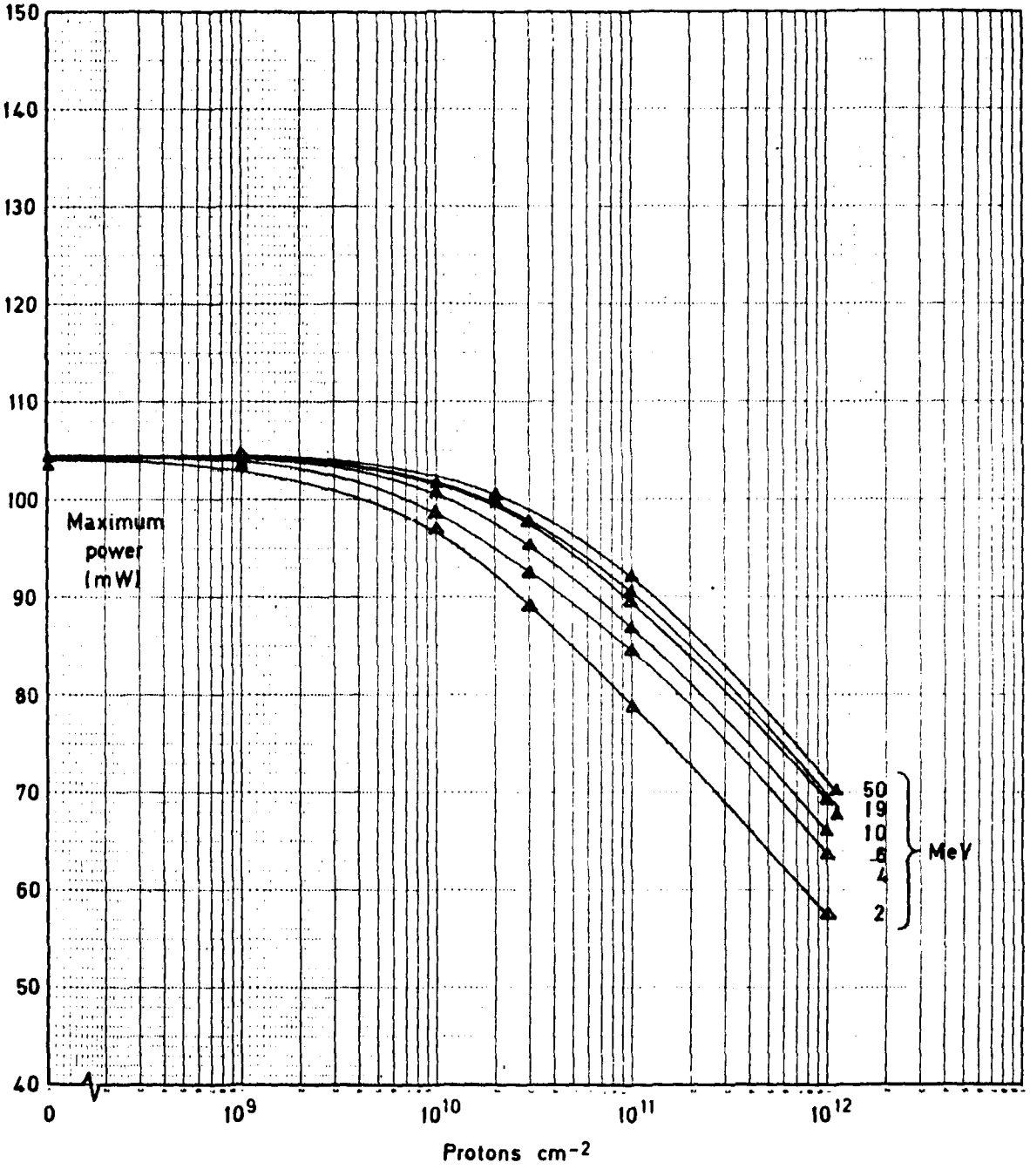

TR 79133

Fig 9 Type A, 90°C, 2-50 MeV proton irradiation

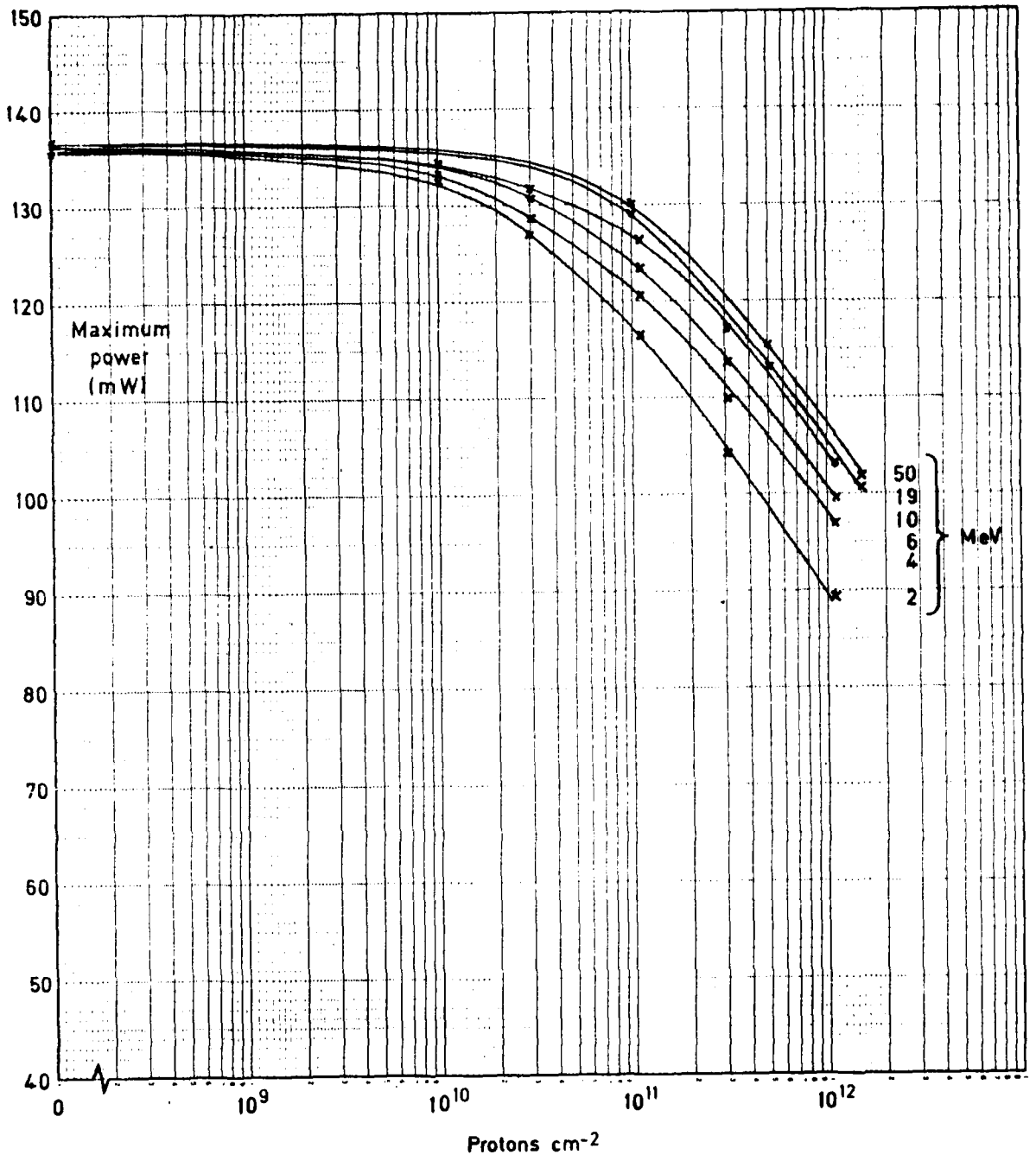

TR 79133

Fig 10 Type B, 25°C, 2-50 MeV proton irradiation

Fig 11

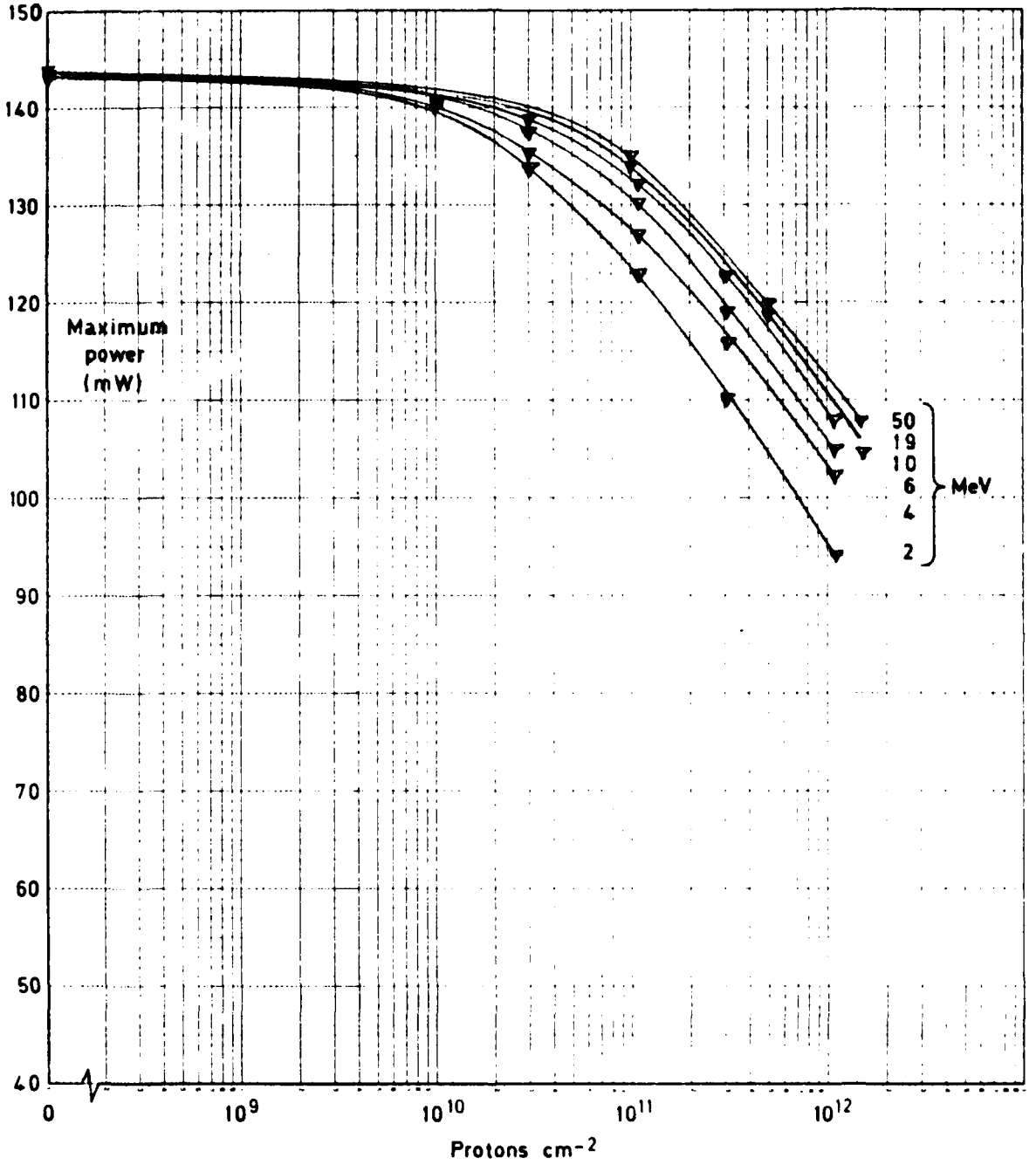

TR 79133

Fig 11 Type B, 15°C, 2-50 MeV proton irradiation

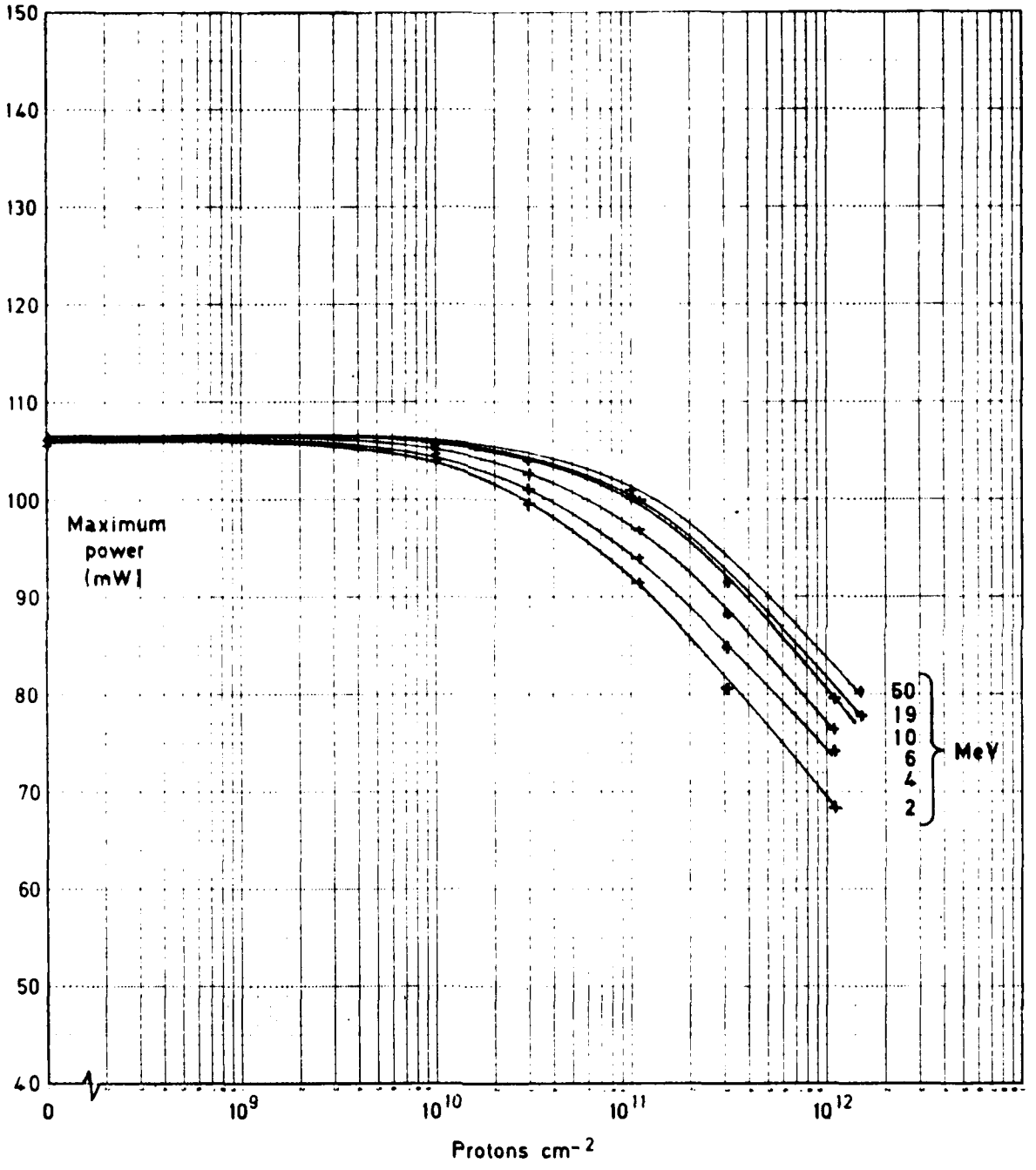

TR 79133

Fig 12 Type B, 65°C, 2-50 MeV proton irradiation

Fig 13

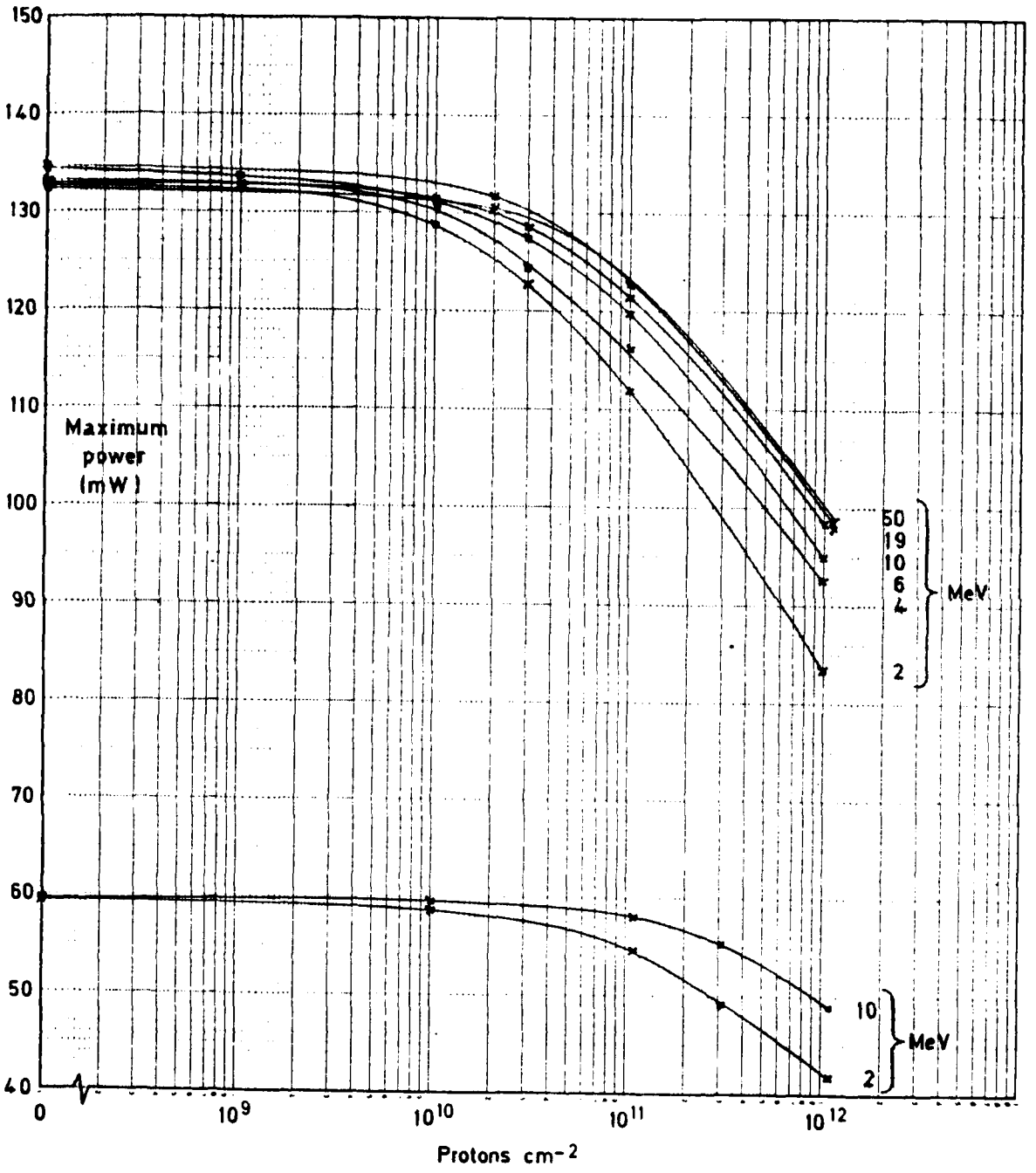

TR 79133

Fig 13 Type C, 25°C, 2-50 MeV proton irradiation; type D, 25°C, 2 and 10 MeV proton irradiation

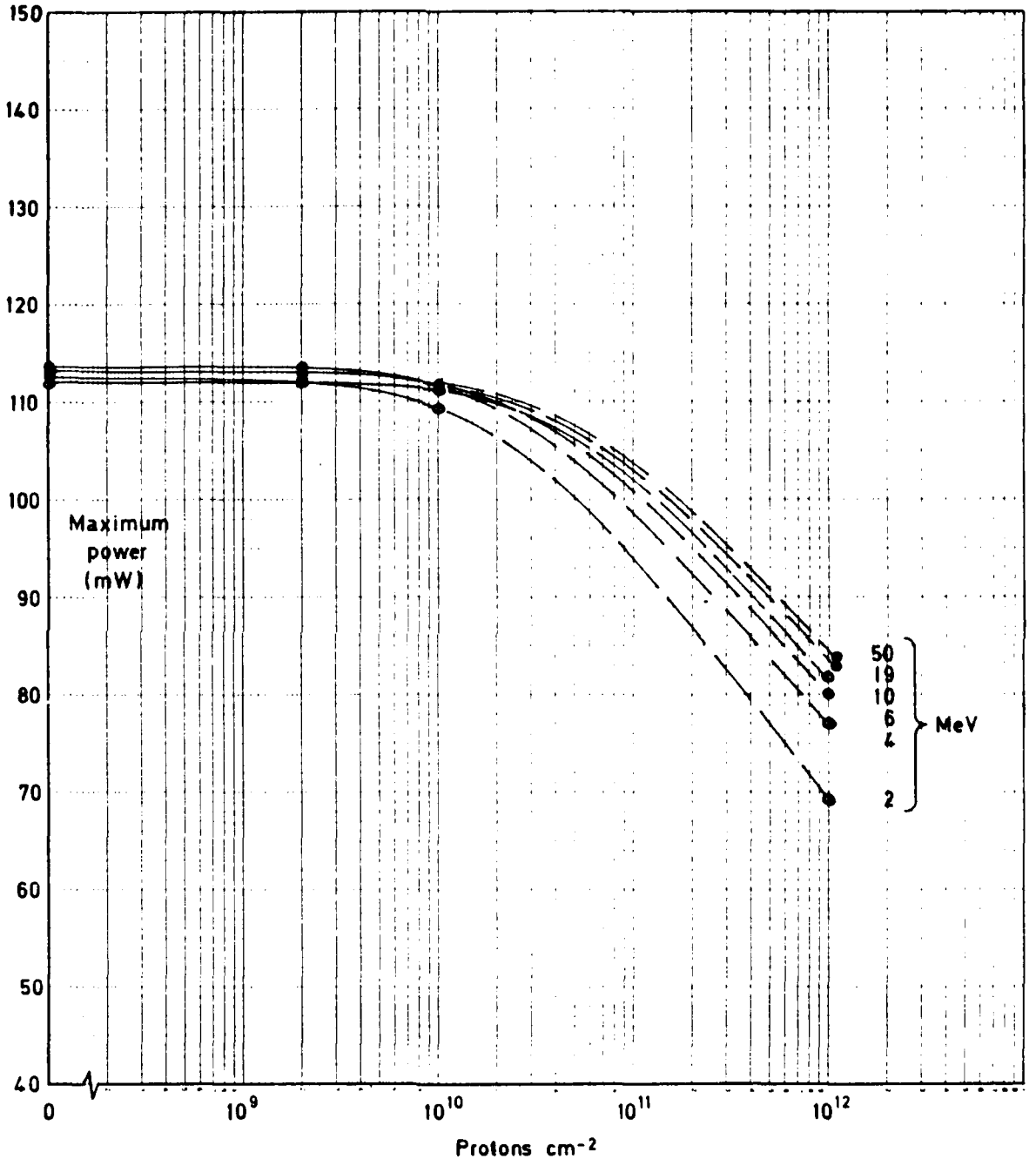

TR 79133

Fig 14 Type C, 55°C, 2-50 MeV proton irradiation

Fig 15

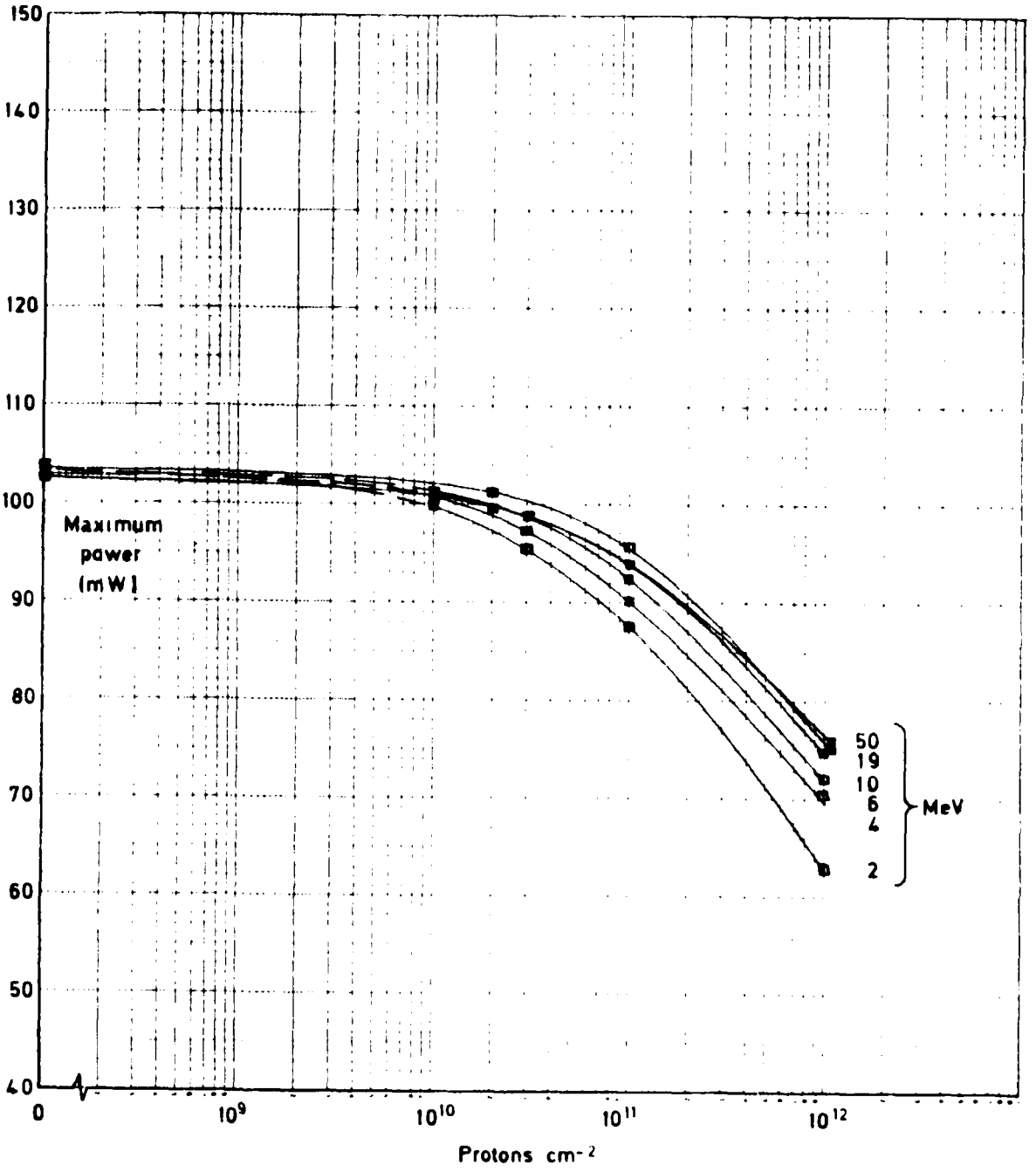

TR 79133

Fig 15 Type C, 70°C, 2-50 MeV proton irradiation

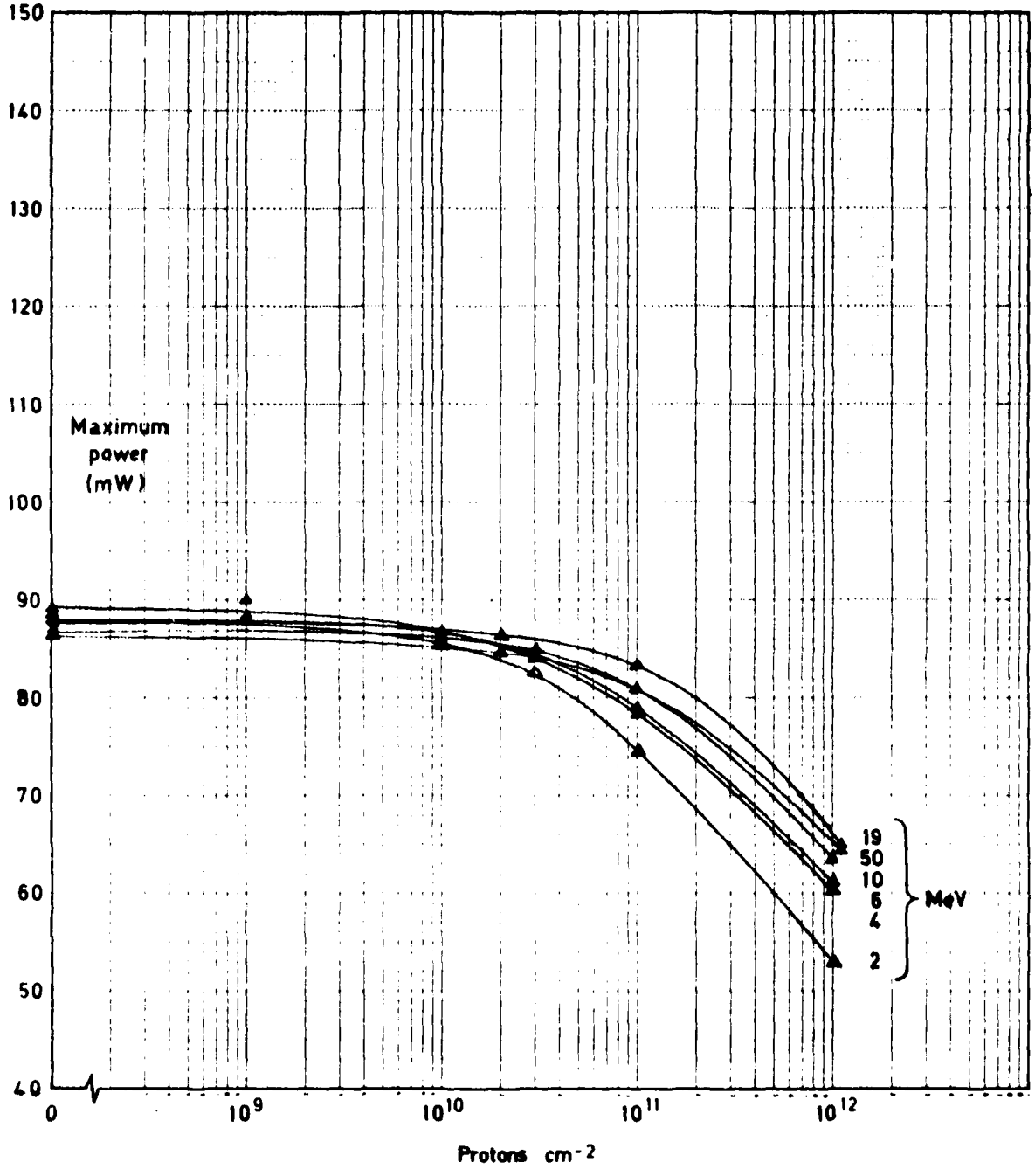

TR 79133

Fig 16 Type C, 90°C, 2-50 MeV proton irradiation

Fig 17

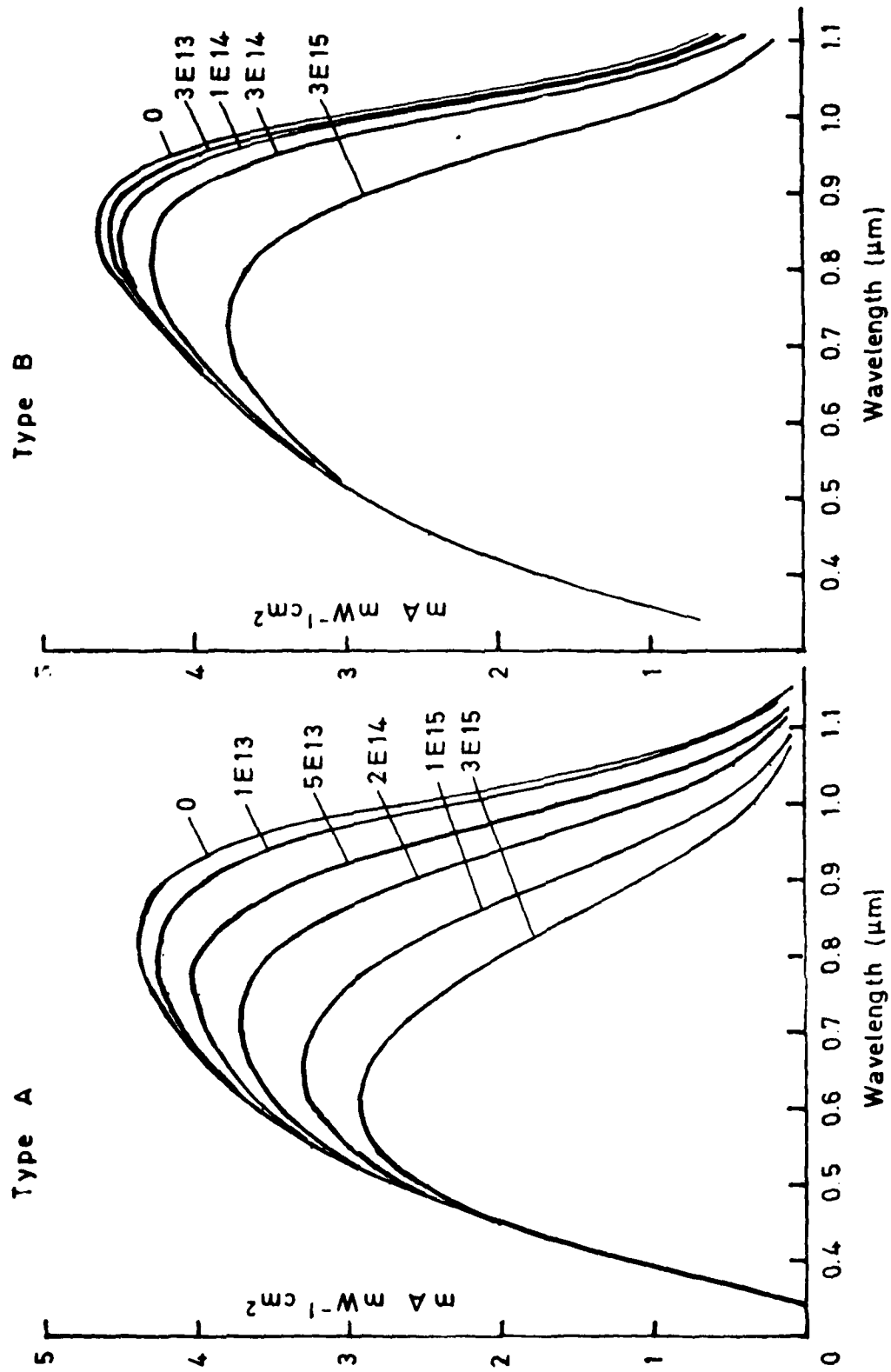

Fig 17 Effect of 1 MeV electron irradiation on spectral response

TR 79133

TR 79133

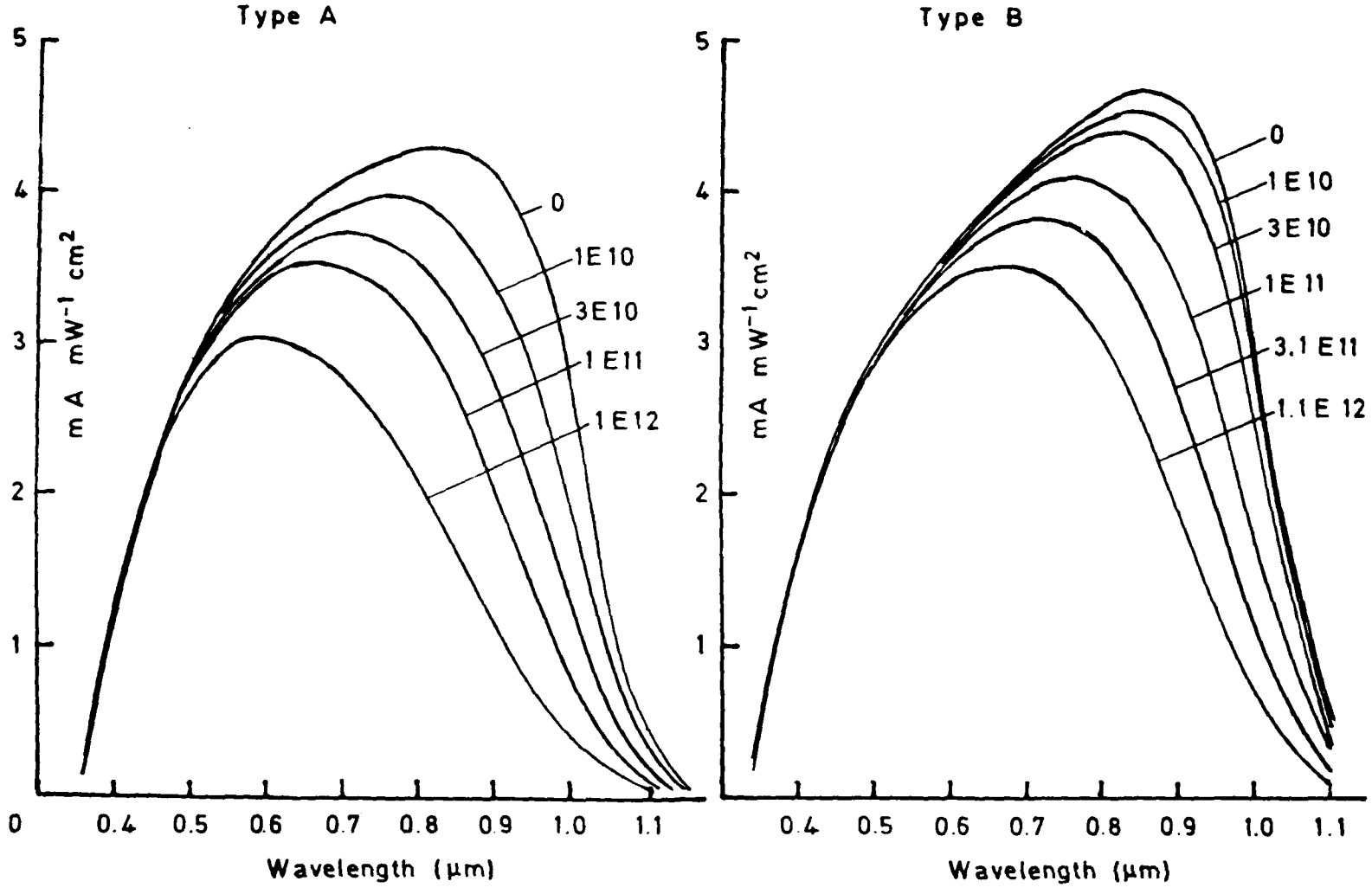

Fig 18 Effect of 2 MeV proton irradiation on spectral response

Fig 18

Fig 19

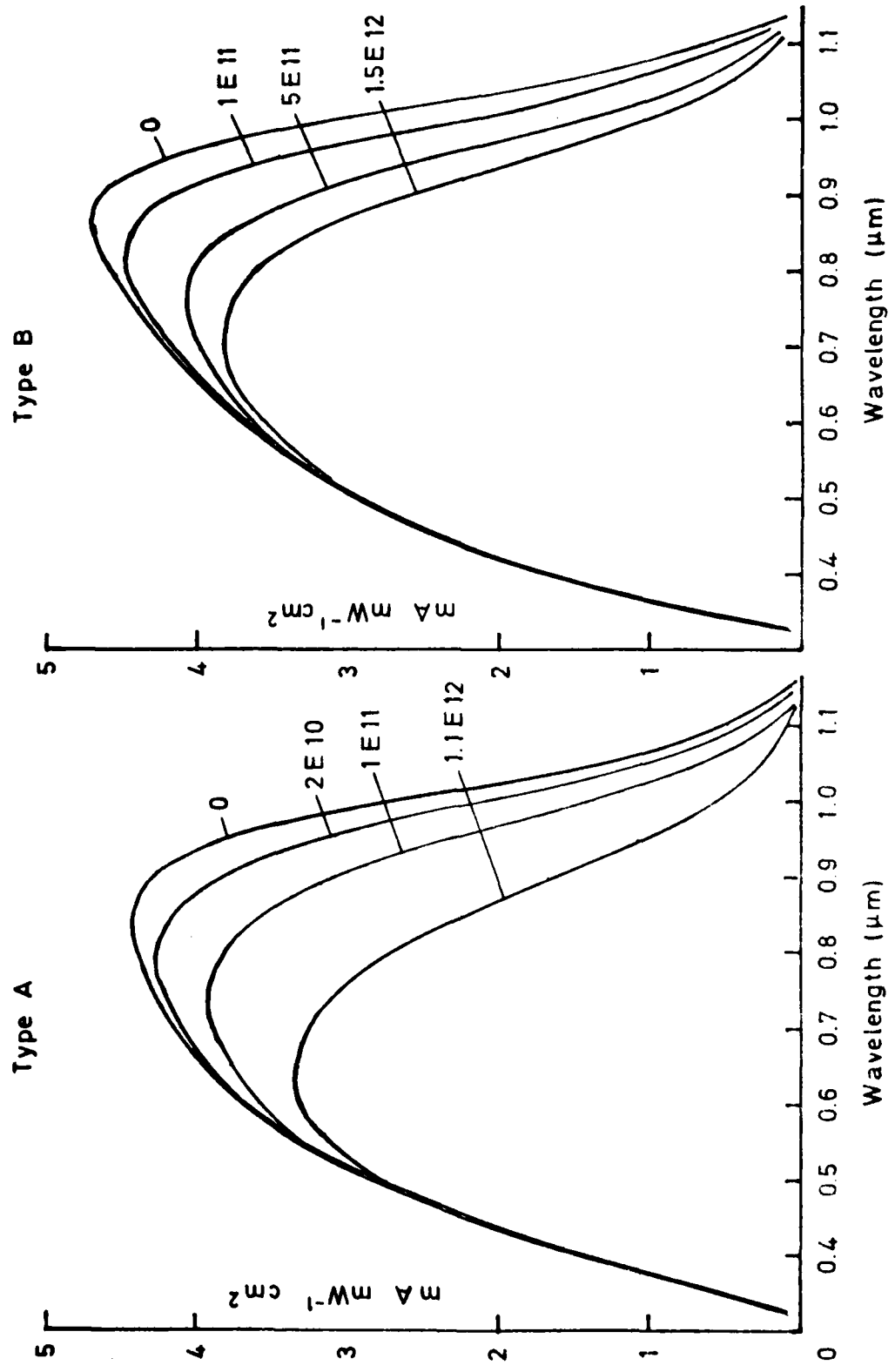

Fig 19 Effect of 50 MeV proton irradiation on spectral response

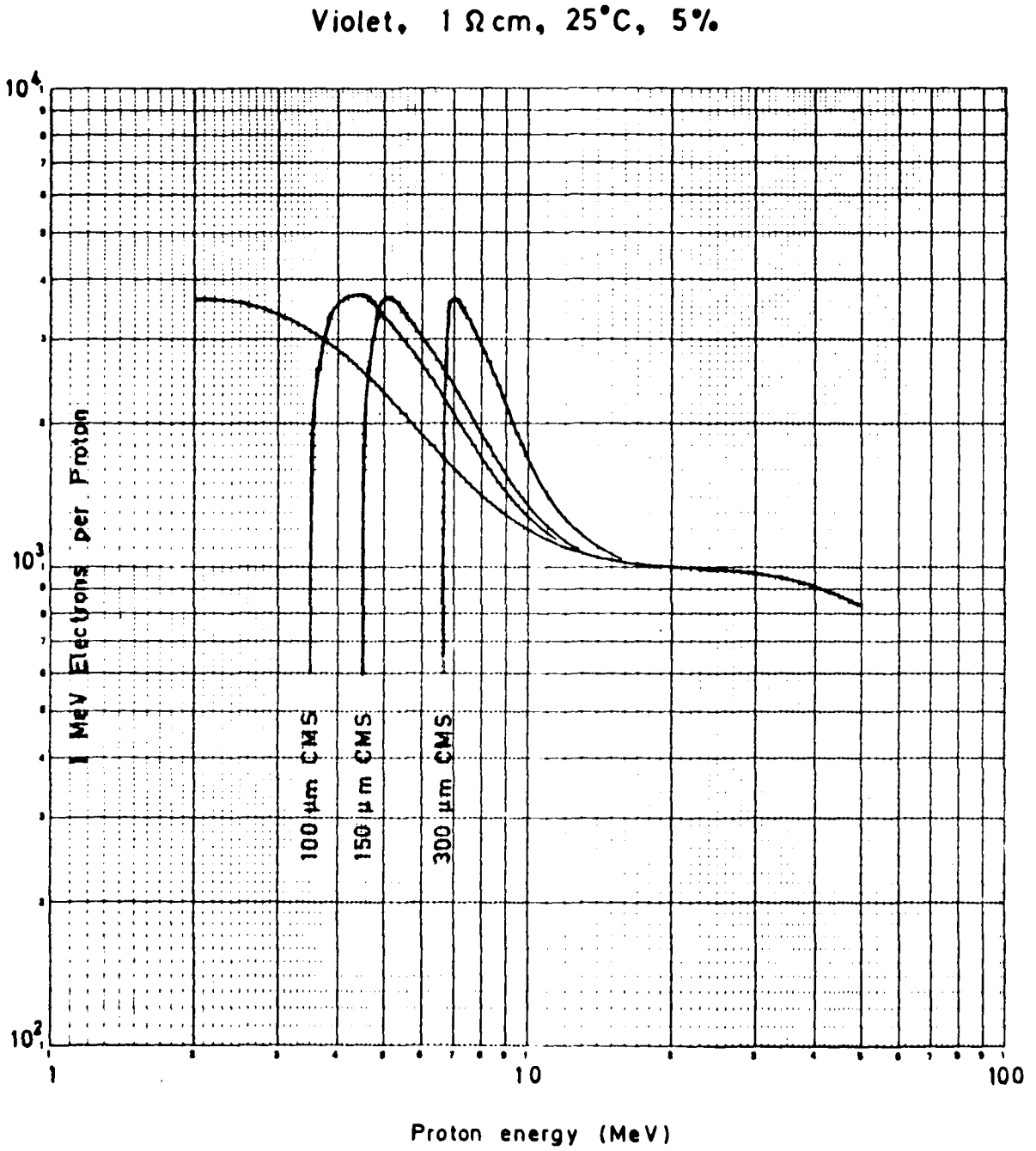

Fig 20 Proton damage ratio, type A

Fig 21

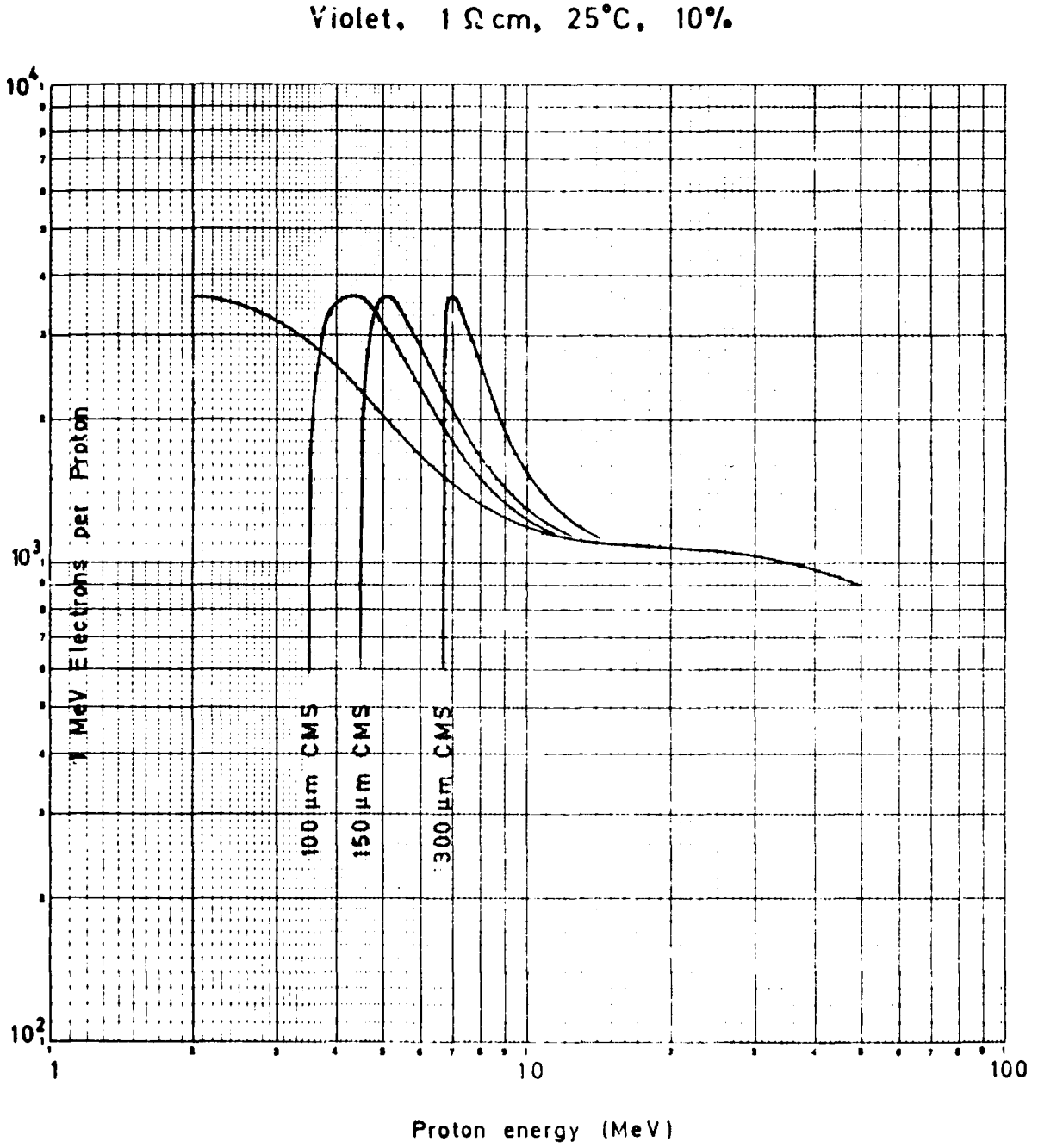

Fig 21 Proton damage ratio, type A

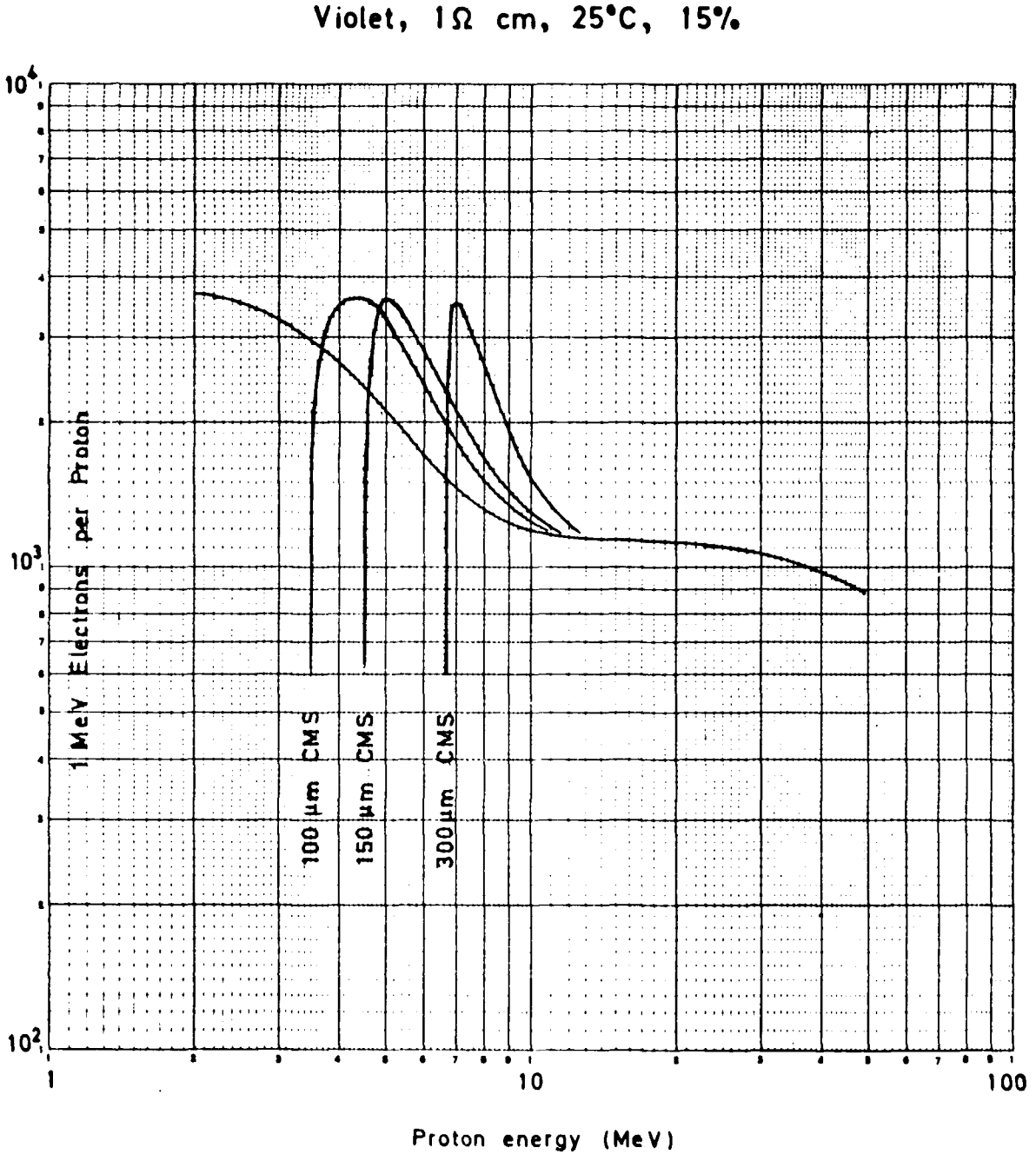

TR 79133

Fig 22 Proton damage ratio, type A

Fig 23

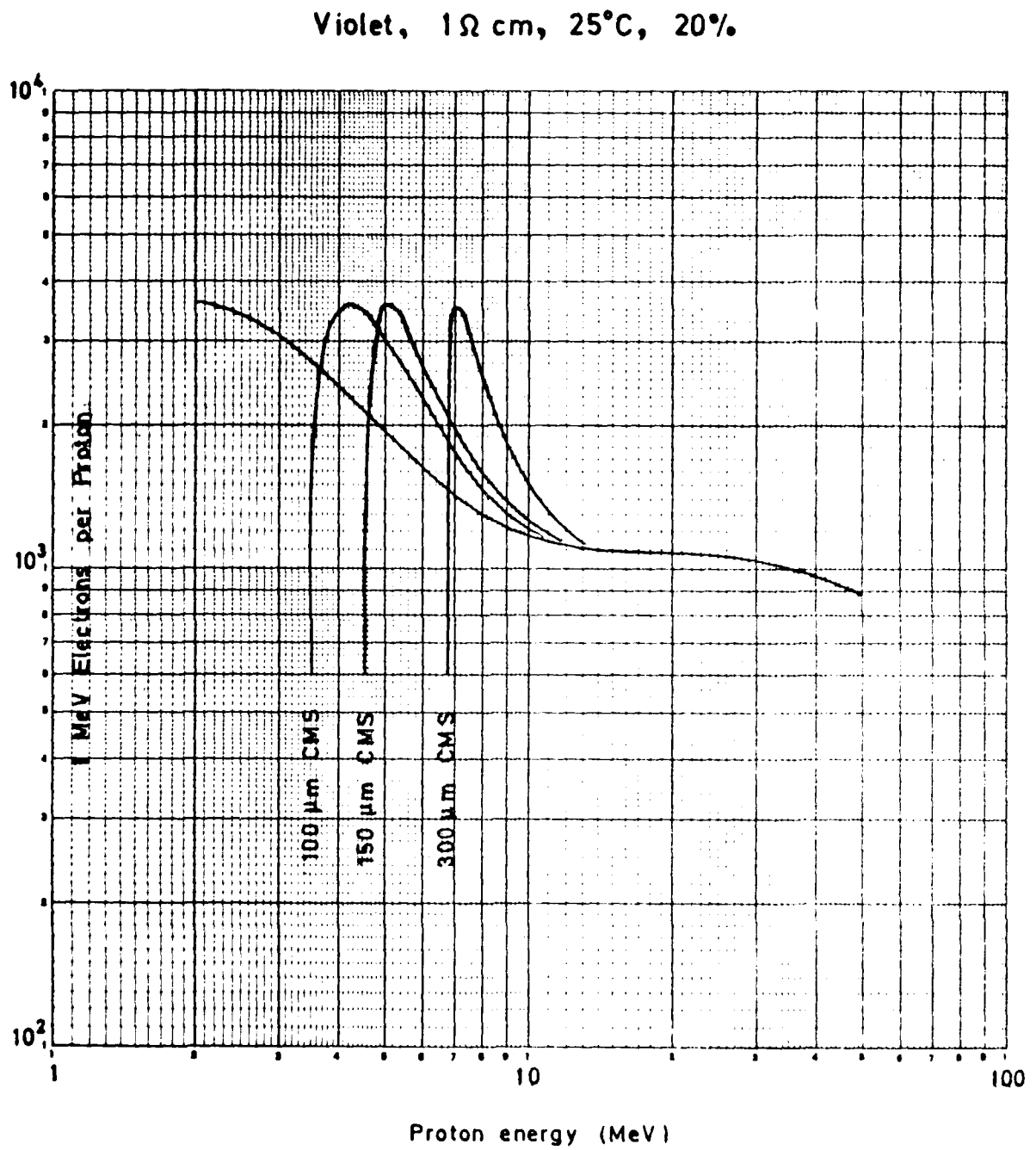

TR 79133

Fig 23 Proton damage ratio, type A

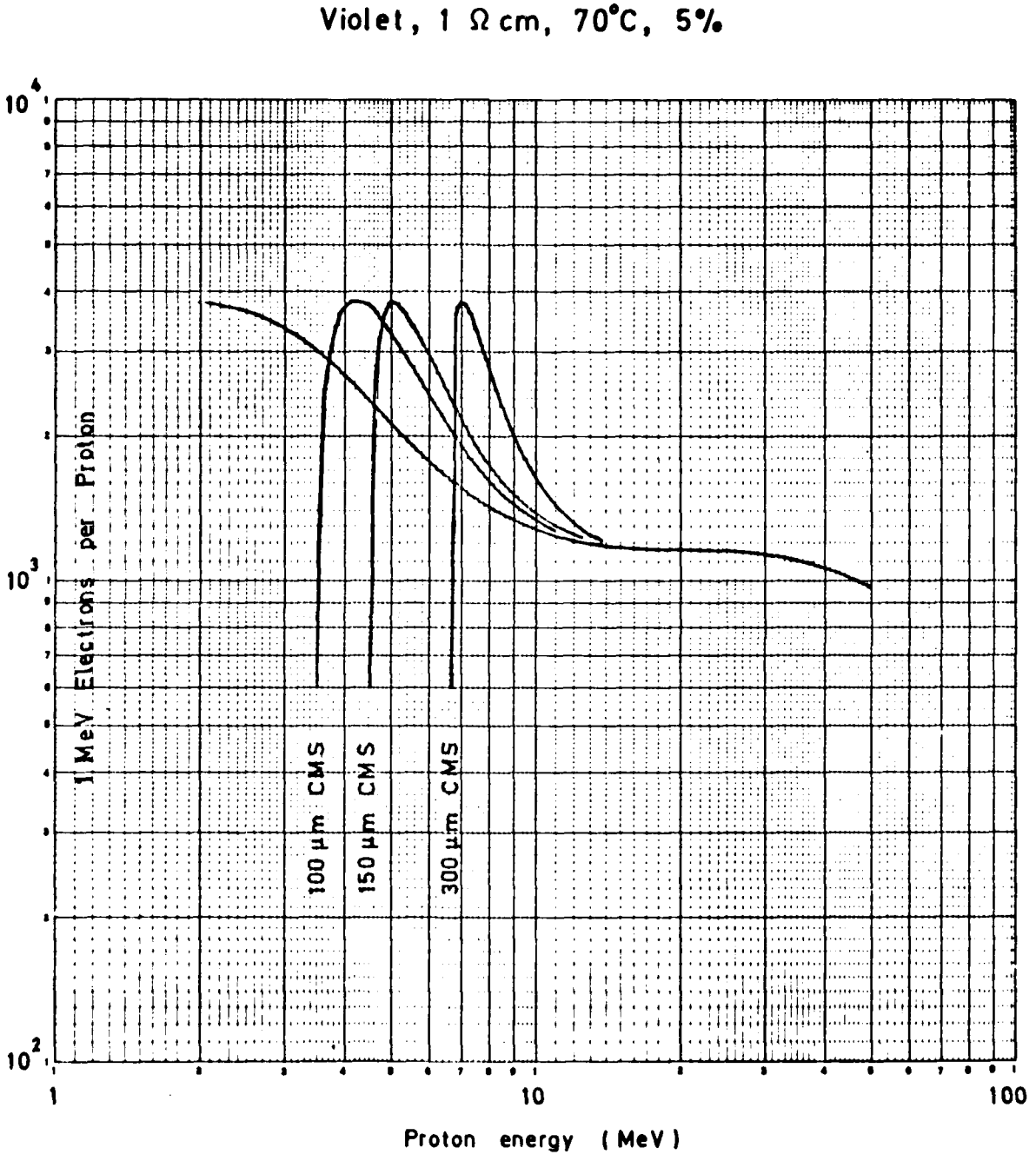

Fig 24 Proton damage ratio, type A

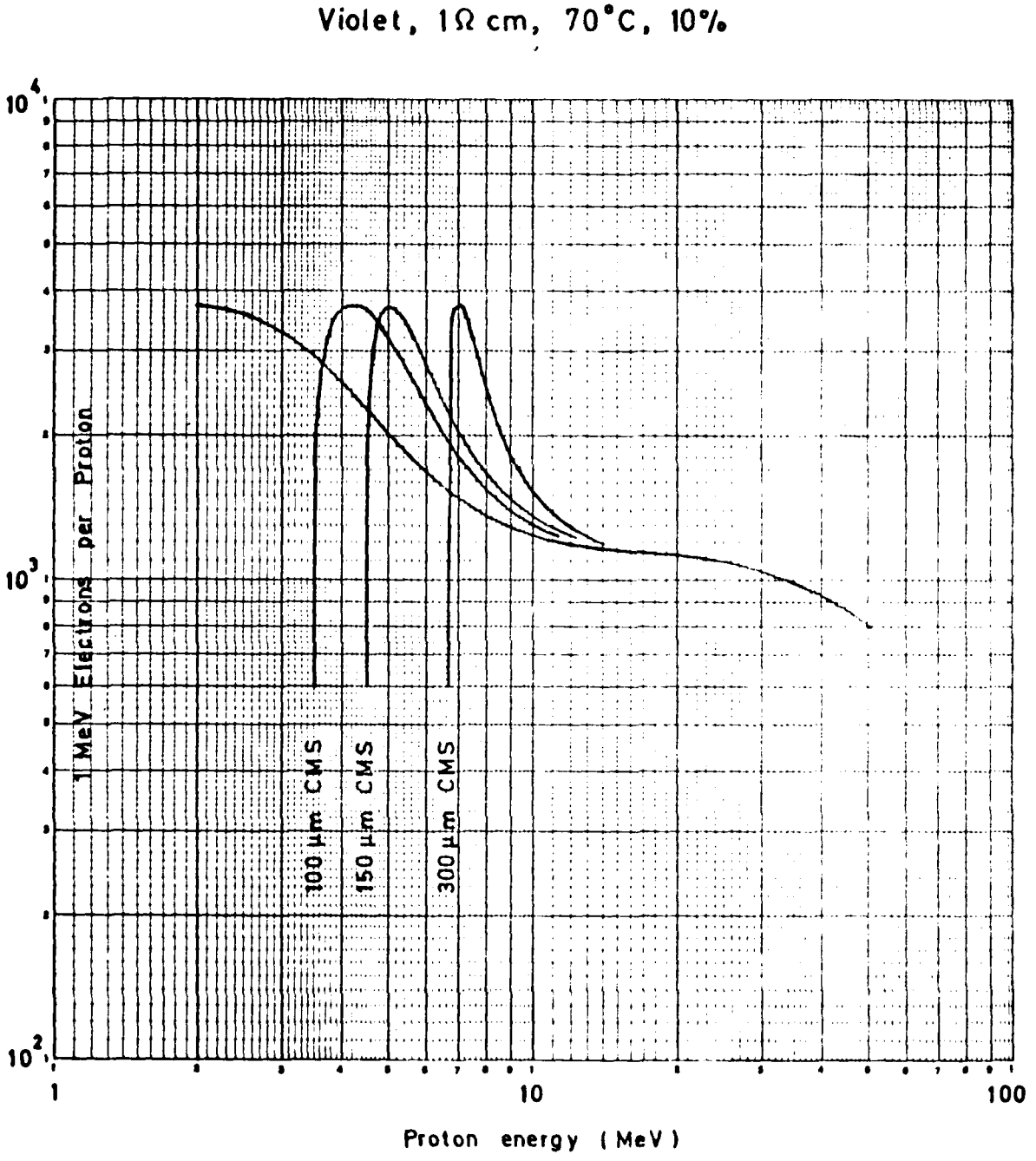

TR 79133

Fig 25 Proton damage ratio, type A

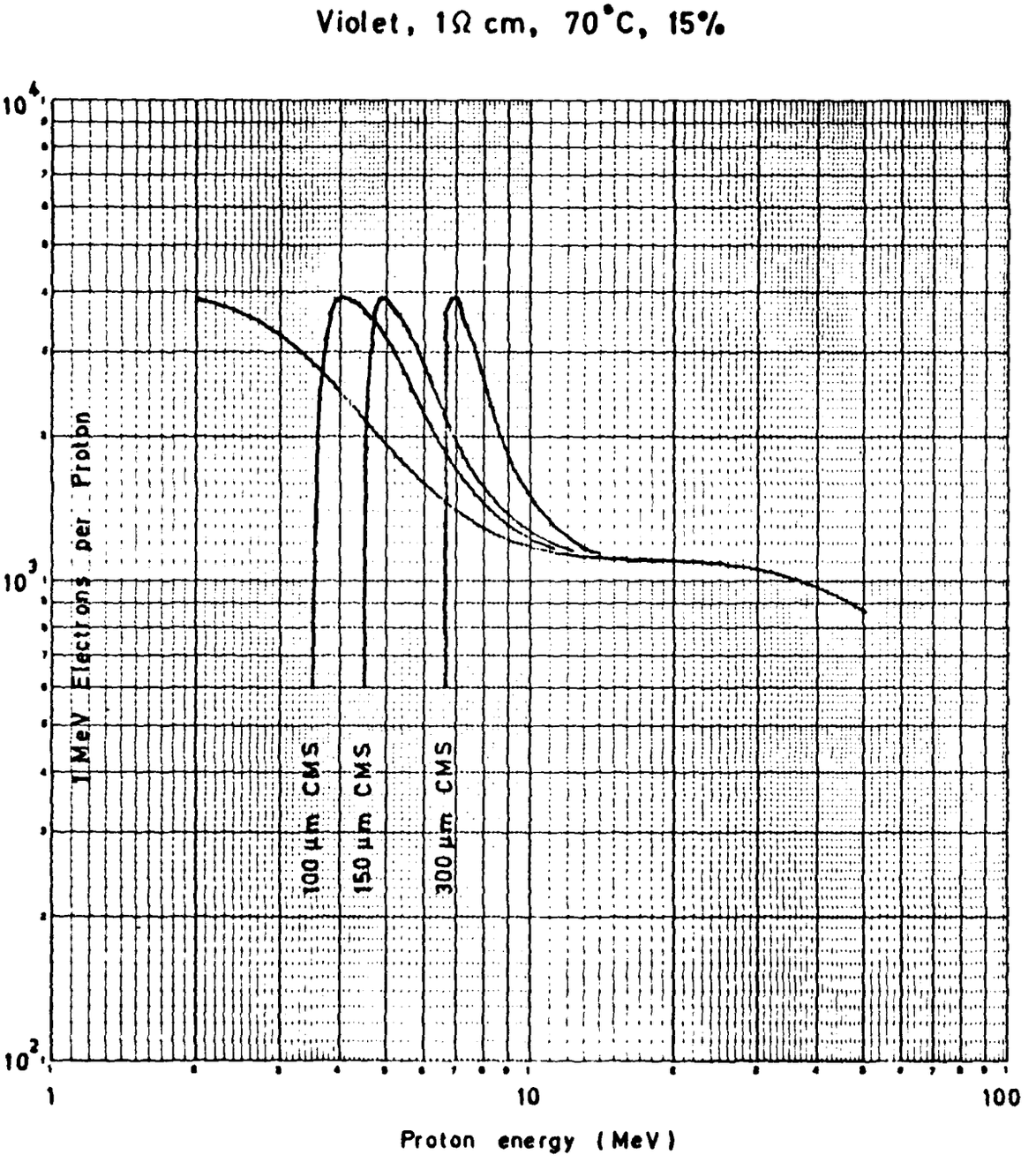

TR 79133

Fig 26 Proton damage ratio, type A

Fig 27

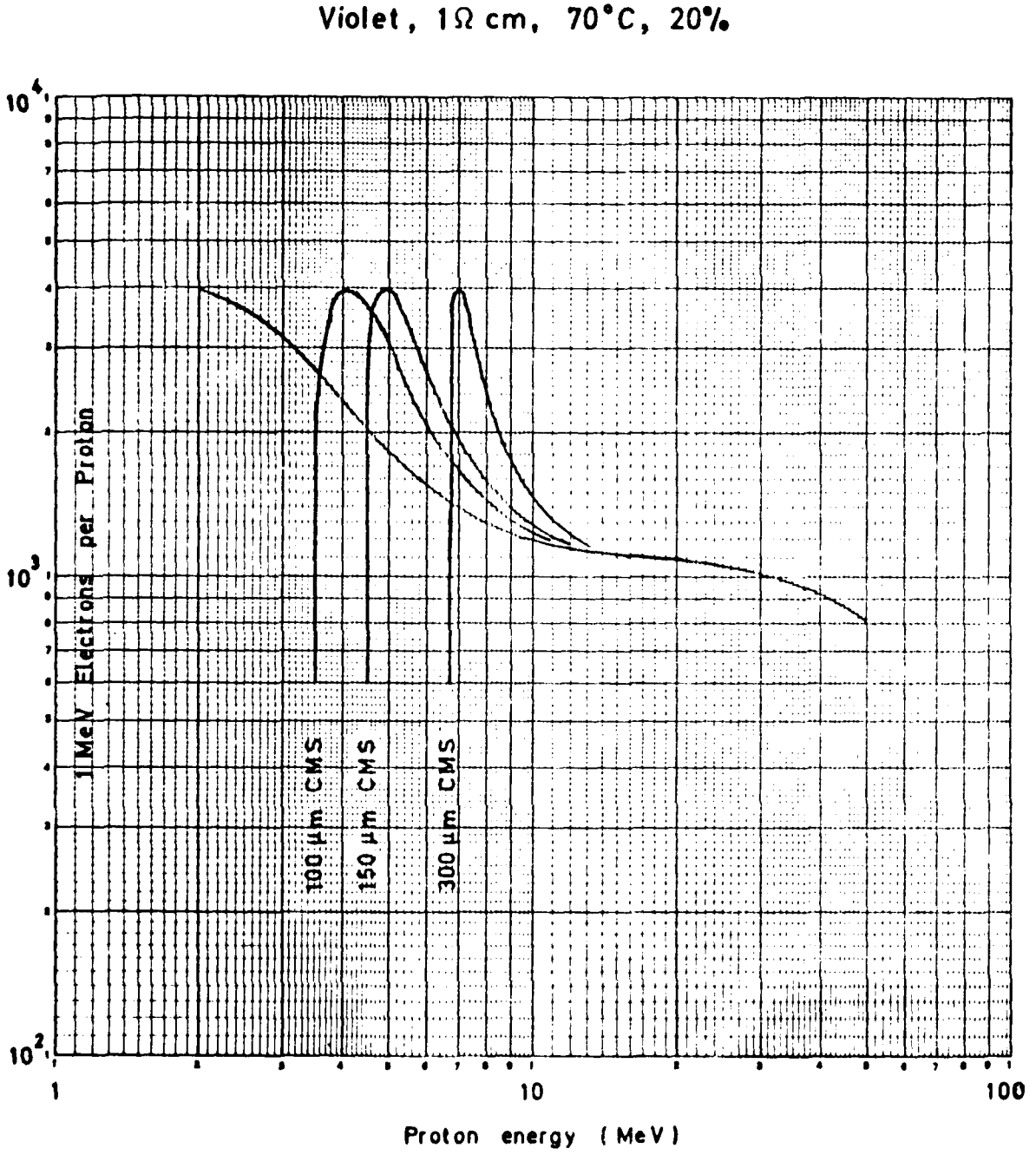

TR 79133

Fig 27 Proton damage ratio, type A

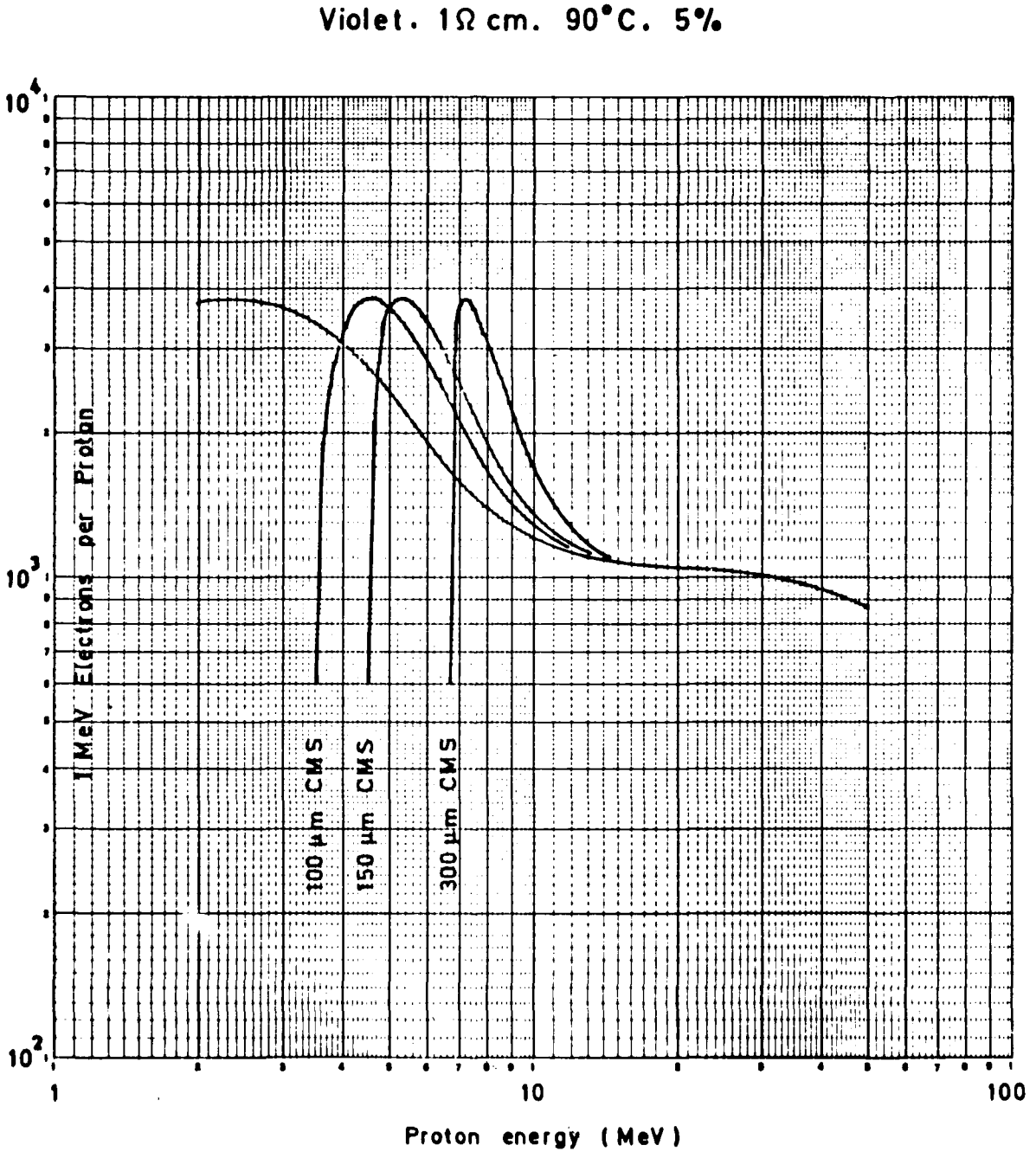

79133

Fig 28 Proton damage ratio, type A

Fig 29

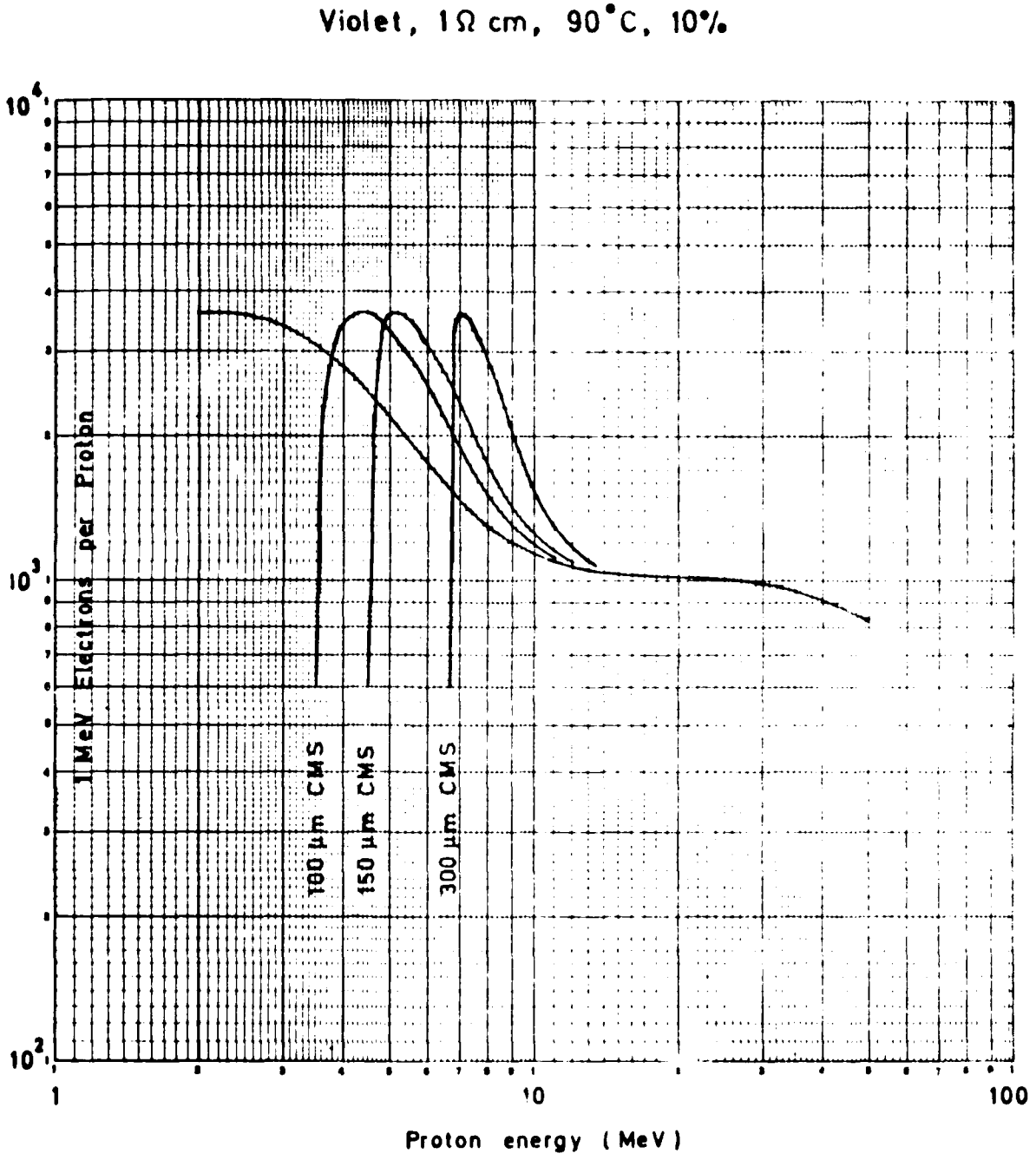

Fig 29 Proton damage ratio, type A

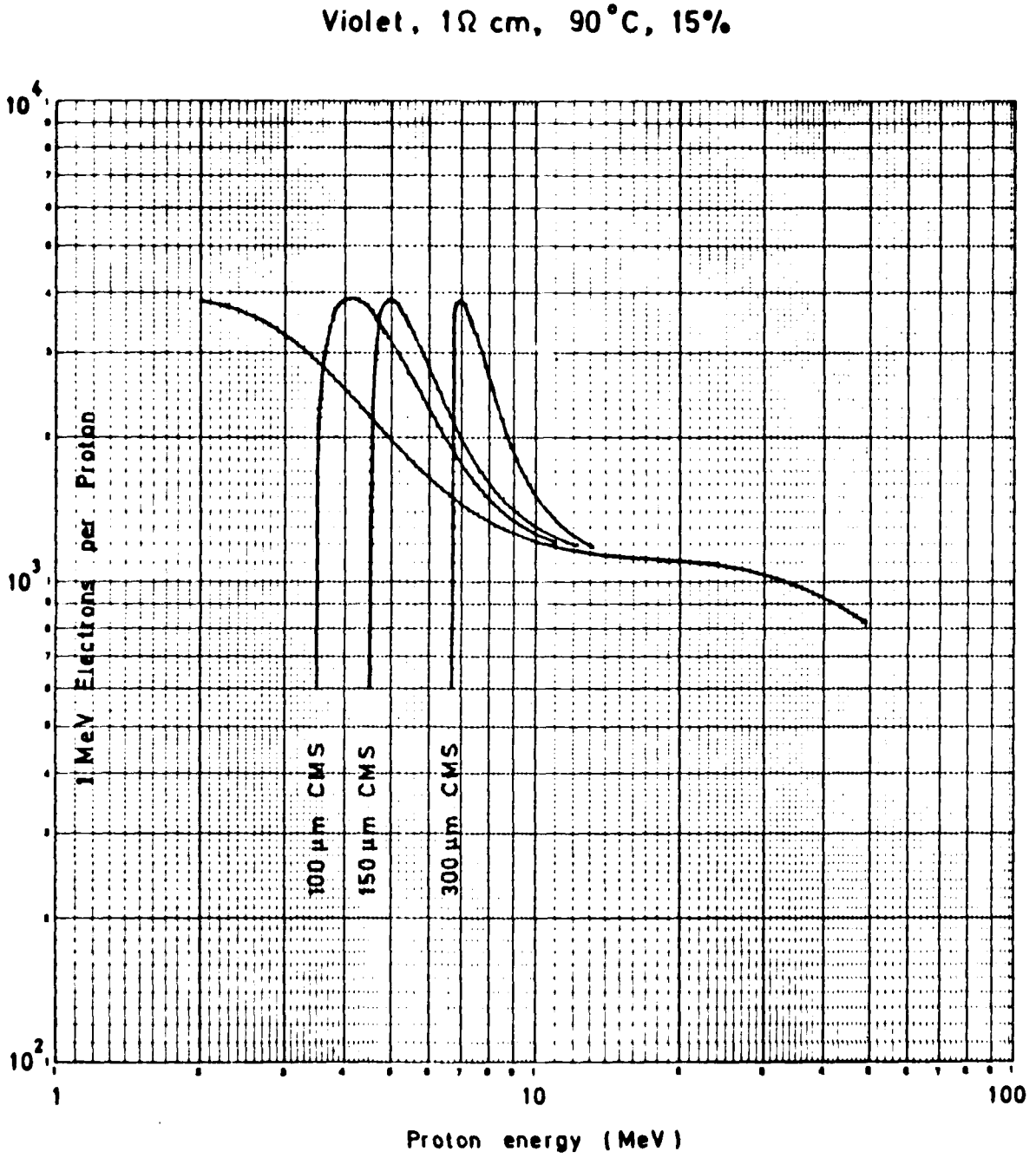

Fig 30 Proton damage ratio, type A

Fig 31

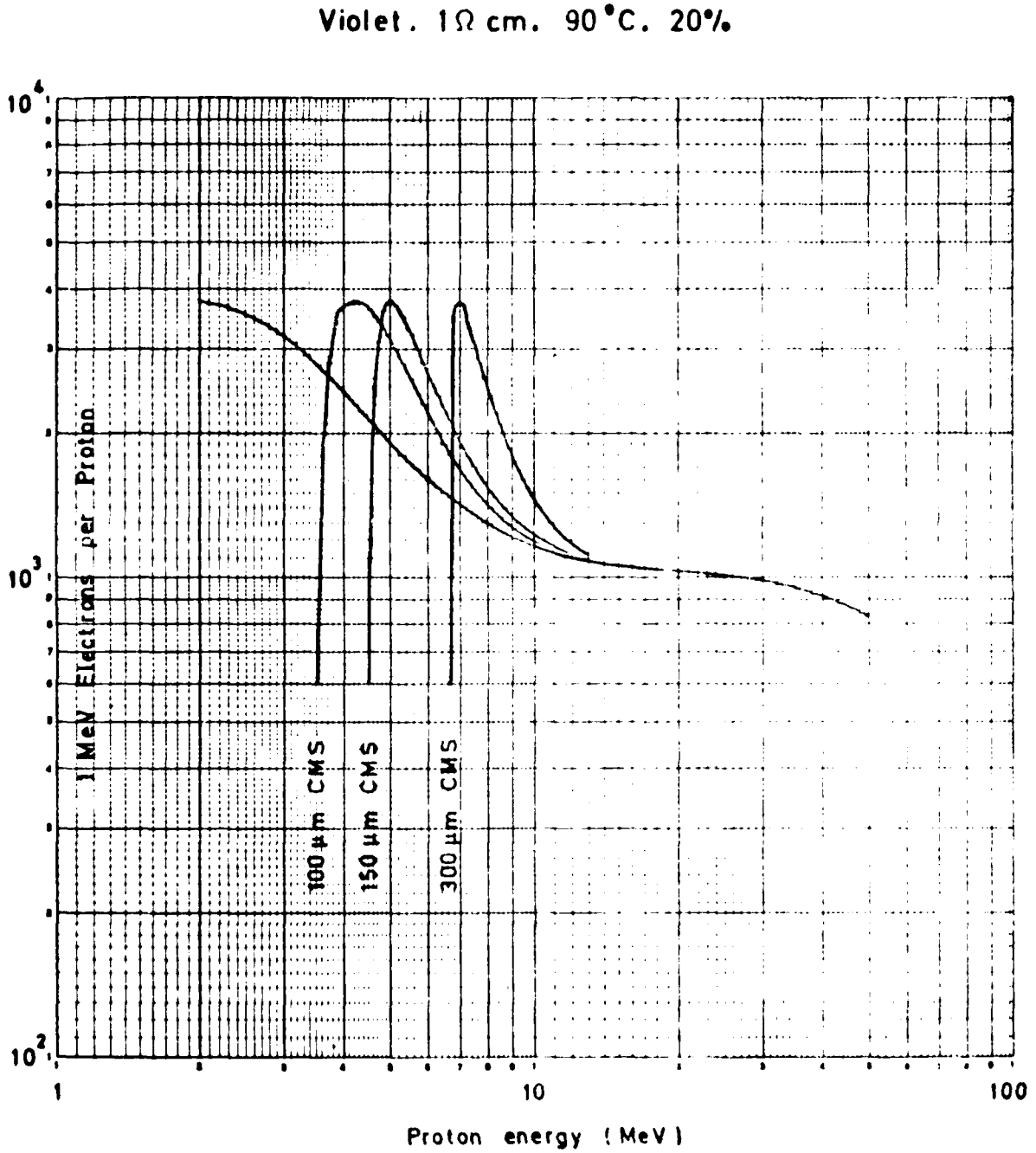

TR 79133

Fig 31 Proton damage ratio, type A

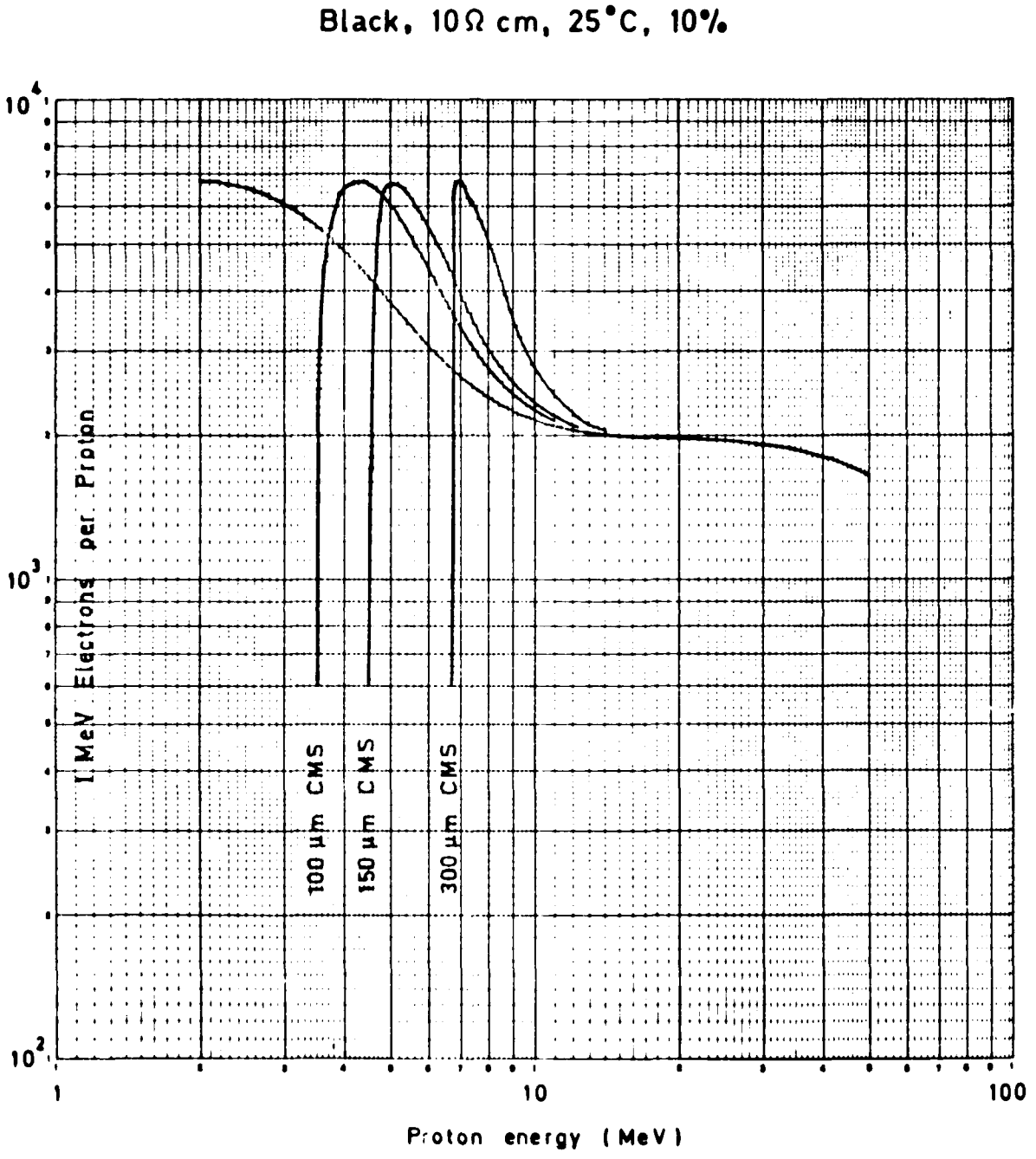

Fig 32 Proton damage ratio, type B

Fig 33

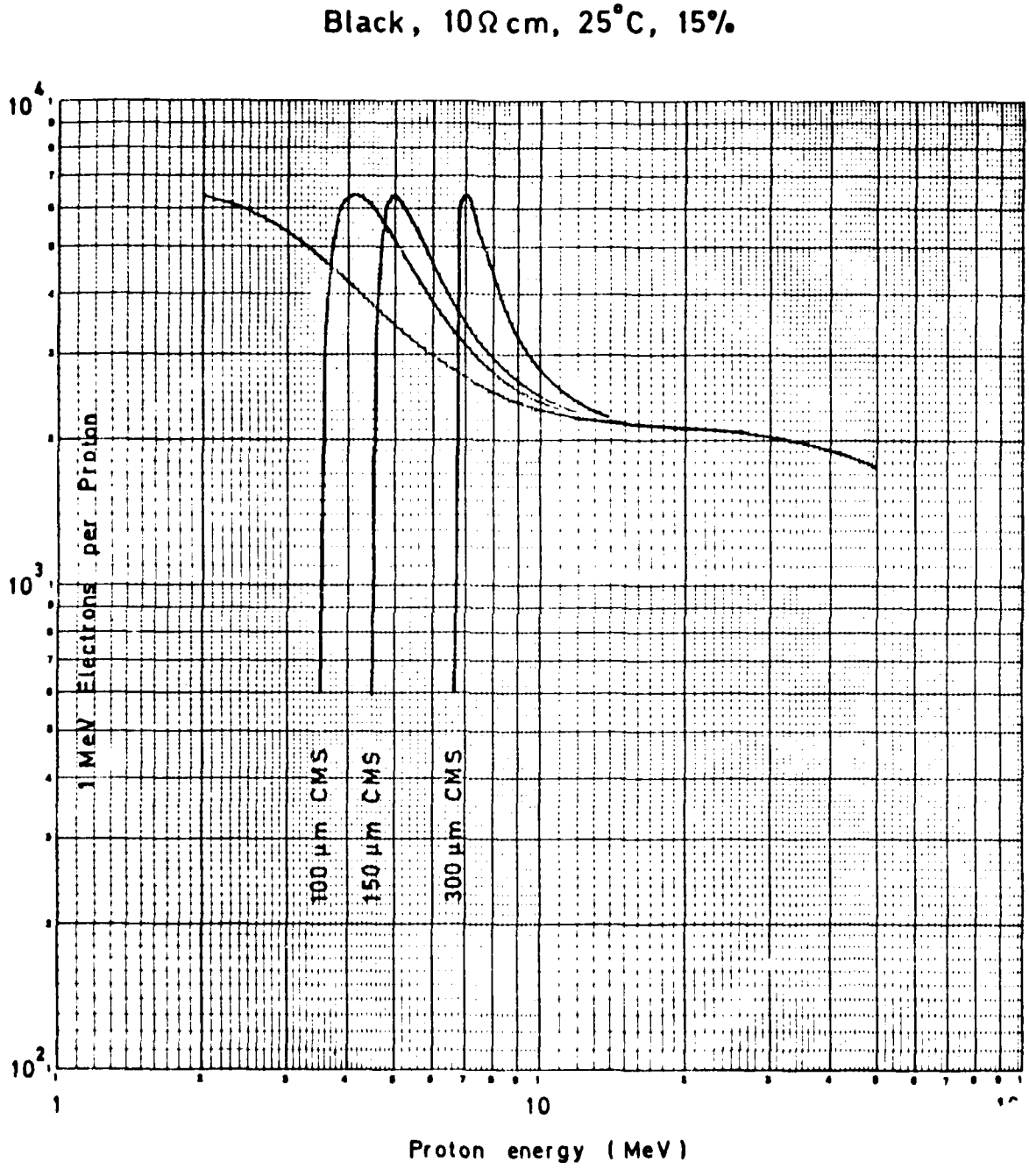

Fig 33 Proton damage ratio, type B

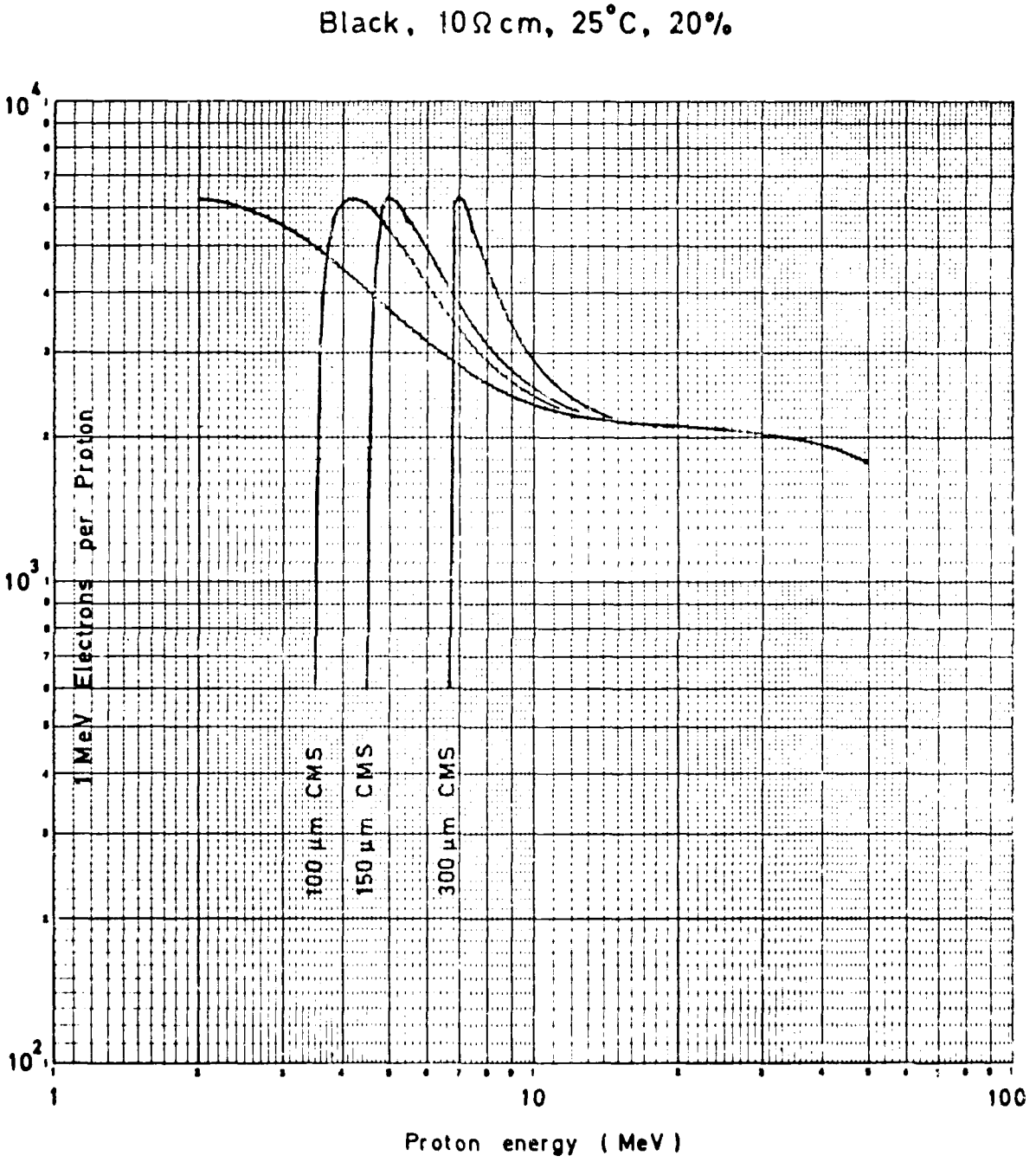

IR 79133

Fig 34 Proton damage ratio, type B

Fig 35

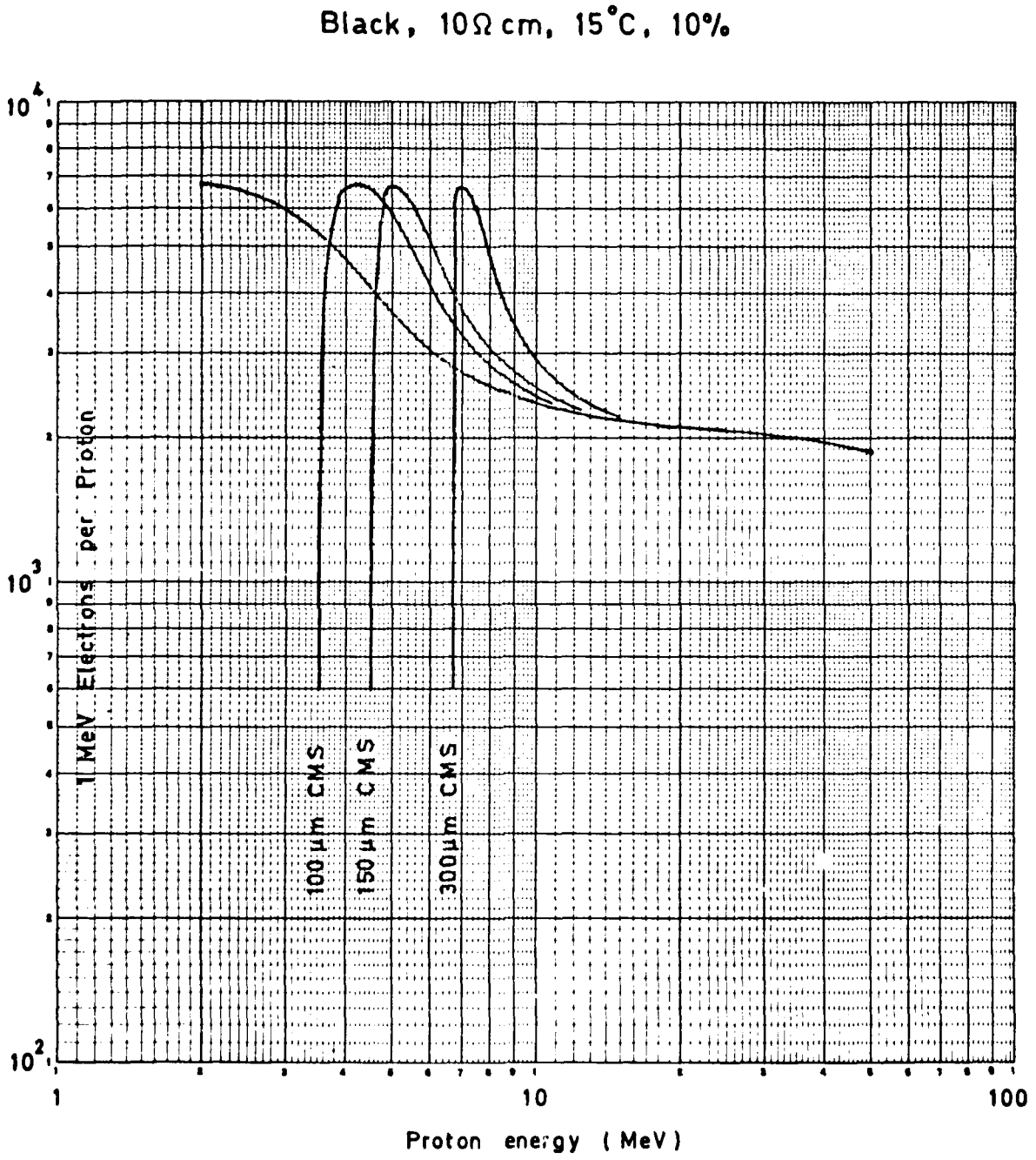

TR 79133

Fig 35 Proton damage ratio, type B

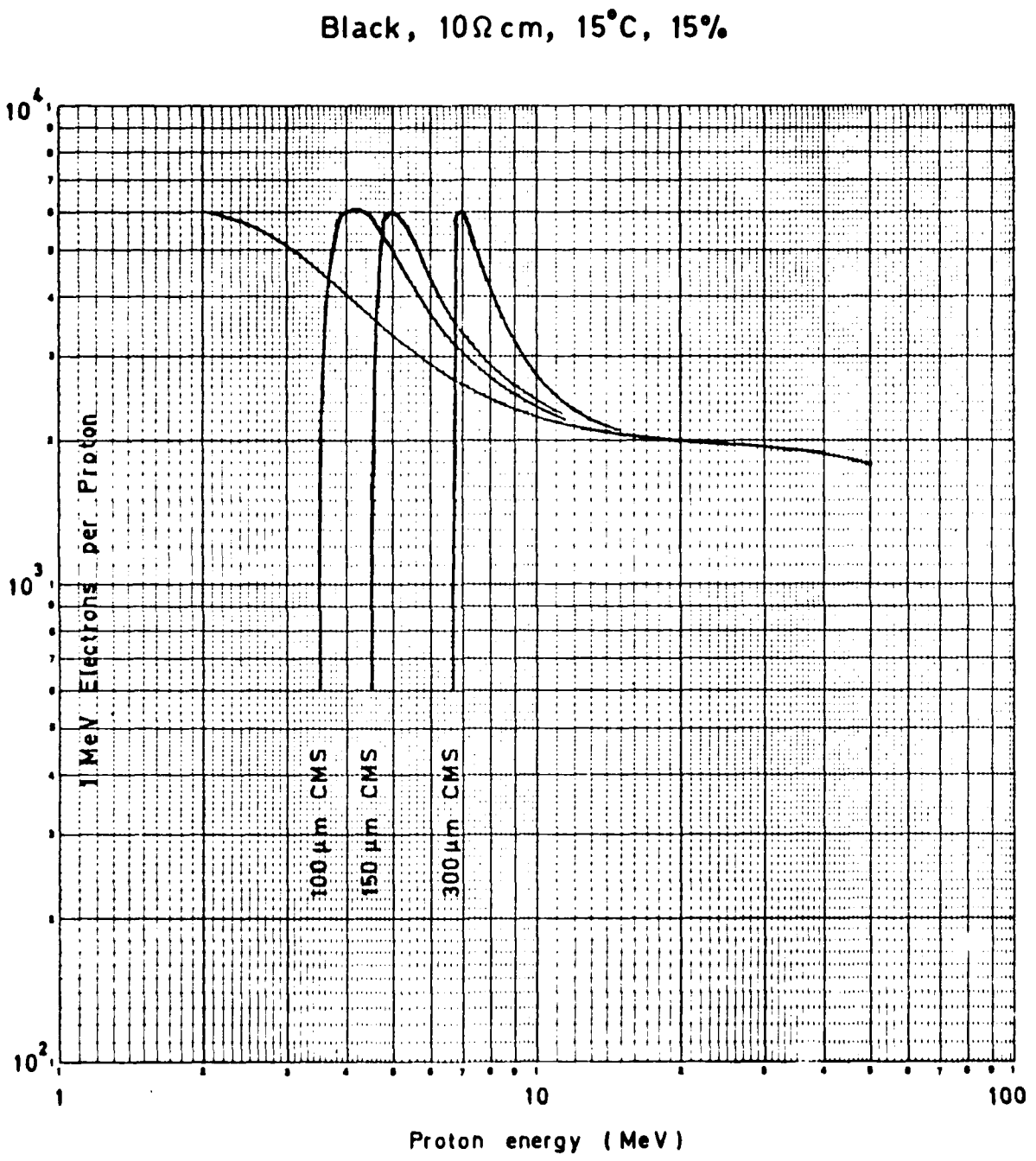

TR 79133

Fig 36 Proton damage ratio, type B

Fig 37

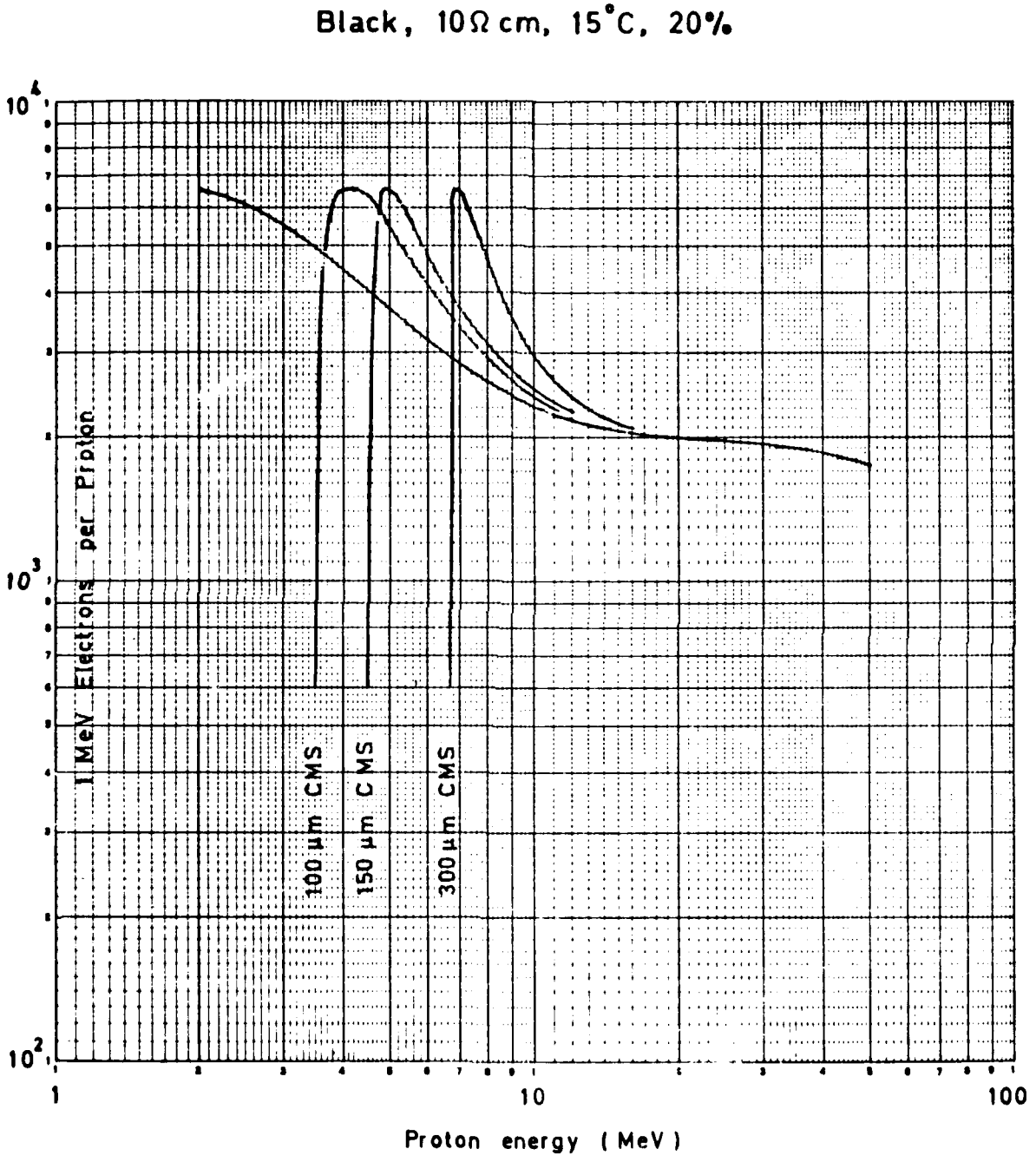

TR 79133

Fig 37 Proton damage ratio, type B

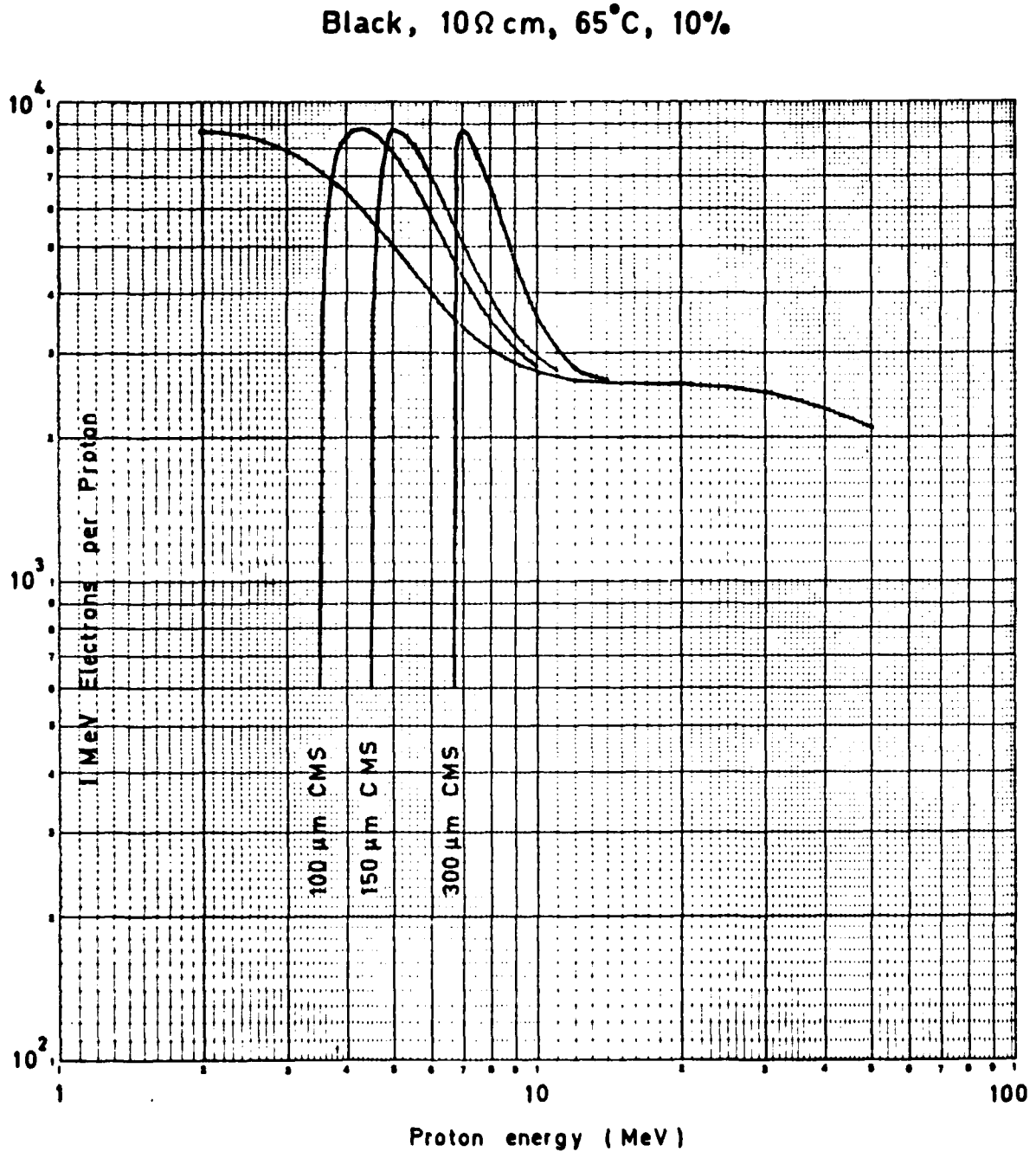

TR 79133

Fig 38 Proton damage ratio, type B

Fig 39

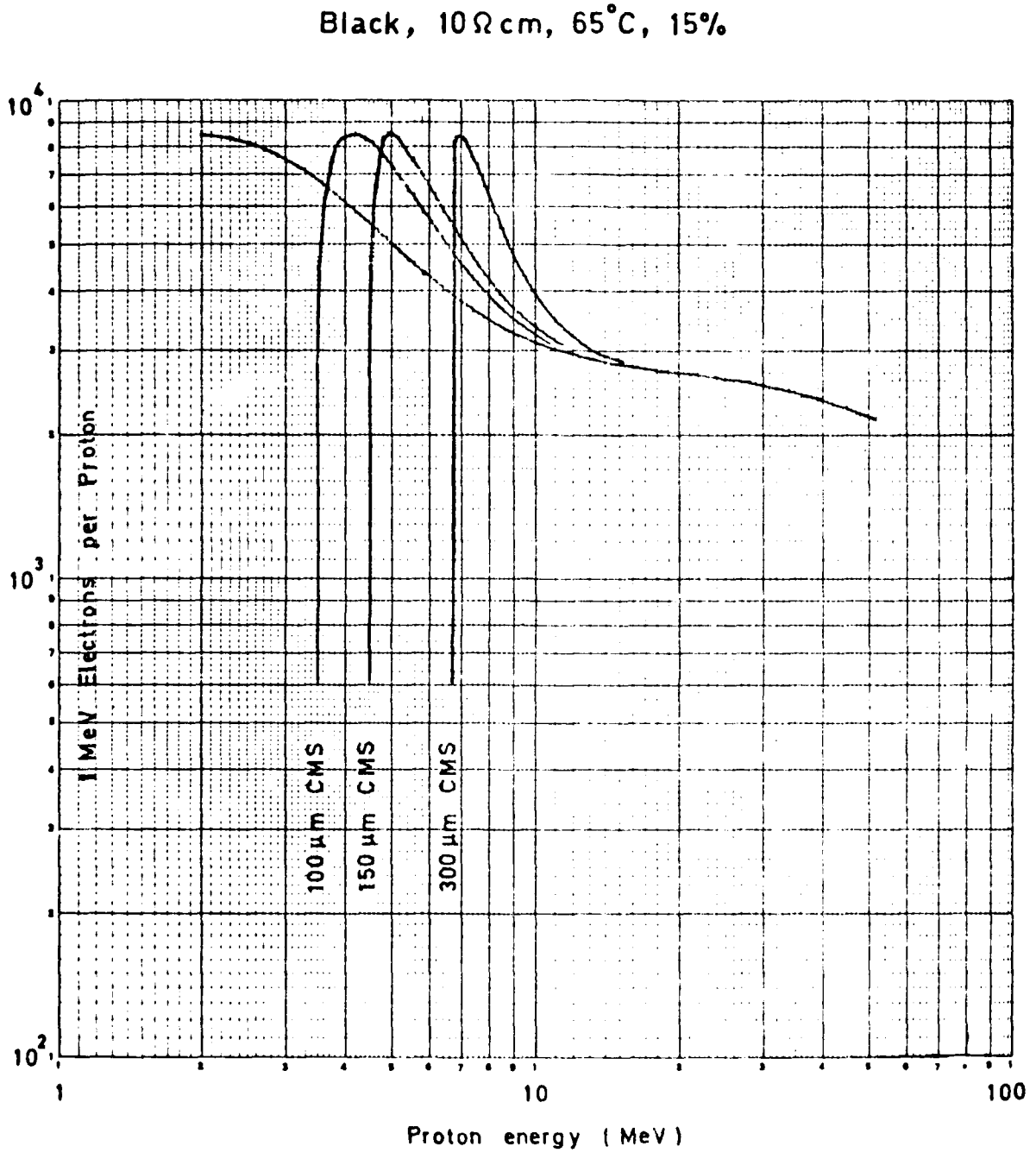

TR 79133

Fig 39 Proton damage ratio, type B

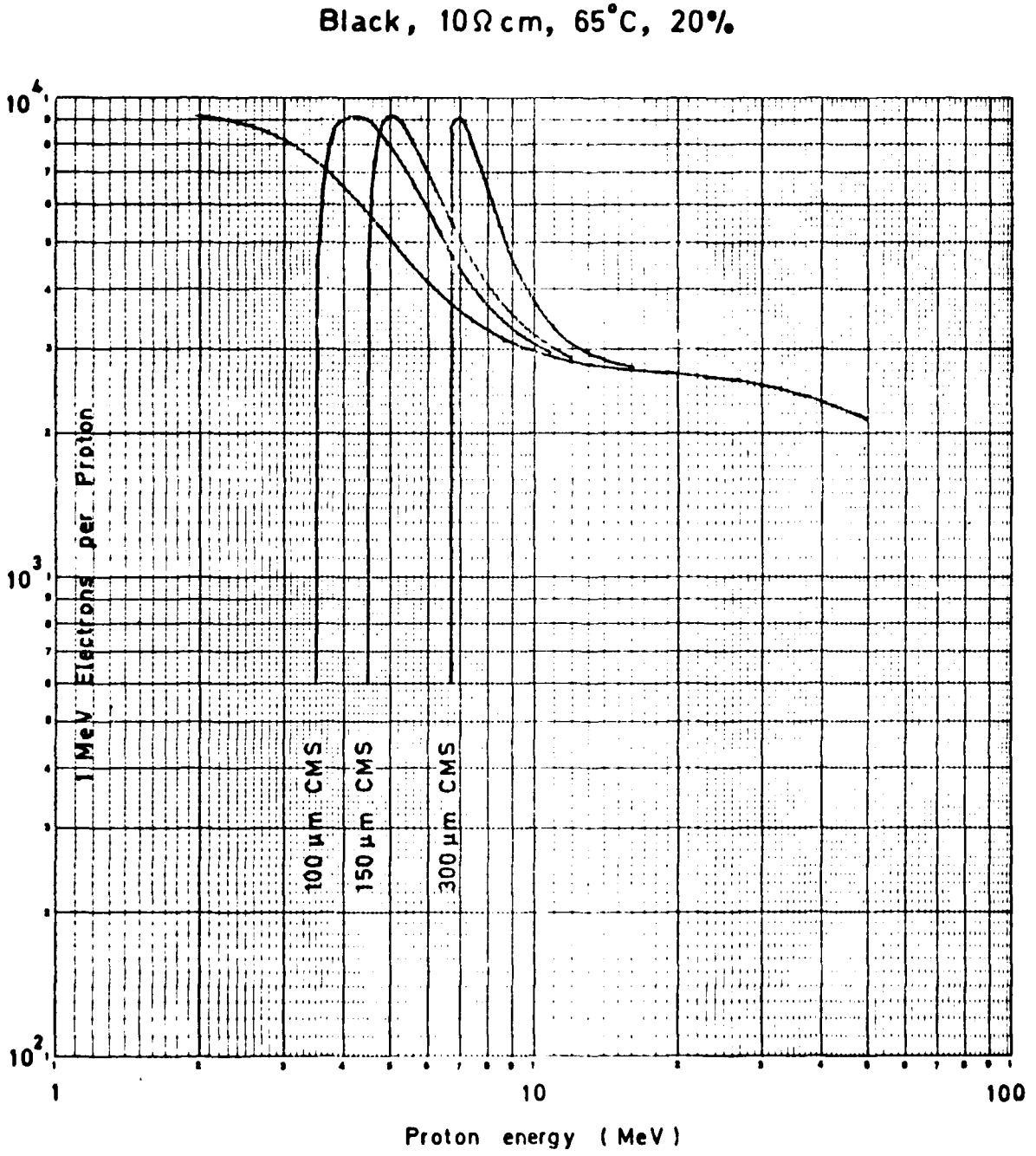

Fig 40 Proton damage ratio, type B

Fig 41

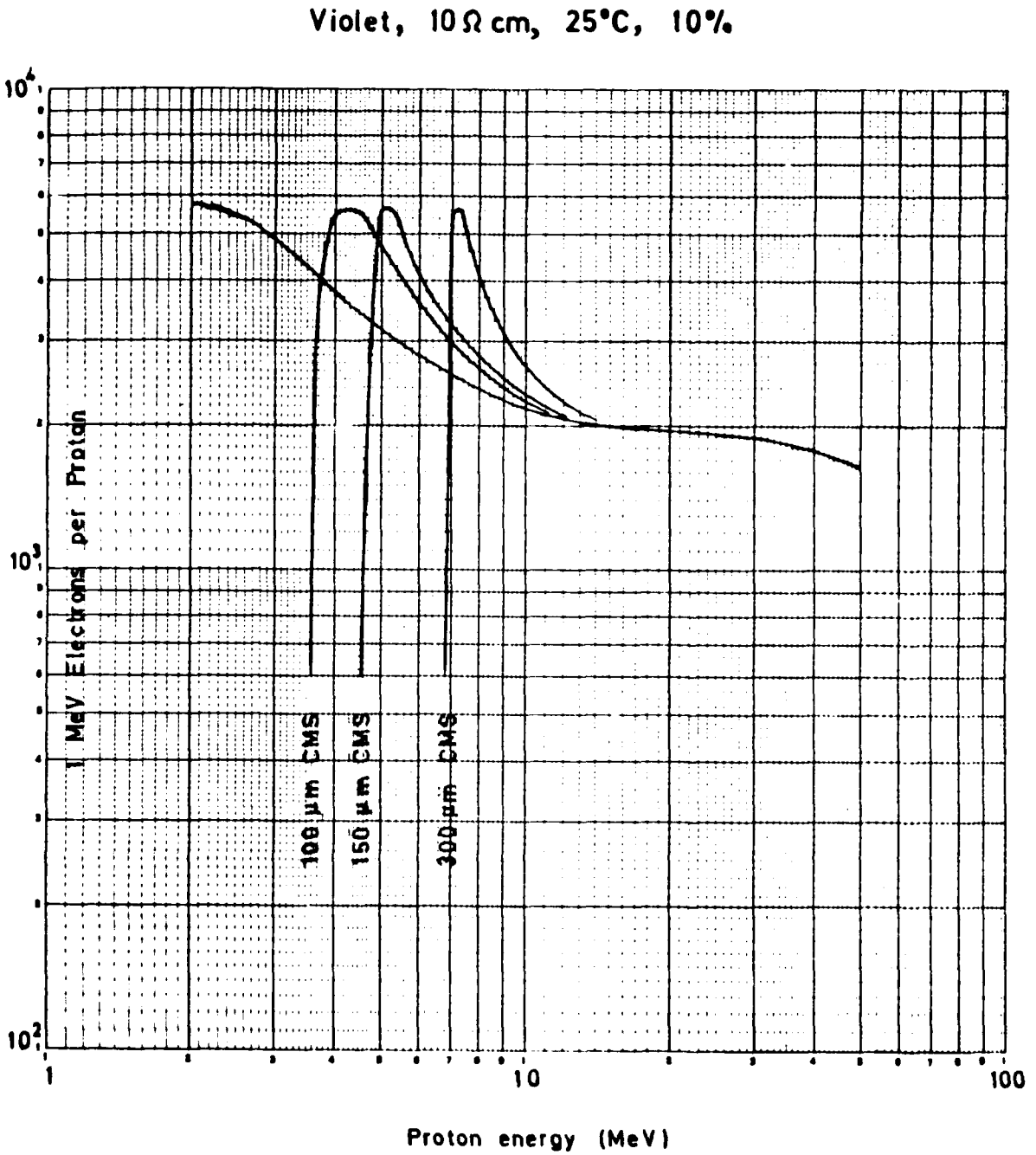

TR 79133

Fig 41 Proton damage ratio, type C

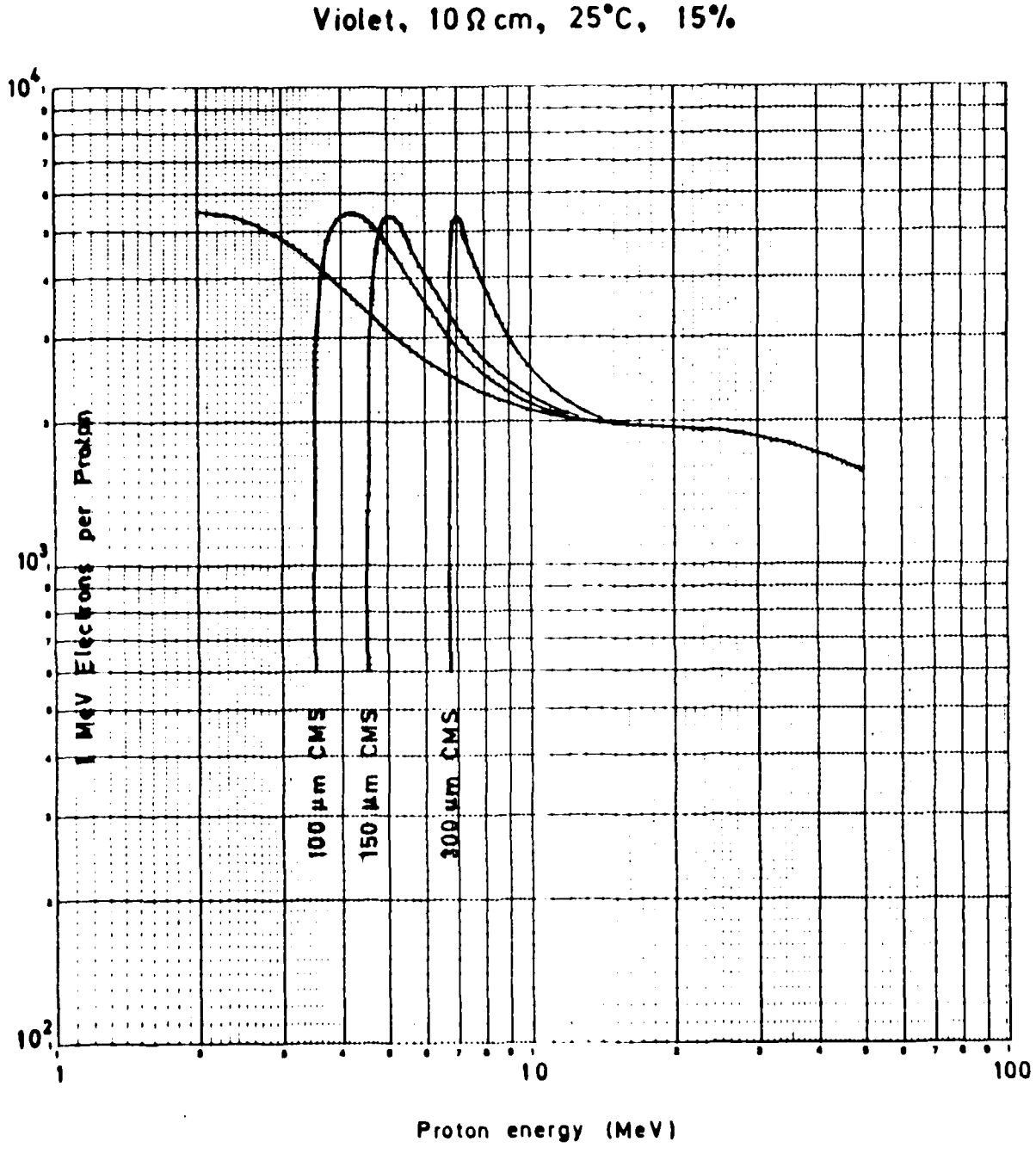

Fig 42 Proton damage ratio, type C

Fig 43

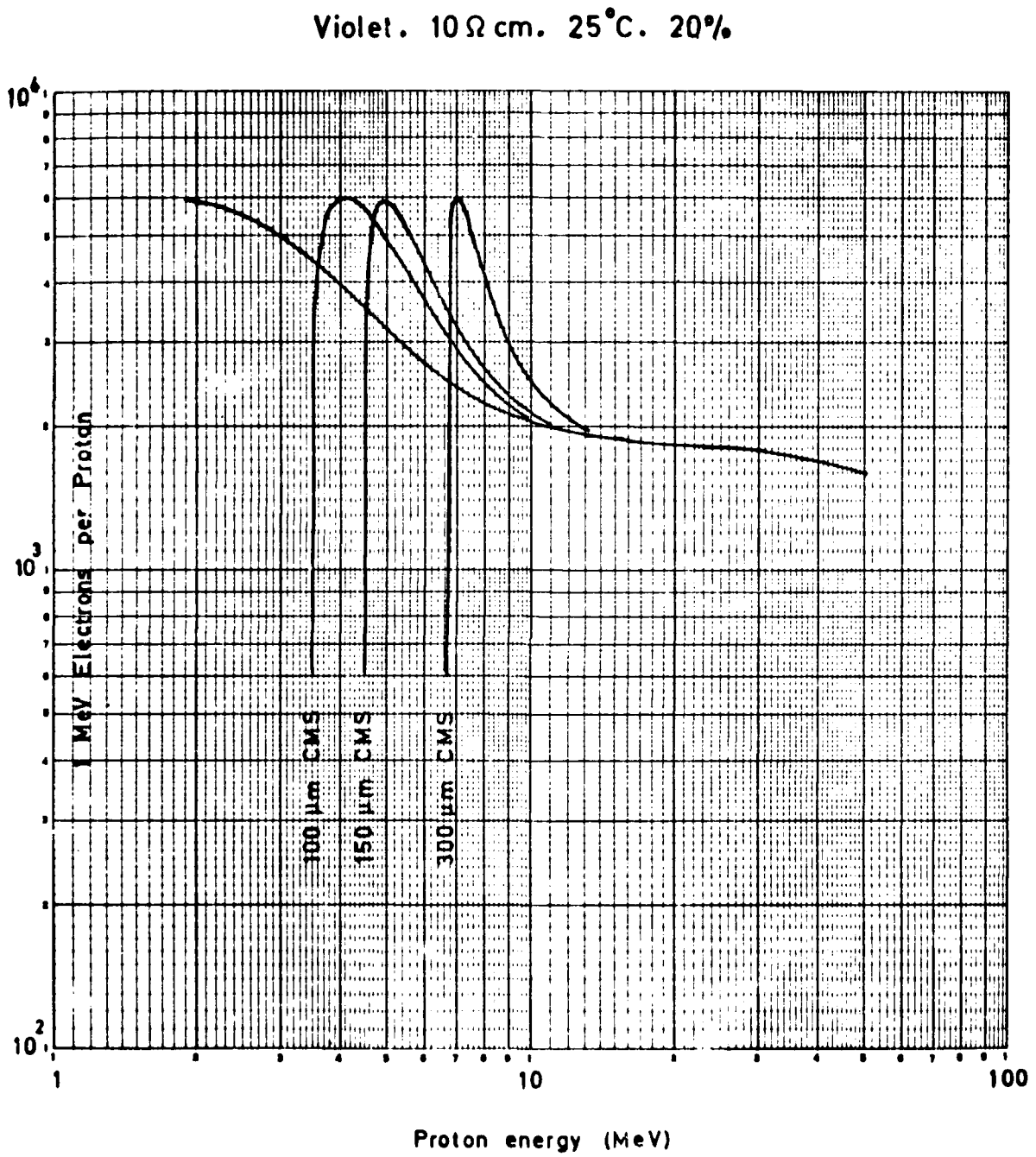

TR 79133

Fig 43 Proton damage ratio, type C

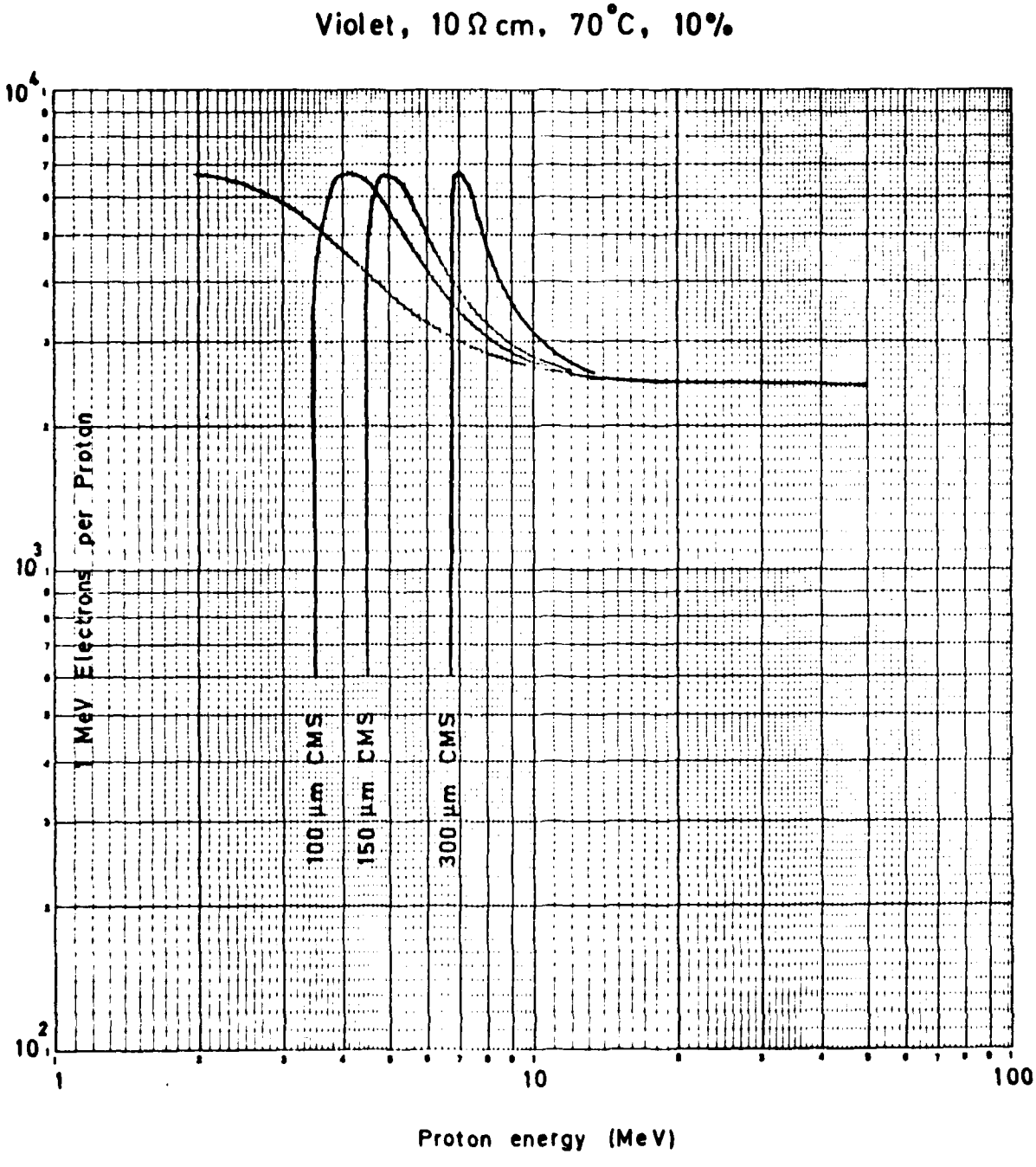

Fig 44 Proton damage ratio, type C

Fig 45

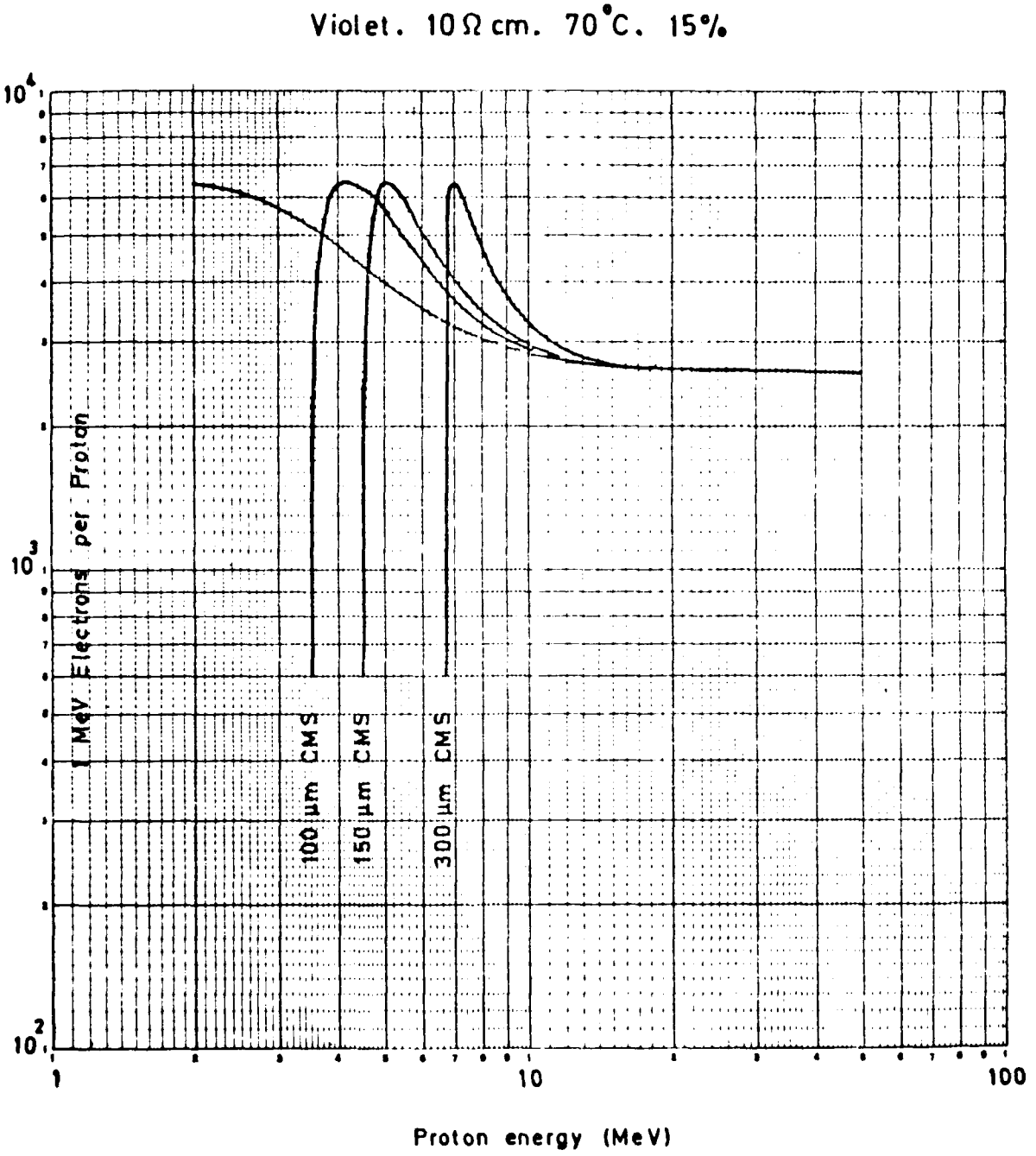

Fig 45 Proton damage ratio, type C

TR 79133

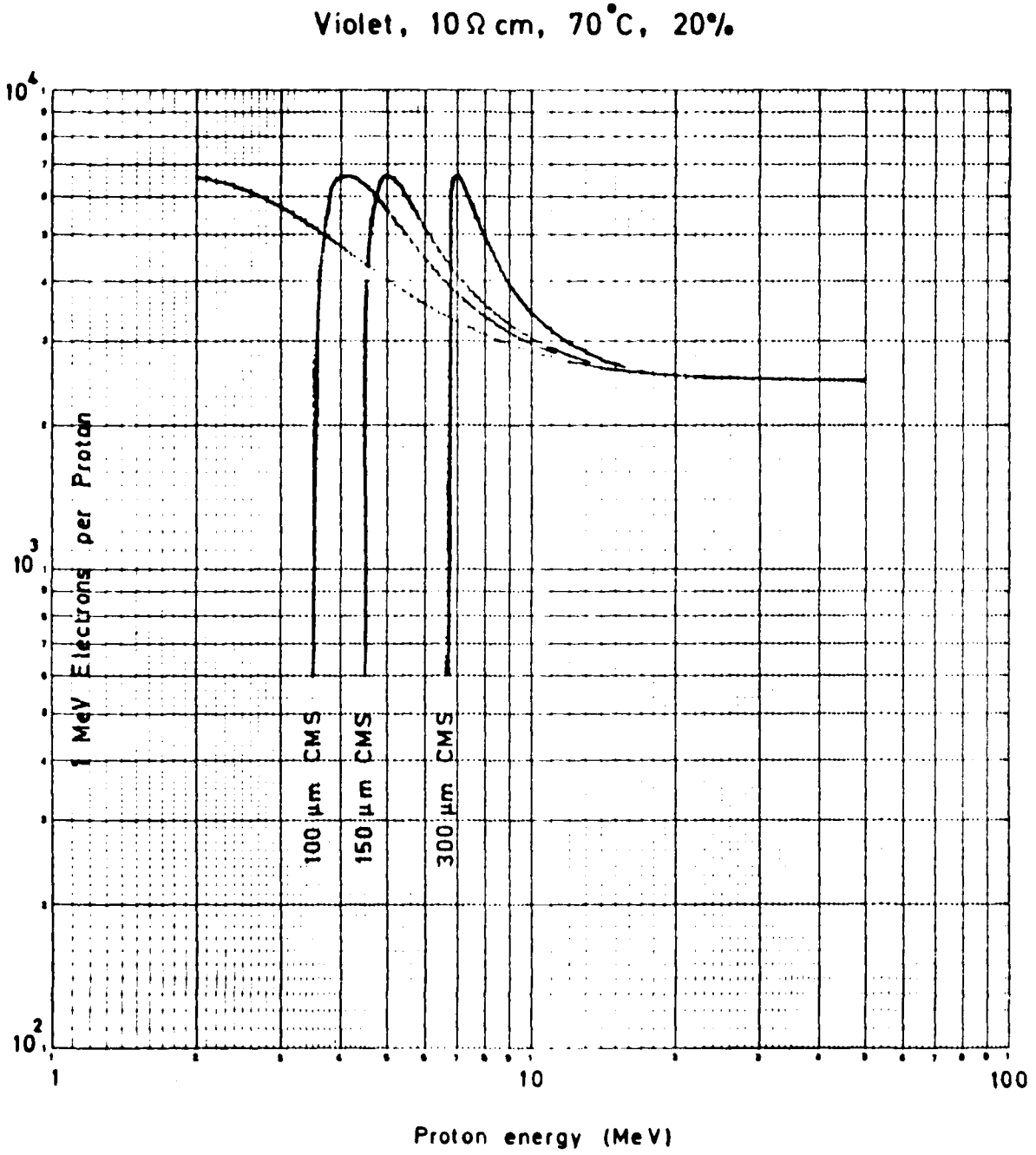

Fig 46 Proton damage ratio, type C

Fig 47

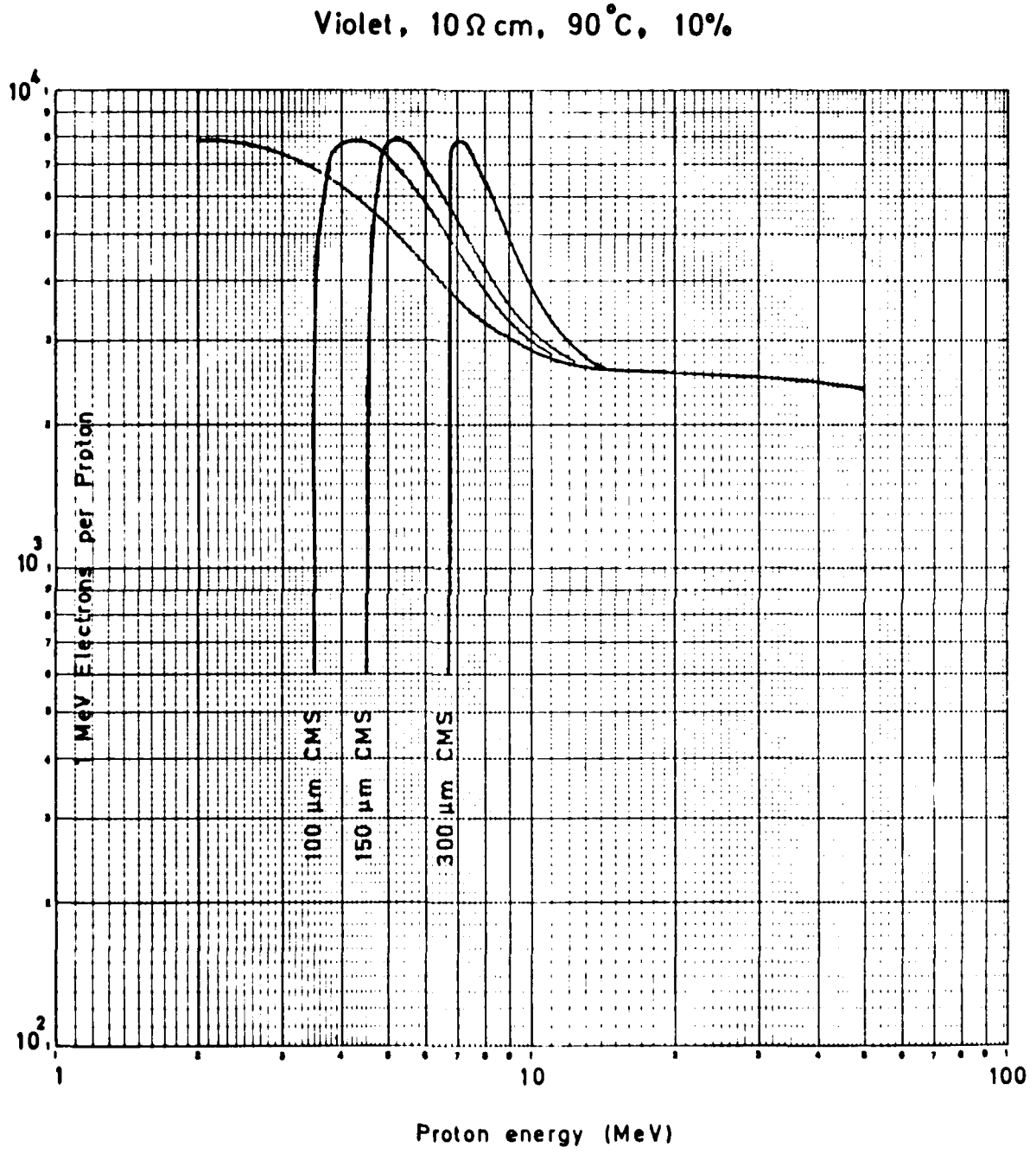

Fig 47 *Proton damage ratio, type C*

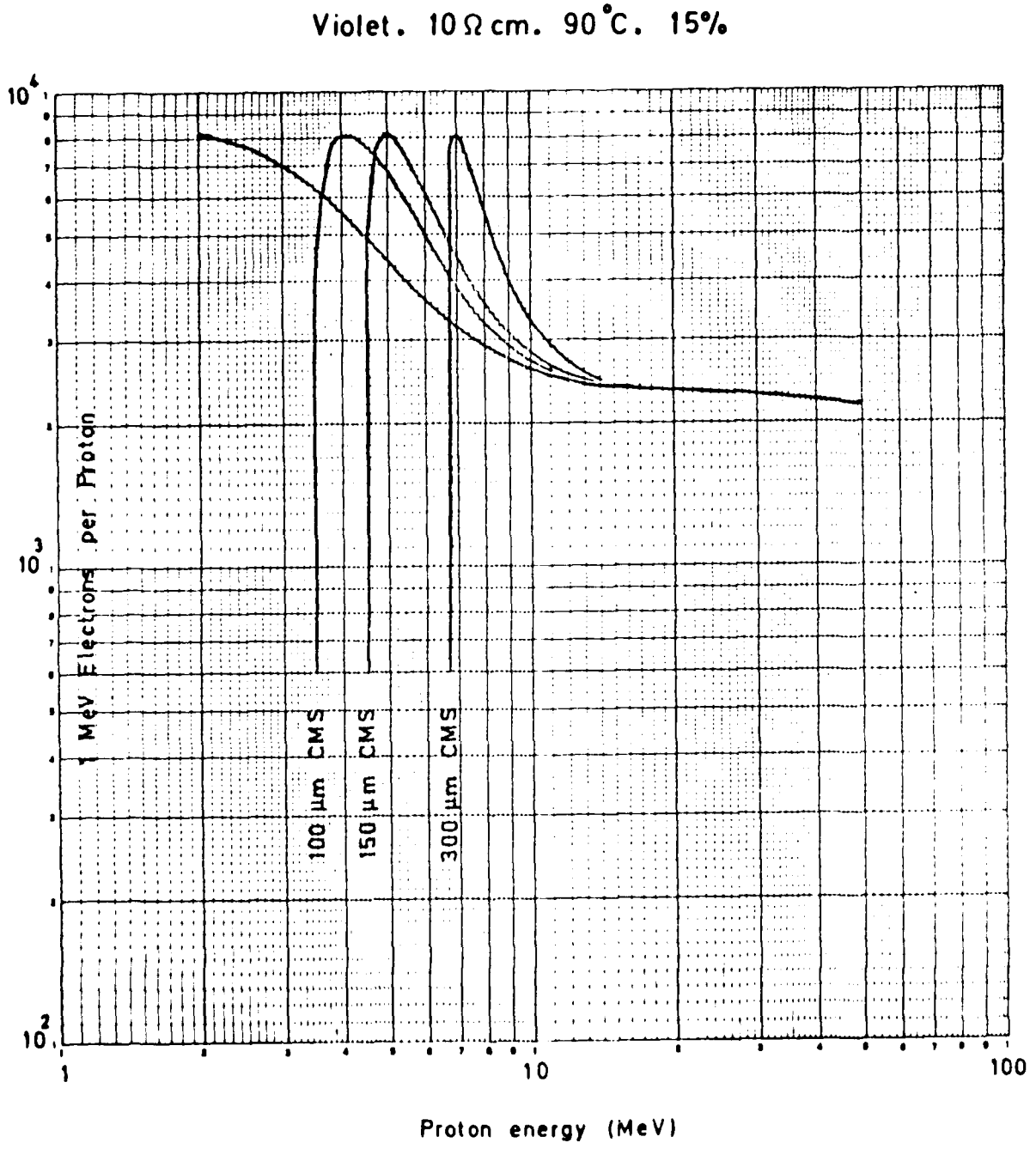

Fig 48 Proton damage ratio, type C

Fig 49

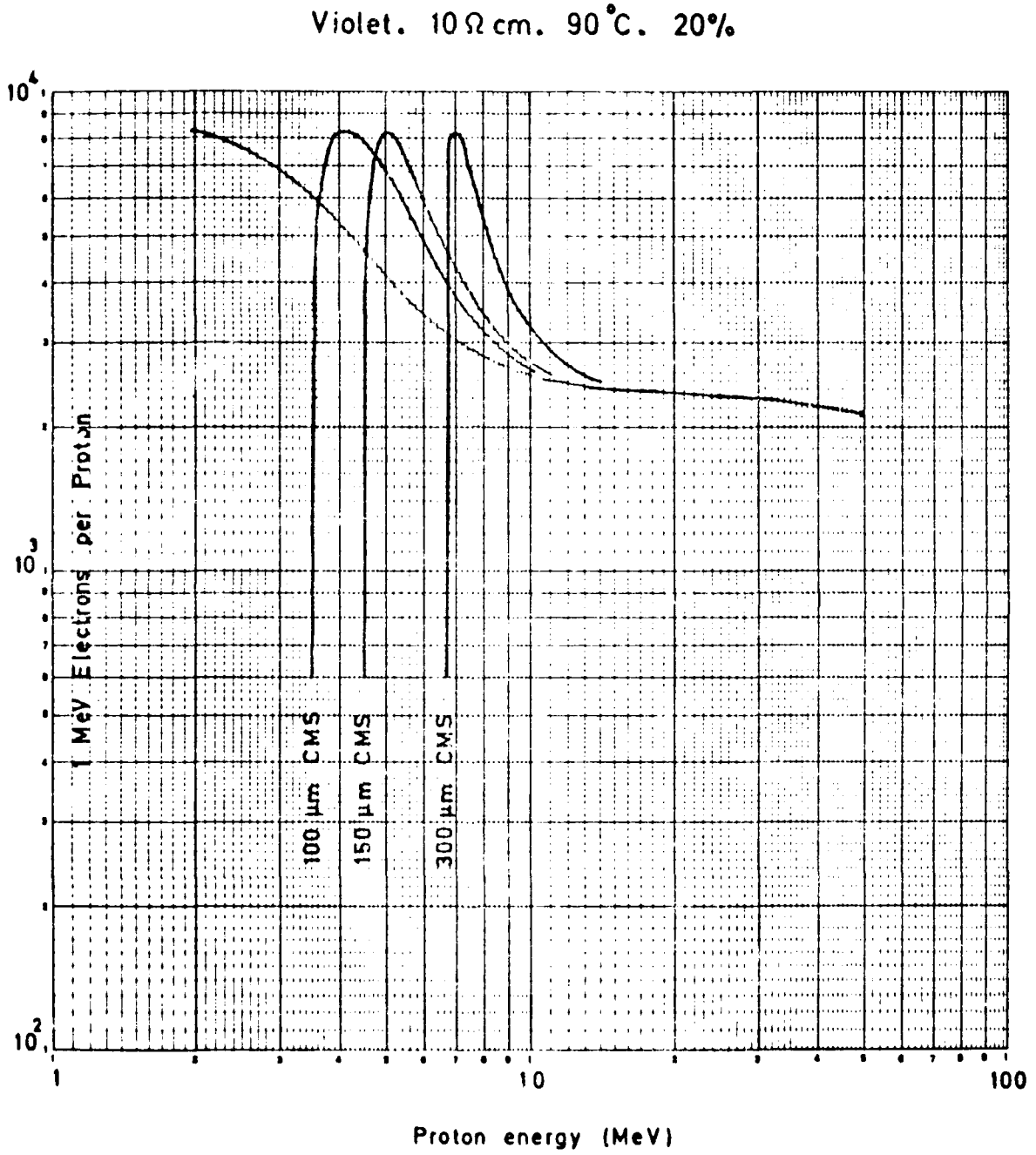

TR 79133

Fig 49 Proton damage ratio, type C

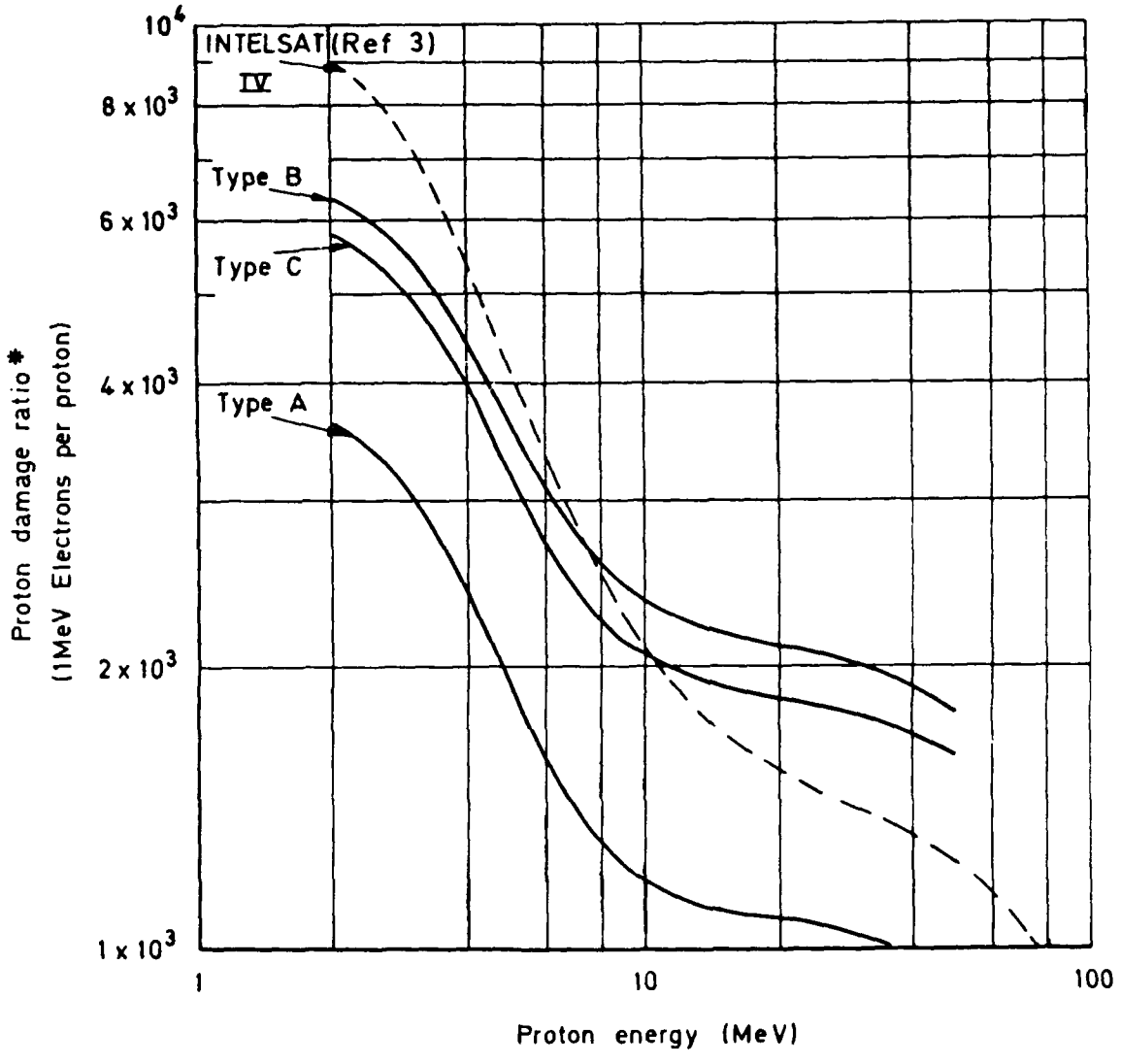

* 25°C, 20% Degradation

Fig 50 Proton damage ratio for different cell types

Fig 51

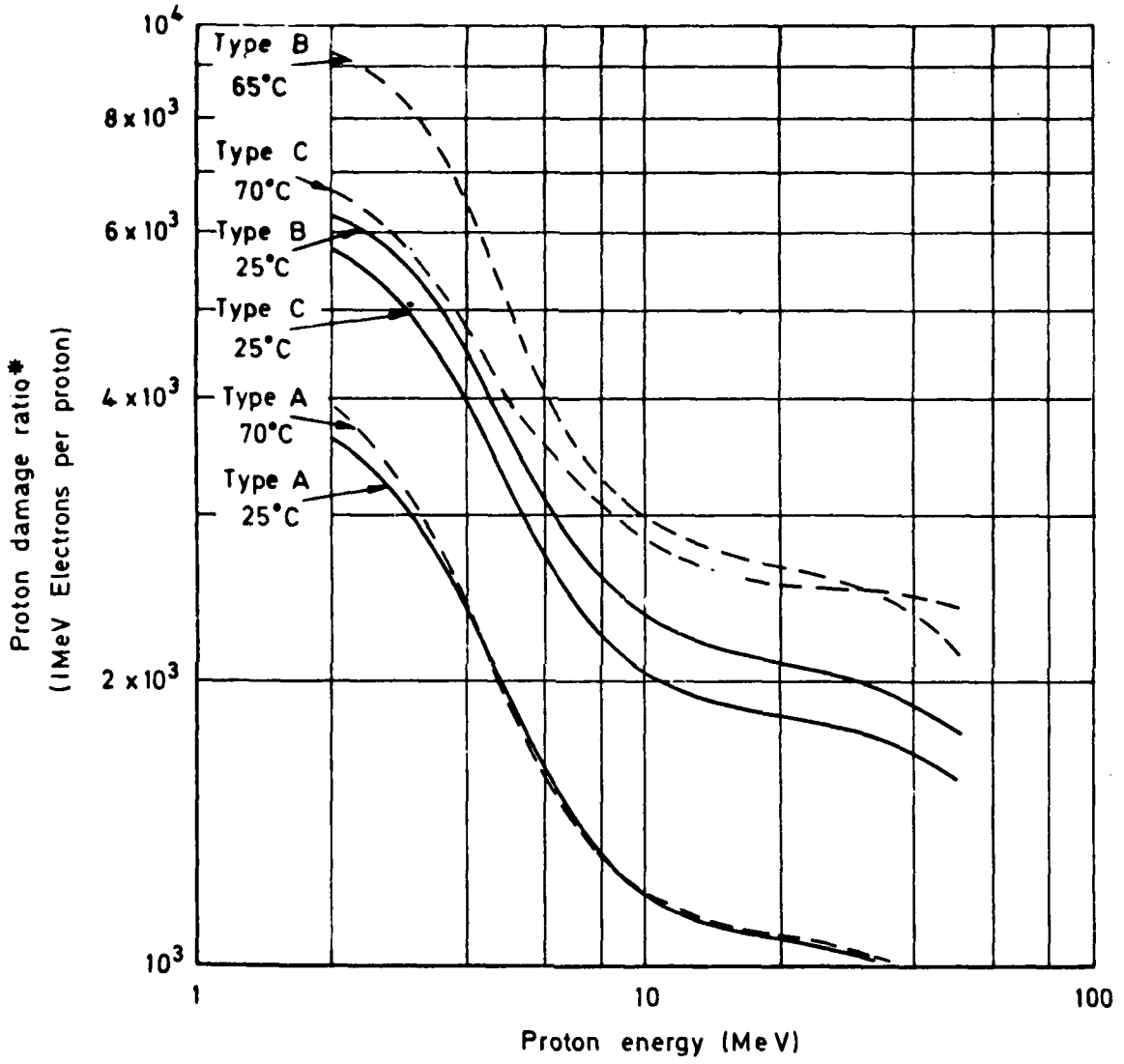

* 20% Degradation

TA 79133

Fig 51 Effect of temperature on proton damage ratios

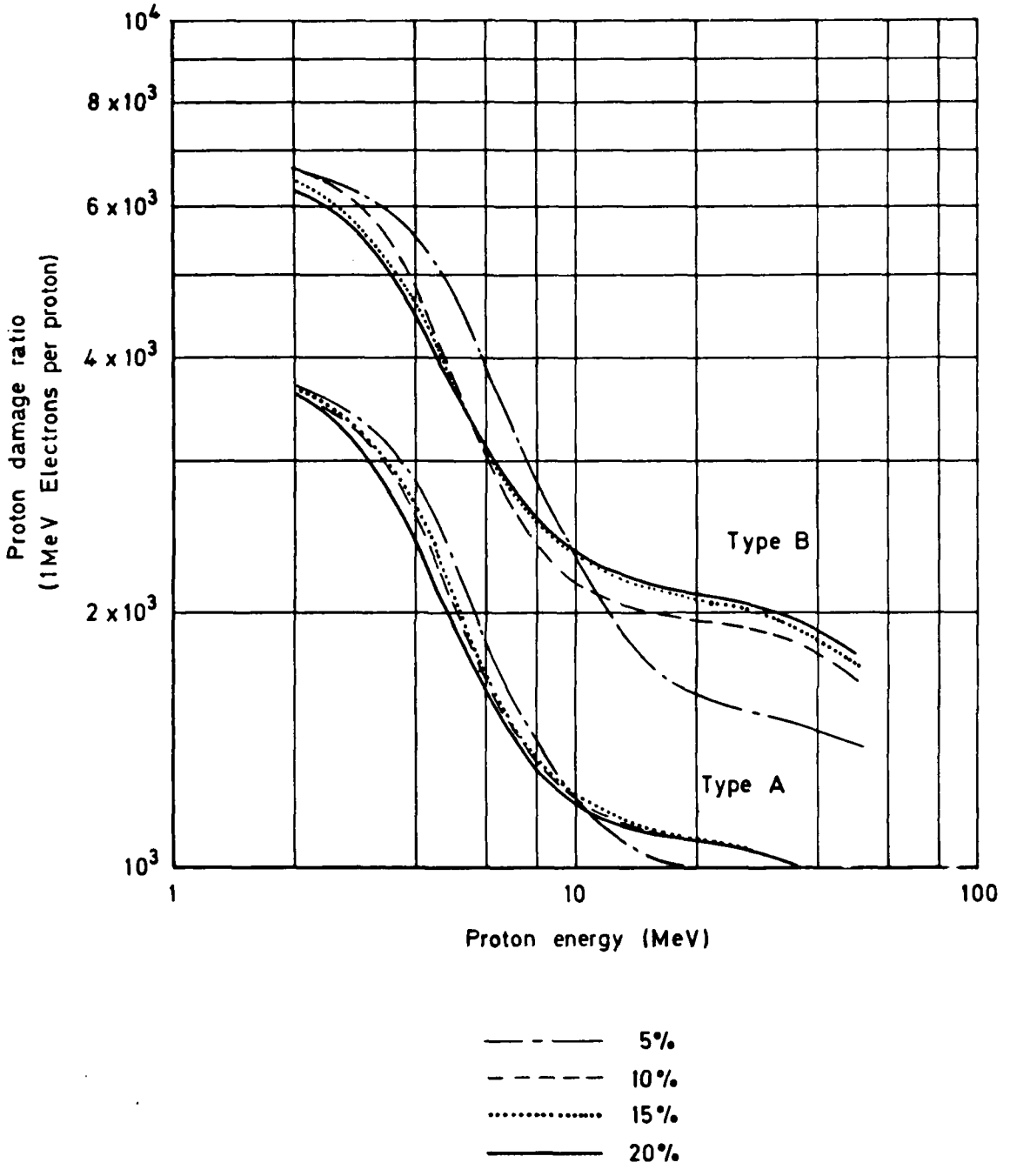

TR 79133

Fig 52 Proton damage ratios based on 5 to 20% degradation of maximum power at 25°C

REPORT DOCUMENTATION PAGE

Overall security classification of this page

UNCLASSIFIED

As far as possible this page should contain only unclassified information. If it is necessary to enter classified information, the box above must be marked to indicate the classification, e.g. Restricted, Confidential or Secret.

1. DRIC Reference (to be added by DRIC)	2. Originator's Reference	3. Agency Reference	4. Report Security Classification/Marking
	RAE TR 79133	N/A	UNCLASSIFIED UNLIMITED

5. DRIC Code for Originator	6. Originator (Corporate Author) Name and Location
7673000W	Royal Aircraft Establishment, Farnborough, Hants, UK
5a. Sponsoring Agency's Code	6a. Sponsoring Agency (Contract Authority) Name and Location
N/A	N/A

7. Title

Proton/electron damage ratios for some violet, black and thin silicon solar cells

7a. (For Translations) Title in Foreign Language

7b. (For Conference Papers) Title, Place and Date of Conference

8. Author 1. Surname, Initials	9a. Author 2	9b. Authors 3, 4	10. Date	Pages	Refs.
Walkden, M.W.			November 1979	71	3

11. Contract Number	12. Period	13. Project	14. Other Reference Nos.
N/A	N/A		Space 571

15. Distribution statement

(a) Controlled by – Head of Space Department, RAE (RAL)

(b) Special limitations (if any) –

16. Descriptors (Keywords) (Descriptors marked * are selected from TEST)

Solar cells. Photon degradation. Radiation. Proton/electron damage.

17. Abstract

In order to determine their proton to electron damage ratios, four different types of modern silicon solar cell have been subjected to 1 MeV electrons and protons in the energy range from 2-50 MeV, followed at each irradiation stage by an exposure to photon irradiation. The cells included non-reflecting and violet cells of normal (200-250 μm) thickness and a thin (50 μm) cell. Cell performance measurements were made on new and irradiated cells at room and at elevated temperatures to obtain the proton damage ratios and to ascertain whether these were temperature dependent.

It was found that the proton damage ratio of one type of cell was approximately one half of that of the other three types. It was also found that the proton damage ratio for this type of cell was independent of temperature, which was not the case with the other types. One cause of these differences is attributed to photon induced changes in solar cell performance following electron and proton irradiation for the particular material from which this type of cell is made.

F5910/1

RAE Form A143

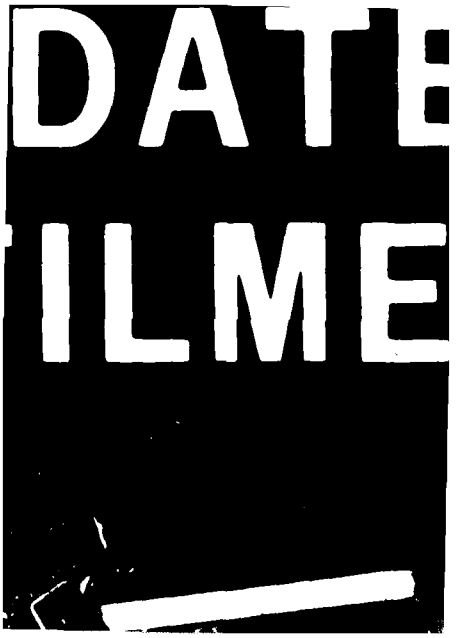
DATE
ILME